Regulation of mitochondrial and nonmitochondrial protein turnover by the PINK1-Parkin pathway

Evelyn S. Vincow

A dissertation
submitted in partial fulfillment of the
requirements for the degree of

Doctor of Philosophy

University of Washington

2013

Reading Committee:

Leo J. Pallanck, Chair

Sandra M. Bajjalieh

Michael J. MacCoss

Program Authorized to Offer Degree:

Neurobiology and Behavior

University of Washington

Abstract

Regulation of mitochondrial and nonmitochondrial protein turnover
by the PINK1-Parkin pathway

Evelyn Sandra Vincow

Chair of the Supervisory Committee:
Associate Professor Leo J. Pallanck
Genome Sciences

The accumulation of damaged mitochondria has been proposed as a key factor in aging and in the pathogenesis of many common age-related diseases, including Parkinson disease (PD). Recently, *in vitro* studies of the PD-related proteins Parkin and PINK1 have found that these factors act in a common pathway to promote the selective autophagic degradation of damaged mitochondria (mitophagy). However, whether PINK1 and Parkin promote mitophagy *in vivo* is unknown. To address this question, I used a proteomic approach in *Drosophila* to study the effects of null mutations in *parkin* or *PINK1* on mitochondrial protein turnover. The *parkin* null mutants showed a significant overall slowing of mitochondrial protein turnover, similar to but less severe than the slowing seen in autophagy-deficient *Atg7* mutants, consistent with the model that Parkin acts upstream of Atg7 to promote mitophagy. By contrast, the turnover of many mitochondrial respiratory chain (RC) subunits showed greater impairment in *parkin* than in *Atg7* mutants, and RC turnover was also selectively impaired in *PINK1* mutants. These findings demonstrate that the PINK1-Parkin pathway promotes mitophagy *in vivo* and, unexpectedly, also promotes selective turnover of mitochondrial RC components. Furthermore, differential tissue expression analyses suggest that selective RC subunit turnover may be particularly important in

neural tissue, as mitophagy appears to account for a relatively low proportion of mitochondrial protein turnover in brain.

Because Parkin is an E3 ubiquitin ligase with multiple known nonmitochondrial substrates, I also examined the effects of *parkin* and *PINK1* mutations on turnover of nonmitochondrial proteins. *parkin* mutants had moderately impaired turnover of most types of nonmitochondrial proteins, including synaptic and plasma membrane proteins, and strikingly impaired turnover of many extracellular proteins. This finding was consistent with previous evidence that Parkin regulates the endocytic/endosomal pathway. *PINK1* mutants, by contrast, had significantly slowed turnover in only 3 of 10 categories of nonmitochondrial proteins, and did not show a defect in endocytic/endosomal turnover. Correlational analysis suggested that PINK1 and Parkin may work together to promote turnover of cytoplasmic proteins, but Parkin's role in endocytic/endosomal protein turnover appears to be independent of PINK1. Further investigation of the roles played by Parkin and PINK1 in both mitochondrial and nonmitochondrial protein turnover will shed light on the contribution of these proteins to human disease.

Table of Contents

List of Figures

List of Tables

Acknowledgments

The idea for this project emerged from a conversation between Leo Pallanck and Michael MacCoss, and my experiments were done in close collaboration with the MacCoss Lab. Gennifer Merrihew performed all the mass spectrometry and patiently guided an ignorant newcomer through the mass spec labyrinth. Nick Shulman created Topograph, the software that made my turnover measurements possible, and responded to feature requests with unfailing good temper. Michael Bereman and Ed Hsieh gave me vital advice on protein abundance analysis.

In the Pallanck Lab, I've been blessed with world-class labmates who answered hundreds (if not thousands) of questions over the years, provided invaluable help and advice, and cheered me on. I owe special thanks to Ruth Thomas, who became an unofficial second mentor. Ruth repeatedly helped sort out my confusion and contributed countless insights.

The Brewer Lab taught me the basics of yeast culture and provided space and equipment for growing labeled yeast. Richard Beyer and Theo Bammler shared their expertise on questions of statistics and data analysis. The University of Washington's Proteomics Resource supported the work with substantial grants of mass spectrometer time.

Finally, I extend thanks to my committee members—Sandra Bajjalieh, Celeste Berg, Martha Bosma, and Michael MacCoss—and to my advisor, Leo Pallanck. Leo encouraged and supported me through a long, risky, and difficult project. With his help and guidance, I have accomplished more than I'd thought possible.

Dedication

This dissertation is dedicated to

JOEL W. DOWNER

for about seven thousand reasons.

...some things travel faster than light.

Chapter 1: Introduction

Mitochondria, as Heidi McBride aptly notes, are far more than "just a powerhouse" for the cell (1). While best known for generating ATP, mitochondria are also essential for calcium homeostasis and creation of iron-sulfur clusters, as well as the metabolism of amino acids, carbohydrates, and lipids (1-3). Mitochondria also play major roles in cell signaling, the cell cycle, differentiation, and apoptosis (1, 4). Maintaining functional mitochondria is therefore vital to cellular health, and the processes involved are collectively called *mitochondrial quality control (QC)*. Vigorous mitochondrial QC is particularly critical because mitochondria are the major cellular producer of reactive oxygen species (ROS), which damage mitochondrial DNA, lipids, and proteins (2, 5).

My dissertation work focuses on two proteins recently identified as key mediators of mitochondrial QC: PINK1 and Parkin. These proteins, which first attracted attention as the products of genes associated with autosomal recessive parkinsonism, are now the focus of a model in which targeted autophagy of dysfunctional mitochondria is a critical form of mitochondrial quality control (6-8). In this first chapter, I will give essential information on mitochondria, briefly discuss nonautophagic forms of mitochondrial QC, review data on mitochondrial autophagy, and discuss the studies on PINK1 and Parkin that have led to my work. Finally, I will discuss early studies of mitochondrial turnover as background for my own turnover measurements.

MITOCHONDRIA: BASIC INFORMATION

Mitochondria are double-membraned structures that, unique among eukaryotic organelles, contain their own genome. This genome encodes a small number of essential mitochondrial proteins, which are transcribed and translated within the organelle itself (2). Most of the mitochondrial proteome, however, is nuclearly encoded, and it is quite large; a 2008 study catalogued nearly 1100 mitochondrial proteins in mouse (9).

Mitochondria contain the protein systems that permit high-efficiency generation of ATP: the tricarboxylic acid cycle enzymes, which produce NADH, and the proteins of the respiratory chain (RC), which use the NADH to generate ATP (2). The RC comprises five protein complexes anchored in the cristae (deep folds) of the mitochondrial inner membrane. Complexes I through IV, often called the electron transport chain, generate an electrochemical gradient across the inner membrane; a healthy mitochondrion thus has a strong negative membrane potential ($\Delta\psi m$). Complex V uses the energy of the electrochemical gradient to power the synthesis of ATP (2).

Mitochondria were originally thought to be much like ribosomes: individual, static organelles that were created, functioned through a defined lifespan, and were eliminated. However, more recent work has shown that mitochondria form a highly dynamic network throughout the cell (1). This network undergoes constant fission, fusion, and movement, processes referred to collectively as mitochondrial dynamics. Mitochondrial dynamics are regulated by specialized proteins within and outside the mitochondria, and the fission-fusion balance shifts with changes in cellular conditions, enabling the mitochondrial network to optimize its functioning for the current state of the cell (1).

NONAUTOPHAGIC FORMS OF MITOCHONDRIAL QC

As mentioned above, mitochondria are the primary source of reactive oxygen species in the cell. Mitochondria therefore have a large repertoire of mechanisms for preventing and removing damage. Mitochondrial damage can be prevented by neutralizing excessive reactive oxygen species, or by reducing biomolecules that have suffered oxidative damage. Mitochondrial superoxide dismutase (SOD2) converts highly reactive superoxide anion to hydrogen peroxide, which in turn is eliminated from mitochondria primarily by the glutathione redox system (5). The glutathione, periredoxin, and thioredoxin systems can also eliminate toxic oxidized molecules and remove some oxidative lesions, such as hydroperoxide groups (5). In addition, mitochondria have a system of resident proteases that can remove misfolded or damaged proteins. Lon protease in particular is known to target oxidatively damaged proteins (10). Intramitochondrial chaperones also buffer against the effects of oxidative stress by inhibiting aggregation of damaged, misfolded proteins (11). Even the ubiquitin-proteasome system, usually considered a mechanism for degradation of cytosolic proteins, can degrade some mitochondrial proteins, including inner membrane and matrix proteins (12-14). Furthermore, cycles of fission and fusion may "dilute" the impact of oxidized mitochondrial components, as damaged mitochondria fuse with healthy parts of the network (15). However, in some cases, all these mechanisms are insufficient to cope with damage, and the best course is to eliminate an entire mitochondrial unit. In this case, mitochondrial autophagy is necessary.

AUTOPHAGY

The term autophagy, or "self-eating," was coined by De Duve in 1963 to explain the presence of cellular components in lysosomes (16). It has since been defined as the lysosome-

dependent intracellular degradation of cytoplasmic components (17, 18). In some types of autophagy (chaperone-mediated autophagy, microautophagy), the cargo to be degraded enters the lysosome directly (18). However, the term "autophagy" without qualification usually refers to the most extensively studied type of autophagy, macroautophagy. In macroautophagy, a double-membraned structure is generated around the cargo. This structure, the autophagosome, then fuses with a lysosome (either directly or after fusion with an endosome), and lysosomal enzymes degrade the contents (19).

The basic machinery of macroautophagy, henceforward simply autophagy, was characterized using genetic screens in yeast (20). As of 2011, 35 components have been identified (21), most of them designated "ATG" (AuTophaGy-related) genes. Homologs of most essential autophagy machinery components have been identified in metazoans. These include proteins that control initiation of autophagy, such as Atg1 and Atg6 (Beclin); proteins involved in nucleation of the autophagosomal membrane, such as Atg9; and proteins involved in extension of the autophagosomal membrane, including Atg7, Atg8, and Atg12 (19, 21). More recently, a form of autophagy has been discovered that does not require some key components of the normal autophagic machinery, such as Atg5 and Atg7 (22). This type of autophagy, still poorly understood, has been designated "alternative autophagy," while autophagy dependent on Atg5 and Atg7 is now called "conventional" or "canonical" autophagy.

Autophagy occurs constitutively at a low level, and can be upregulated by multiple stimuli, especially nutrient deprivation (19). Starvation autophagy recycles amino acids and energy to maintain cellular function. Autophagy is frequently described as a nonselective or bulk degradation process in which random portions of cellular contents are engulfed and digested (19, 23). Bulk autophagy also contributes to the reshaping of tissues during development (24).

In recent years, multiple cargo-selective forms of autophagy have been noted. Organelles such as peroxisomes, ribosomes, the endoplasmic reticulum, and mitochondria have all been found to undergo targeted autophagy (25). Peroxisomes, for instance, are selectively eliminated when yeast are transferred to a less toxic environment (26), and selective ER autophagy regulates ER expansion during unfolded protein stress (27). Cytoplasmic protein aggregates (28) and extracellular pathogens (29) have also been identified as targets of cargo-selective autophagy. Selective autophagy of mitochondria was first described in yeast as a response to altered growth conditions (16). Since that time, multiple types of selective mitochondrial autophagy have been described.

MITOCHONDRIAL AUTOPHAGY (MITOPHAGY)

Before the word "autophagosome" was coined, electron micrographs showing mitochondria inside liver cell lysosomes had already been published (30). Over the decades since that time, abundant evidence of mitochondrial autophagy has accumulated, and several different types of mitochondrial autophagic turnover have been described. These are as follows:

1) Bulk (random) mitochondrial autophagy
2) Targeted mitochondrial autophagy in yeast
3) Nix/BNIP3-mediated mitochondrial autophagy
4) Damage-selective mitochondrial autophagy

I will discuss the first three types of mitochondrial autophagy very briefly, and focus on the last.

Bulk mitochondrial autophagy

Especially under nutrient deprivation conditions, mitochondria are found in autophagosomes along with cytosol and other organelles (30). This form of mitochondrial autophagy is considered random, although it has been suggested that autophagy spares mitochondria and other organelles in the early stages of nutrient deprivation (31).

Targeted mitochondrial autophagy in yeast

Cargo-selective mitochondrial autophagy in yeast has been demonstrated in response to nutrient deprivation and rapamycin, both classic autophagy-inducing stimuli, as well as the stressful environment of stationary phase growth (32). This targeted mitochondrial degradation has been suggested to require factors including the selective autophagy factor Atg11, the protein phosphatase homolog Aup1, and the outer mitochondrial membrane proteins Atg32 and Uth1 (32, 33). As this machinery lacks orthologs in higher eukaryotes, I will not discuss it further here.

Nix/BNIP3 mitochondrial autophagy

Nix (BNIP3L), a Bcl-2 family member with roles in both autophagy and apoptosis (34), has been linked to targeted mitochondrial autophagy. Nix resides on the outer mitochondrial membrane and is best known for promoting clearance of mitochondria during reticulocyte maturation (16, 35). This process appears to be accomplished primarily through alternative, rather than conventional, autophagy (16, 22). The action of Nix is mitochondria-specific; ablation of Nix does not interfere with the clearance of ribosomes, which are also eliminated during reticulocyte maturation (36). Nix promotes dissipation of the mitochondrial membrane potential (37), and this may be its primary role in reticulocyte mitochondrial clearance;

mitochondrial autophagy can be restored in $Nix^{-/-}$ reticulocytes by inducing depolarization with the uncoupler FCCP. However, Nix's mechanism of action remains somewhat controversial (34). BNIP3, a protein that shares > 50% sequence identity with Nix (38), has also been implicated in mitochondrial autophagy, especially autophagy induced by hypoxia (34).

SELECTIVE TURNOVER OF DAMAGED MITOCHONDRIA

De Duve speculated in 1966 that autophagy might be capable of "discriminating between normal and abnormal cellular constituents, and thus serving an important scavenging function" (39). More than thirty years passed, however, before published data first suggested that autophagy could at least distinguish between normal and abnormal mitochondria. In 1997, the Lemasters group observed that occasional individual mitochondria in hepatocytes spontaneously lost membrane potential, as observed by confocal FRET, and about two-thirds of these depolarized mitochondria colocalized with a lysosomal marker. The rate of spontaneous depolarization and apparent autophagy could be increased by nutrient deprivation (40). Lemasters theorized that this type of mitochondrial autophagy was triggered by opening of the mitochondrial permeability transition pore (41). The same group noted in 2001 that autophagosomes formed about 20 minutes after mitochondrial depolarization (42). Mitochondrial autophagy in response to depolarization was later also demonstrated in yeast (43).

Also in 2001, the Tolkovsky group observed that, if apoptosis was initiated and then inhibited in cultured rat sympathetic neurons, mitochondria disappeared within three days (44). Other organelles were unaffected. An inhibitor of lysosomal acidification prevented the disappearance of mitochondrial markers, suggesting that the disappearance was due to autophagy. Importantly, the investigators noted that neurons without mitochondria survived

considerably longer in an anaerobic chamber than did neurons with mitochondria; thus, the absence of mitochondria rendered neurons temporarily resilient to hypoxic insult.

In a 2005 review, Lemasters formally proposed that damaged mitochondria were selectively removed by autophagy, and coined the term "mitophagy" to describe the process. Two years later, his group demonstrated that individual mitochondria damaged by photoirradiation underwent rapid autophagy (45). A paper from the Shirihai group then demonstrated that mitochondrial dynamics played an important role in depolarization-induced mitophagy (46). The authors found that 89% of normal mitochondrial fission events in INS1 cells produced daughter mitochondria of unequal membrane potential. Slightly depolarized daughter mitochondria were less likely to re-fuse with the mitochondrial network and more likely to be degraded by autophagy. Furthermore, knockdown of fission factors or overexpression of a fusion factor decreased mitophagy.

By 2008, there was thus strong evidence that mitochondrial damage and decreased mitochondrial membrane potential could lead to mitophagy. However, the mechanism by which depolarization triggered mitophagy was still unknown. At this point, the Youle group published a paper that changed the direction of the mitophagy field (47). They demonstrated that Parkin was recruited to depolarized mitochondria, which then underwent autophagic turnover. Soon afterward, Youle and others demonstrated that PINK1 acted upstream of Parkin in this mitophagy pathway (8, 48). Within a remarkably short time, these proteins were widely accepted as essential mediators of selective autophagic mitochondrial degradation. I will now discuss PINK1, Parkin, and the current model of their functions in mitophagy.

PINK1 AND PARKIN

PINK1 (phosphatase and tensin homolog–induced putative kinase 1) and Parkin first became targets of scientific inquiry separately, but for a common reason: the genes encoding these proteins were identified as causes of autosomal recessive parkinsonism. The *parkin* gene (*PARK2*), encoding a cytosolic E3 ubiquitin ligase (49, 50), was identified in 1998 (7); *PINK1* (*PARK6*), encoding a mitochondrially targeted serine/threonine kinase, was linked to familial PD in 2004 (6).

During the first few years of research on Parkin, Parkin was not considered a regulator of mitochondrial biology, although a 2000 immunohistochemical study had revealed Parkin on the outer mitochondrial membrane in mouse brain (51). Investigators focused first on its potential role in preventing protein aggregate formation (52) and searched for critical substrates. Over the next several years, many remarkably diverse Parkin substrates were reported, implicating Parkin in regulation of processes including endoplasmic reticulum stress response (53, 54), protein synthesis (55, 56), neuronal apoptosis (57), nucleocytoplasmic transport (58), and microtubule stability (59). Several substrates with possible roles in neurotransmission and/or vesicle trafficking were also proposed, including septin family members CDCrel-1 and -2 (50, 60, 61), synaptotagmin XI (62), and a glycosylated form of α-synuclein (52).

By contrast, few PINK1 substrates were proposed before the protein became known as a mitophagy regulator. PINK1 was reported to phosphorylate the mitochondrial chaperone TRAP1 (63) and the serine protease HtrA2/Omi (64, 65), which has a role in apoptosis. In addition, an early report showed that PINK1 inhibited neuronal apoptosis by preventing mitochondrial cytochrome *c* release (66).

Connection to mitochondria

In 2003, the link between Parkin and mitochondria began to be elucidated. Darios et al. noted that Parkin protected against ceramide-stimulated apoptosis by delaying mitochondrial swelling and release of cytochrome *c* (67). Furthermore, they reported that Parkin was enriched in the mitochondrial fraction of mouse brain homogenate and was associated with the outer mitochondrial membrane. A month later, Greene and Whitworth described mitochondrial pathology in the newly created *Drosophila parkin* null mutant (68). The *parkin* null flies had shortened lifespans, male sterility, thoracic indentations associated with degeneration of indirect flight muscle, and impairment of flight and climbing. A 2005 followup paper demonstrated age-related progressive loss of dopaminergic neurons from the PPL1 cluster (protocerebral posterior lateral cluster 1), and showed that abnormal mitochondrial morphology was first detectable between 48 and 96 h after the initiation of the pupal stage. In addition, although *parkin* null mice did not demonstrate neurodegeneration (69), brain mitochondria from these mice were reported to have decreased respiratory capacity (70) and abnormal morphology (71).

The PINK1-Parkin pathway

In 2006, multiple groups reported that *PINK1* deletion in *Drosophila* caused the same phenotype as *parkin* mutations, including mitochondrial abnormalities (72-75). In addition, overexpression of Parkin rescued *PINK1* mutants, but overexpression of *PINK1* did not rescue *parkin* mutants. PINK1 was thus considered to operate upstream of Parkin in a pathway with effects on mitochondrial integrity. Understanding of the pathway advanced when Poole and Thomas (74) demonstrated that *PINK1* and *parkin* regulated mitochondrial morphology, either by promoting fission or by inhibiting fusion. Genetic manipulations that increased fission or

decreased fusion rescued *PINK1* and *parkin* mutant phenotypes, while manipulations that decreased fission severely enhanced those phenotypes. These results were confirmed by other groups in *Drosophila* (76, 77) and cultured rat neurons (78). In 2010, Poole and Thomas then demonstrated that the PINK1-Parkin pathway specifically inhibited fusion by promoting degradation of a mitochondrial fusion factor (79).

THE PINK1-PARKIN PATHWAY AND MITOPHAGY

As early as 2005, the Pallanck group proposed that Parkin might target individual mitochondria for degradation by autophagy, and in 2008, they suggested that Parkin's effect on mitochondrial dynamics might facilitate isolation and turnover of damaged mitochondrial units (74, 80). The Youle group, noting that mitochondrial fission had been linked both to autophagy and to mitochondrial integrity, tested this theory in 2008. Narendra et al. used the uncoupler CCCP, which abolishes mitochondrial membrane potential, to produce severe mitochondrial dysfunction (47). After CCCP treatment of cultured cells, Parkin underwent rapid translocation from cytosol to mitochondria. If the CCCP treatment continued for 24-48 h, autophagy-dependent clearance of mitochondria was observed. Experiments in Mfn1/2 KO cells, which have heterogeneous mitochondrial membrane potential, demonstrated that Parkin recruitment was selective for mitochondria with low membrane potential (47). These findings drew widespread notice, and multiple groups turned their attention to the PINK1-Parkin pathway. In 2010, Parkin recruitment and mitophagy after CCCP were shown to be dependent on PINK1 (8, 48). From this work, a model of PINK1-Parkin pathway regulation of mitophagy rapidly emerged. I will outline the model and then discuss findings associated with each step.

1. Mitochondrial depolarization leads to accumulation of PINK1 on the mitochondrial outer membrane.

2. PINK1 accumulation triggers recruitment of Parkin to mitochondria.

3. Parkin ubiquitinates proteins in the outer mitochondrial membrane.

4. The depolarized mitochondrion undergoes autophagic degradation.

Mitochondrial depolarization leads to PINK1 accumulation

In the absence of mitochondrial dysfunction, the level of PINK1 on the mitochondrial outer membrane (OM) is so low that endogenous PINK1 is difficult to detect by immunoblot (8). Two groups have demonstrated that PINK1 is constitutively expressed, but is rapidly imported into mitochondria, cleaved, and either released to the cytoplasm or degraded within the mitochondria (8, 81, 82). When a mitochondrion is depolarized, PINK1 ceases to be imported and processed. This may occur through failure of mitochondrial protein import, which requires a membrane potential (83), or because the cleaving protease is voltage dependent (8). In any case, PINK1 accumulates on the mitochondrial surface, most likely with its transmembrane domain across the OM and its kinase domain facing the cytoplasm (8, 84, 85).

PINK1 accumulation triggers recruitment of Parkin to mitochondria

After PINK1 accumulates on the depolarized mitochondrion, Parkin translocates to mitochondria from the cytosol. Although the mechanism of recruitment is not well understood, PD-associated mutations in various domains of the protein can block recruitment of Parkin (8). Also, PINK1 is required for the process; recruitment did not occur in *PINK1* null MEFs or in cells expressing shRNA to *PINK1* (8, 86). Conversely, PINK1 overexpression without

depolarization was sufficient to trigger both Parkin recruitment and mitophagy in cells coexpressing PINK1 and Parkin (8, 48). Ectopic PINK1 expression on peroxisomes or lysosomes also caused recruitment of Parkin to those organelles, and led to selective autophagy of peroxisomes (85).

Again, the manner in which PINK1 recruits Parkin, and interacts with Parkin, is still not clear. The recruitment of Parkin does depend on PINK1's kinase activity (8, 86). Some investigators have reported that PINK1 directly phosphorylates Parkin (87, 88), although one group failed to find evidence of phosphorylation *in vitro* (48) and another found no evidence of phosphorylation at two specific threonines (8). Very recently, there have been reports that PINK1 phosphorylates Parkin at Ser65 in Parkin's ubiquitin-like domain (89, 90). Other investigators have reported physical interaction of the two proteins (86, 91, 92), leading to consequences such as increased PINK1 levels (92) or protection of PINK1 from proteasomal degradation (91). PINK1 has also been reported to relieve constitutive inhibition of Parkin's ubiquitin ligase activity (81). In addition, PINK1 phosphorylates Parkin substrates, as in the case of Miro, and may enhance Parkin's ability to ubiquitinate these targets (93).

Parkin ubiquitinates proteins in the outer mitochondrial membrane

Once Parkin has been recruited, it ubiquitinates mitochondrial OM proteins. Known OM targets of Parkin include the anion channel VDAC1 (86, 94); the mitochondrial motor adaptor protein Miro (93, 95); the mitochondrial fusion factors Mitofusin 1 and 2 (96, 97); and the single fly mitofusin, Marf (79, 98). The glycolytic enzyme hexokinase I (HKI), which associates with the mitochondrial OM, has recently been added to the list (99). The function and downstream consequences of Parkin's activity at the mitochondrial OM are still being ascertained. However,

it appears that CCCP treatment leads to at least two different kinds of Parkin-mediated ubiquitination, with different functions: degradation of specific substrates, and possible tagging of the entire mitochondrion for mitophagy.

Substrates are generally targeted for proteasomal degradation through K48-linked polyubiquitination (100), and Parkin-dependent increases in K48 ubiquitination of mitochondria after CCCP treatment have been demonstrated (101). While Parkin has been reported to target multiple mitochondrial proteins for proteasomal degradation (95, 101, 102), the most definitive evidence for Parkin-mediated ubiquitination and proteasomal degradation of a substrate comes from studies of the mitofusins (79, 96-98). Degradation of Mfn1 and Mfn2 is proteasome dependent (97), and proteasomes translocate to CCCP-treated mitochondria (101, 102). Mitofusins may be particularly important targets, as they are required for re-fusion with the mitochondrial network; degrading mitofusins helps to isolate the mitochondrion in preparation for autophagy. However, as CCCP-induced mitophagy occurs in Mfn1/2 null cells, the absence of these fusion factors cannot be the sole requirement for mitophagy (47). It has also been proposed that widespread proteasomal degradation of mitochondrial substrates must take place before mitophagy can occur. Parkin-dependent degradation of multiple mitochondrial substrates after CCCP has been reported by two separate groups (101, 102). One group found that this process was a necessary prerequisite for mitophagy (101), while the other found that mitophagy proceeded even when the proteasome was inhibited (102).

Parkin also performs ubiquitination of mitochondrial targets that is not intended to cause proteasomal degradation, including K63-linked ubiquitination. K63-linked ubiquitin chains are known to recruit autophagy adaptor proteins such as p62 and HDAC6 (103, 104). Geisler and colleagues (86) noted both K63- and K27-linked polyubiquitin chains colocalizing with Parkin

and mitochondria after CCCP treatment. In particular, they noted that VDAC1 underwent K27-linked ubiquitination, and found that the presence of VDAC1 was necessary for mitophagy. Unspecified polyubiquitination (105) and K63-linked ubiquitination (94) have been reported by other groups as well, and K63 ubiquitination of mitochondria has been proposed as a trigger for mitophagy. A particular mutant form of Parkin (R275W) that is defective in promoting mitophagy has a decreased ability to perform K63 ubiquitination of mitochondria (94). The same paper, however, found that the mere presence of ubiquitin on the mitochondrial surface was insufficient to trigger mitophagy. A drug-inducible fusion protein system was used to recruit a protein tagged with mutant ubiquitin (UbG76V) to mitochondrial membrane anchors. While the mitochondria recruited p62, they did not undergo mitophagy. This experiment does not, however, constitute a conclusive test of mitochondrial surface ubiquitination as a mitophagy signal. Specific ubiquitin linkages, or ubiquitination of native mitochondrial proteins, could be required to trigger mitophagy.

The depolarized mitochondrion undergoes autophagic degradation

The final stage of mitochondrial turnover via the PINK1-Parkin pathway is autophagic degradation of the isolated mitochondrial unit. This process requires conventional autophagy and is almost completely blocked in *Atg5*$^{-/-}$ and *Atg7*$^{-/-}$ MEFs (47, 81). The final signals that trigger autophagic engulfment of a mitochondrion after Parkin recruitment, however, remain unclear. The mere presence of Parkin is not sufficient to trigger mitophagy; R275W mutant Parkin is recruited to mitochondria almost normally, but cannot promote mitophagy (8). As mentioned above, absence of mitofusins is necessary but not sufficient for mitophagy (97). Ubiquitination of VDAC, which has been proposed as necessary for mitophagy (86), also does not appear to be

an essential trigger, as mitophagy occurs normally in VDAC1/3$^{-/-}$ MEFs (94). Evidence is mixed for the autophagy adaptor protein p62, which binds both K63-linked ubiquitin and LC3 (104, 106). At least three reports have found p62 essential for Parkin-dependent mitophagy (37, 86, 105), but other groups report that mitophagy can proceed without p62 (94, 107). A single report gives evidence that another autophagy adaptor protein, HDAC6, is required for mitophagy (105). It remains possible that a sufficient quantity of K63-linked (and/or K27-linked) ubiquitin on mitochondrial OM proteins is the trigger for mitophagy.

LIMITATIONS OF THE CURRENT MITOPHAGY MODEL

Although there is substantial support for the role of the PINK1-Parkin pathway in selective mitochondrial degradation, it is still not clear that this pathway promotes mitochondrial degradation *in vivo*. While there is substantial evidence that mitochondrial dysfunction can lead to Parkin recruitment, there is much less evidence that it leads to actual mitophagy. In discussing the limitations of the model, therefore, I will focus primarily on studies demonstrating mitophagy.

1. The model is based on *in vitro* data.

First and foremost, PINK1/Parkin-dependent mitophagy has been demonstrated exclusively in cultured cells. In addition to other obvious differences from cells *in vivo*, cells in culture rely more heavily on glycolysis (108), and their relative lack of dependence on respiration may affect their readiness to eliminate mitochondria.

2. The few *in vivo* studies have not clearly demonstrated PINK1/Parkin-dependent mitophagy.

There are dozens or scores of studies *in vitro*, but only five *in vivo*, to the best of my knowledge. While some of the *in vivo* studies are highly suggestive, none conclusively documents the occurrence of mitophagy driven by the PINK1-Parkin pathway. The studies examining neuronal mitochondria *in vivo* reported no Parkin recruitment to dopaminergic neuron mitochondria in two different mouse models of mitochondrial dysfunction and neurodegeneration (109, 110). Two studies attempted to characterize Parkin-mediated mitophagy after cardiac ischemia in rodents. Huang et al. (111) demonstrated translocation of endogenous Parkin and p62 to rat heart mitochondria after three brief bouts of ischemia, and showed that *parkin* null mice did not obtain the normal benefit from ischemic preconditioning. Kubli et al. (112) noted the appearance of autophagosomes in the border zone of the infarcted area in wild-type (WT) mice, while the border zone in *parkin* null mice contained no autophagosomes and instead contained swollen, abnormal mitochondria. Unfortunately, this very interesting finding was reported in a qualitative manner, and no comparison of mitochondrial mass or area was performed.

The fifth *in vivo* study examined skeletal muscle of mice with severe mitochondrial abnormalities due to defective phospholipid biosynthesis (113). The investigators found increased levels of PINK1, Parkin, p62, polyubiquitin, LC3-I, and LC3-II in isolated muscle mitochondria, but, as in the Kubli study, gave only a qualitative report of mitophagy. There was also no difference in total mitochondrial area between mutants and littermates, and it is not clear that mitochondria were being degraded.

3. The model is based largely on data involving overexpressed Parkin.

While Parkin recruitment has been documented using endogenous Parkin, actual PINK1/Parkin-dependent mitophagy has been documented primarily in the presence of overexpressed Parkin (114), which may not behave identically to the endogenous protein (115). CCCP-induced mitophagy, as measured by a decrease in total mitochondrial mass using MitoTracker Green, has twice been reported without overexpression of Parkin (8, 116), but a recent study in human primary fibroblasts and iPS-derived neurons found no mitophagy with endogenous levels of Parkin (117).

4. There is a lack of evidence for mitophagy in cultured neurons.

Although the findings on mitophagy are interpreted as a model of neurodegenerative disease, mitophagy has not yet been demonstrated in cultured neurons. Studies to date have discussed Parkin recruitment alone. Two groups saw rapid recruitment of Parkin to neurons in culture after treatment with CCCP (48) or antimycin A (93). A third group saw recruitment, but over a much longer timeframe than in other cell types (118), and yet another study reported no Parkin recruitment whatsoever (119). This last study noted that even in culture, neurons, unlike most cell types, are dependent on mitochondrial respiration. They found that HeLa cells forced to rely on respiration did not recruit Parkin.

5. The model simulates acute crisis, not ongoing quality control.

Actual PINK1/Parkin-dependent mitophagy, as opposed to recruitment of Parkin, has been documented primarily after the acute application of mitochondrial toxins, such as CCCP

and paraquat (35). One study documented mitophagy after a more naturalistic stimulus, simulated ischemia in cardiomyocytes, but this still represents an extreme, acute stressor (111).

More generally, the studies clearly demonstrating PINK1/Parkin-dependent mitophagy depict the cellular response to sudden, catastrophic mitochondrial dysfunction, rather than the response to gradual accumulation of damage. The treated cells undergo rapid and widespread mitochondrial degradation, with many cells eliminating all mitochondria within 24 h (47). Such an extreme response may well be beneficial in the context of ischemia-reperfusion, but would be harmful under most conditions, and it may not occur through the same processes involved in ongoing mitochondrial quality control. Because PINK1-Parkin pathway dysfunction is implicated in aging and in slowly progressive diseases, it is necessary to study the mechanisms of mitochondrial turnover under nonstressed physiological conditions. This was the task I undertook for my graduate work.

I performed my studies using the fruit fly *Drosophila melanogaster*. As mentioned above, the role of the PINK1-Parkin pathway in mitochondrial morphology and integrity was first elucidated using *Drosophila*. Genetic manipulation can be easily and quickly performed in this organism. Furthermore, *PINK1* and *parkin* mutant flies have robust phenotypes and experience DA neuron loss, which is not the case for the corresponding mouse mutants (69). I therefore set out to determine whether *PINK1* and/or *parkin* mutations affected the rate of mitochondrial turnover.

MEASUREMENT OF MITOCHONDRIAL TURNOVER

While there are no data on mitochondrial turnover in *Drosophila*, measurement of mitochondrial "half-lives" in mammals dates back to 1961. I will briefly outline some of the early findings.

Most studies of mitochondrial turnover were published in the 1960s through the 1980s. At that time, it was not yet known that mitochondria constantly merged and redistributed their contents through cycles of fusion and fission. Mitochondria were considered individual organelles with defined lifespans, and investigators performed radioactive pulse-chase experiments to measure those lifespans. The basic method involved administering oral or injected radiolabel and sacrificing the animals (nearly always rats) at various time points after administration. After purifying mitochondria from the tissue of interest, the experimenters extracted mitochondrial proteins, lipids, and/or DNA, and measured the radioactivity remaining. Plotting the exponential decay of radioactivity over time yielded a half-life value. While the results varied with the component studied, the radiolabel used, and other parameters, some basic facts emerged. Mitochondrial half-lives were at least several days long, but varied considerably across tissues. In particular, mitochondrial half-lives were strikingly long in brain—about three times the half-lives in liver. Table 1.1 presents results for different rat tissues from several mitochondrial turnover studies.

Aside from determining half-lives, the early mitochondrial turnover studies sought to learn whether or not mitochondrial turnover was unitary. In other words, did all mitochondrial components (lipids, DNA, proteins) turn over together, or was turnover piecemeal? The first study of mitochondrial turnover in an adult organism, reported by Fletcher and Sanadi in 1961, measured half-lives of cytochrome *c*, insoluble protein, soluble protein, and lipids in

Table 1.1. Mitochondrial half-lives for various tissues in rat.

Study	**Menzies & Gold (1971) (120)**	**Beattie et al. (1967) (121)**	**Swick et al. (1968) (122)**	**Gross et al. (1969) (123)**	**Aschenbrenner et al. (1970) (124)**		**Rajwade et al. (1975) (125)**	***mean***
Component	protein	whole mitochondria	protein	mitochondrial DNA	protein		protein	
Label(s)	^{3}H-leucine	^{14}C-leucine	^{14}C-$CaCO_2$	^{3}H-thymine deoxy-ribonucleoside	$^{3}H_2$-leucine	guanido-^{14}C-arginine	^{14}C-leucine	
brain	24.4	26.3		31			19.5	**27.2**
kidney	6.0	8.7		10.4	6.1	6.2	8.6	**8.4**
heart	17.5			6.7				**10.1**
liver	9.3	8.4	~4-6	9.4	7.0	5.0		**7.6**
lung	16.6							
small intestine	17.6							
testis	12.6							

mitochondria from rat liver (126). The authors found half-lives for all four components within a narrow range (9.7 to 10.6 d), and reported that mitochondria therefore appeared to be "turning over as an entity." This finding had a profound impact on all future studies of mitochondrial turnover. The appearance in 1962 of photographs showing whole mitochondria in lysosomes (30) reinforced the idea by providing an obvious mechanism for unitary mitochondrial turnover.

Subsequent studies, therefore, tested the assumption that mitochondria turned over as units. Evidence against completely unitary turnover rapidly accumulated (e.g., (122, 127, 128)). For instance, Bailey et al. (129) found that dietary manipulation altered the half-life of mitochondrial phospholipids without changing the half-life of mitochondrial protein. They also noted that mitochondrial phospholipids and mitochondrial soluble protein each showed at least two separate decay components. They remarked, "It seems likely that, if the groups of proteins measured were separated into their individual components, then these would also be found to turn over at different rates."

By the late 1960s, after the publication of studies that measured turnover of individual mitochondrial compartments, many authors adopted a modified view. They suggested that the inner membrane and matrix turned over as a unit, but that the outer membrane turned over separately and somewhat more quickly (summarized in (120)). It is interesting to note that even authors professing this view frequently reported findings such as multiple-component decay curves for mitochondria in a nonproliferating tissue, or different half-lives for mitochondrial DNA and phospholipids (120, 123). Nevertheless, the model of unitary inner membrane/matrix turnover was still predominant in 1982, when Lipsky and Pedersen reported half-lives in liver mitochondria of 3.3 d and 4 d for the outer membrane and inner membrane/matrix respectively (130).

In that same year, Hare and Hodges provided striking *in vitro* evidence for nonunitary turnover. Using cultured hepatoma cells, they demonstrated heterogeneous degradation rates not only for mitochondrial matrix polypeptides, but for different peptides of individual respiratory complexes (131, 132). Despite such findings, and despite the discovery of mitochondrial resident proteases (133), the unitary turnover model gained ground. By 2008, the outer membrane vs. inner membrane/matrix turnover distinction seemed largely forgotten. Review-article statements such as "Mitochondria are degraded through autophagy" (134) expressed a common attitude, along with passing acknowledgments that "at least some mitochondrial protein turnover" is mediated by proteases (135). And, of course, the PINK1/Parkin model of mitophagy rests on the assumption that unitary (autophagic) turnover is critical to mitochondrial quality control. Thus, to test the model thoroughly, it was desirable to determine the extent to which mitochondria do turn over as units.

In 2008, Dr. Pallanck and Dr. Michael MacCoss conceived an approach to turnover measurement that permitted me both to investigate the question of unitary turnover and to test the effects of *PINK1* and *parkin* mutations on mitochondrial turnover. They proposed to measure mitochondrial protein turnover via stable isotope labeling and shotgun proteomics. Publications using this concept to measure general protein turnover (136) and mitochondrial protein turnover (137) in mice have since appeared. I will discuss the development of our own stable isotope labeling assay in the next chapter.

Chapter 2: Development and validation of a mitochondrial protein turnover assay

ASSAY DEVELOPMENT

As mentioned in the previous chapter, the Pallanck and MacCoss laboratories developed a method of measuring mitochondrial turnover *in vivo*, using stable isotope labeling of protein followed by mass spectrometry. This method has several advantages over the two main alternatives, which were radiolabeling and inducible overexpression of fluorescent mitochondrial proteins. The stable isotope labeling assay produces more accurate half-life values than radiolabeling (see below) and provides information on multiple individual proteins simultaneously. It measures half-lives of native, untagged mitochondrial components, and it does not depend on obtaining pure mitochondrial fractions.

Although stable isotope labeling had not been previously used in flies to measure protein turnover, it had been performed successfully in *Drosophila* (138), and Geoff Findlay of Genome Sciences kindly shared his labeling technique. Dr. MacCoss suggested [5,5,5 – $^{2}H_{3}$]-leucine, or D3-leucine, as a label. Leucine is an essential amino acid that occurs frequently in protein and is efficiently incorporated; 75% to 80% of leucine in blood enters the intracellular amino acid pool, compared to 58% for methionine (139, 140).

Process overview

Full technical details are described in Materials and Methods. Briefly, I fed adult flies D3-leucine-labeled yeast for 120 h or 240 h, and used mass spectrometry to monitor the rates at which unlabeled proteins were degraded and replaced by labeled proteins. To reduce sample

complexity and enrich for neural tissue, as well as to avoid the degenerating tissue in *PINK1* and *parkin* mutant thoraces, I performed all experiments on homogenates from adult heads. I fed one-day-old flies yeast paste fully labeled with D3-leucine. At each labeling time point, I prepared postnuclear protein homogenates from heads and subjected the homogenates to trypsin digestion, mass spectrometry, and half-life analysis (Fig. 2.1). All mass spectrometry experiments were performed by Gennifer Merrihew of the MacCoss Lab.

Pilot experiments and establishment of time points

In my earliest experiments, I labeled larvae and measured the decline of D3-leucine over time in adults given unlabeled food. Newly eclosed adults were completely labeled (median precursor enrichment 100%). However, I soon realized that it would be equally effective, and much simpler, to label adults and track the accumulation of D3-leucine over time. In this method, either D3-leucine or unlabeled leucine can be regarded as "label"; turnover measurements are always based on the ratio of D3-leucine to total leucine (see below). Tracking the accumulation of D3-leucine in adults offered another advantage: I could omit a zero time point, as there was obviously no D3-leucine present in the flies until I began feeding it to them. This omission allowed us to conserve our limited mass spectrometer time.

Another concern addressed in my pilot experiments was the question of whether I could detect an adequate number of mitochondrial proteins without creating mitochondria-enriched fractions. I found that I reliably detected substantial numbers of mitochondrial proteins in simple postnuclear homogenates, and that mitochondrial proteins made up a surprisingly large percentage of all proteins detected. The four main datasets analyzed in my dissertation work contained 106 to 170 mitochondrial proteins (27% to 34% of all proteins detected). If flies have a

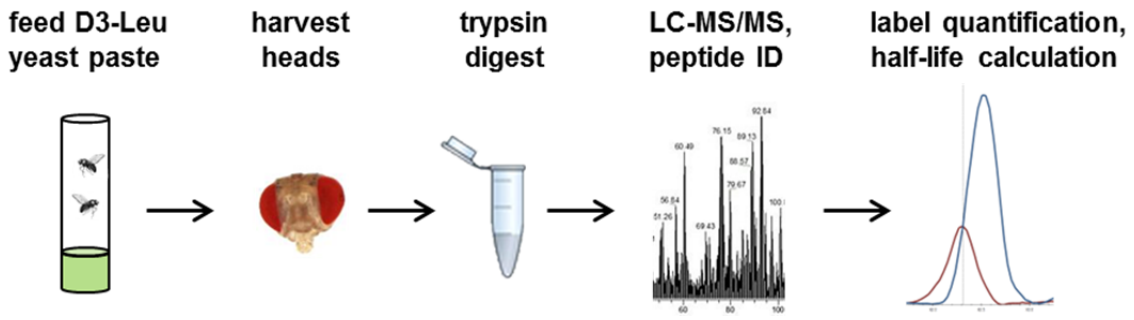

Figure 2.1. Basic assay workflow.

total number of mitochondrial proteins somewhere between the 1000 predicted for yeast (141) and the 1500 predicted for mammals (142), I was able to detect 7%-17% of all mitochondrial proteins without enriching for mitochondria. I therefore performed all experiments using postnuclear homogenates, a strategy that decreased the number of flies required and allowed me to compare mitochondrial and nonmitochondrial proteins in the same sample.

As I had no information on fly mitochondrial protein turnover, I determined labeling periods empirically. I initially tried time points as short as 24 h, but found that periods of 120 and 240 h (5 and 10 d) provided an adequate level of labeling for most mitochondrial proteins.

Determination of half-lives (Topograph)

The greatest challenge of this method was analyzing the data obtained. When I began my experiments, the software for computing half-lives from stable isotope labeling data was in the early stages of development. Over the course of my project, Nick Shulman of the MacCoss Lab developed Topograph, software that computed both half-life and total protein abundance from stable isotope labeling mass spectrometry data.

A substantial advantage of Topograph is its ability to compute precursor enrichment, which allows it to compensate for a major source of error: incomplete labeling of the amino acid precursor pool. Traditional radiolabeling calculations presume that a label, such as a radioactive amino acid, is eliminated from the body when a protein is degraded. However, amino acids from degraded proteins often return to the "precursor pool" from which new peptides are synthesized (143, 144). This causes problems for turnover measurement in two ways. First, reutilization of labeled amino acids causes them to remain in the body after a labeled protein has been degraded. Second, unlabeled as well as labeled amino acids are incorporated into the protein made during a

labeling period. Some of these unlabeled amino acids come from breakdown of existing proteins; others are part of the precursor pool at the time labeling begins. Especially if the label is administered in food, the precursor pool is not instantly saturated, and new protein continues to incorporate a percentage of unlabeled amino acids. The net result is substantial inaccuracy in calculated half-lives. Topograph calculates the percentage enrichment of the precursor pool, as described below, and thus avoids artifacts from incomplete precursor pool labeling.

The software has been described fully elsewhere (145), and I will give only a brief, qualitative overview here. For each peptide, Topograph uses MS1 data to quantify the amount of the peptide that is fully labeled, partially labeled, and unlabeled. A peptide with three leucines would have forms with 0, 1, 2, and 3 D3-leucines, and each D3-leucine adds 3 units to the peptide's mass. However, peptides also normally have multiple mass forms due to the natural occurrence of "heavy" isotopes, and the mass signal from the tracer is superimposed on this normal mass distribution. Topograph deconvolutes the complex distribution and determines the signal intensity for each form, or isotopolog, of the peptide. Topograph then plots signal intensity against elution time, resulting in a separate chromatographic peak for each isotopolog, and measures the abundance of each isotopolog as area under the curve. The ratio of labeled peptide abundance to total peptide abundance is then reported as "percent D3-leucine."

At this point, Topograph calculates precursor enrichment, using an algorithm based on the distribution of partial labeling in multi-leucine peptides. The median precursor enrichment is used to correct all percent D3-leucine values, and the resulting corrected values are designated "percent newly synthesized." To calculate protein half-life, Topograph subtracts percent newly synthesized values from 100%, $\log_2$-transforms the resulting values, and creates a plot vs. time using all data points for peptides derived from that protein. The program fits a line to the data,

assuming first-order exponential decay, and the slope of the line is the rate constant for synthesis of new protein.

The fact that Topograph calculates "percent newly synthesized" and calculates a rate constant for synthesis, rather than degradation, highlights a key issue for users of the program. Topograph half-life computations assume that protein synthesis rate equals degradation rate, and therefore that protein abundance remains constant throughout the experiment. If protein abundance increases or decreases significantly during the labeling period, the rate of protein degradation may be overestimated or underestimated. Adult *Drosophila* heads are composed entirely of postmitotic cells (146), and I chose to accept the assumption of constant protein abundance when computing WT half-lives for assay validation. When comparing half-lives across genotypes, however, I tested for abundance change artifacts. This procedure will be described in Chapter 3.

Experimental validation of precursor pool enrichment algorithm

As mentioned above, the most significant advance of Topograph was its built-in, label-independent estimation of precursor enrichment. Adjustment for precursor enrichment had dramatic effects on computed protein half-lives. For example, galactokinase had an unadjusted half-life of 99.4 h in the *parkin* control group. After correction for precursor enrichment, the half-life was 48.0 h. Given the major impact of this algorithm on the results, I felt it essential to test the algorithm's accuracy in determining precursor enrichment.

For this test, I created samples with known precursor enrichment by growing yeast to saturation in incompletely labeled growth medium (33.3% or 66.7% D3-leucine). After lysate preparation, trypsin digestion, and mass spectrometry by Gennifer Merrihew, the data were

analyzed using Topograph's precursor enrichment function. Figure 2.2 shows histograms of precursor enrichment values from the two samples. The mean calculated enrichments, using the insoluble fraction of the samples, were 32.7±8.3% and 67.5±6.1% respectively. Similar results were obtained using the soluble fraction (32.1±8.5% and 65.6±6.2%). Thus, the algorithm was capable of accurate estimates of precursor enrichment.

Filtering for high-confidence data

I developed a set of standards and cutoffs to ensure that I analyzed only high-confidence data. Automated peak detection is challenging at best, and my complex, unfractionated samples posed additional difficulty. During Topograph's early stages of development, I frequently checked its accuracy by inspecting raw signal vs. time plots for individual peptide replicates. A substantial minority of the time, Topograph misidentified peaks or used incorrect start and end points. I noted that apparent outliers in the data for a peptide or protein were most frequently the result of such "missed calls," or of poor signal-to-noise ratio. I therefore developed the set of data filtering standards described in Materials and Methods. These standards were purely empirically based, but were designed to be automated, reproducible, and conservative.

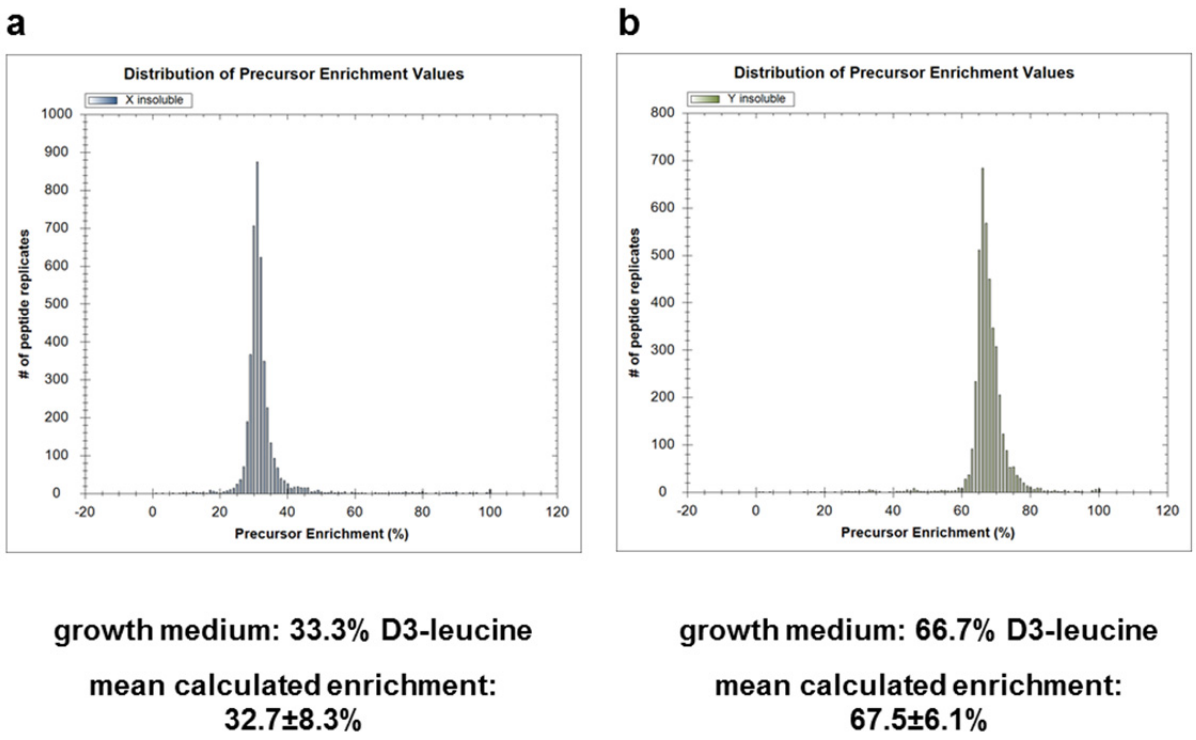

Figure 2.2. Experimental validation of precursor pool algorithm. Histograms of precursor enrichment values for peptides containing ≥ 2 leucines. (Enrichment could not be calculated for peptides with only one leucine.) An enrichment value was calculated for each replicate of each peptide, and the *y*-axis indicates the total number of occurrences of a given enrichment value. Insoluble fraction histograms are shown; soluble fraction findings were comparable. **(a)** Enrichment values for yeast grown in 33.3% D3-leucine medium. **(b)** Enrichment values for yeast grown in 66.7% D3-leucine medium.

Protein annotation

Because I did not fractionate my samples, determining the previously documented localization of each protein was the only way to differentiate mitochondrial from nonmitochondrial proteins. Unfortunately, little information on localization is available for many fly proteins. This was especially true when I began my project; lists of vertebrate orthologs had not yet been added to FlyBase at that time.

Initially, I adopted a conservative strategy and based localization primarily on information available in the main FlyBase screen for a protein, linkouts to UniProt, and the MitoDrome database (147). To minimize confounds from multiple localization, I excluded from analysis any mitochondrial protein that appeared to have a significant degree of nonmitochondrial localization. However, toward the end of the project I found this method inadequate. Too many proteins had to be listed as "localization unknown." In addition, FlyBase, like any large resource, contains errors, and many of the localization terms listed are based solely on uncurated electronic annotation. I also found, upon more thorough investigation, that many proteins regarded as exclusively mitochondrial had some degree of nonmitochondrial localization as well.

I therefore adopted a new approach and created a manually curated database of protein localization information. Starting from the FlyBase record, I drew on a variety of databases and consulted primary literature where available and feasible. I also used a suite of computational localization predictors, which were especially valuable for the many proteins with little or no information available in FlyBase. See Materials and Methods for a more detailed description of my procedures.

FINDINGS

For initial validation of the assay, I analyzed protein half-lives in heads from wild-type (WT) flies with three different genetic backgrounds. Proteins detected in any of the three genotypes were compiled into a composite WT dataset. For the proteins detected in more than one genotype (59% of the total), half-life values were averaged. Of the 524 proteins that met all data filtering criteria, 160 were exclusively or primarily mitochondrial (31%). The distribution of localizations is shown in Figure 2.3. As noted above, I was using postnuclear homogenates, so the small percentage of nuclear proteins detected is not surprising. On the other hand, I detected fewer proteins than I expected from organelles such as the endoplasmic reticulum (17), the Golgi apparatus (0), and the lysosome (6). Especially in the case of the lysosome, the low detection rate for these proteins may be partly due to lack of published information on fly homologs.

The proteins detected exhibited an extensive range of half-lives, and mitochondrial proteins were generally longer-lived than nonmitochondrial proteins (Fig. 2.4). The broad range of mitochondrial protein half-lives is consistent with the fact that mitochondrial protein turnover occurs through mitochondrial proteases and the ubiquitin-proteasome system as well as through autophagy, as discussed in Chapter 1.

An incidental finding of interest was that ribosomal proteins appeared to be turned over primarily as intact 60S and 40S (large and small) subunits. The mean half-life of the large ribosomal subunit was 191.9±16.8 h, with a coefficient of variation (CV) of 0.09. The small subunit had a slightly longer mean half-life of 208.0±26.7 h (CV 0.13), and the subunit means differed significantly by *t* test ($p = 0.018$; $n = 25$ and 19 proteins respectively). This finding is consistent with autophagic turnover of whole ribosomal subunits, as described in yeast (148). However, the endoplasmic reticulum, also a known target of autophagy (27), had remarkably

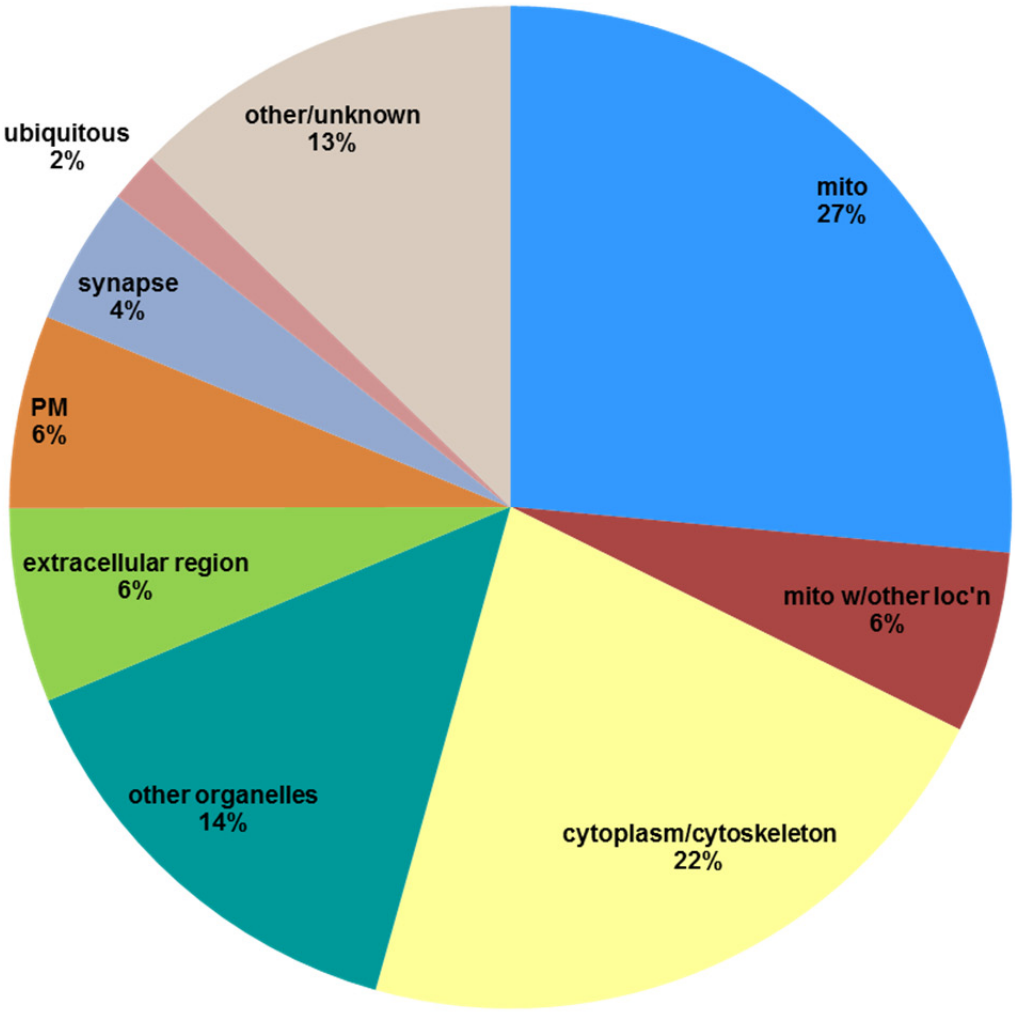

Figure 2.3. Localization of proteins detected in WT fly heads. Composite data from three WT genotypes (n = 524). The "mito" category refers to exclusively mitochondrial proteins (M), and "mito with other loc'n" refers to mitochondrial proteins with significant secondary localization (M/N; see Materials and Methods). The "other organelles" category includes proteins from ER, ribosome, lysosome, and nucleus. "Ubiquitous" proteins have multiple diverse localizations, with none clearly primary.

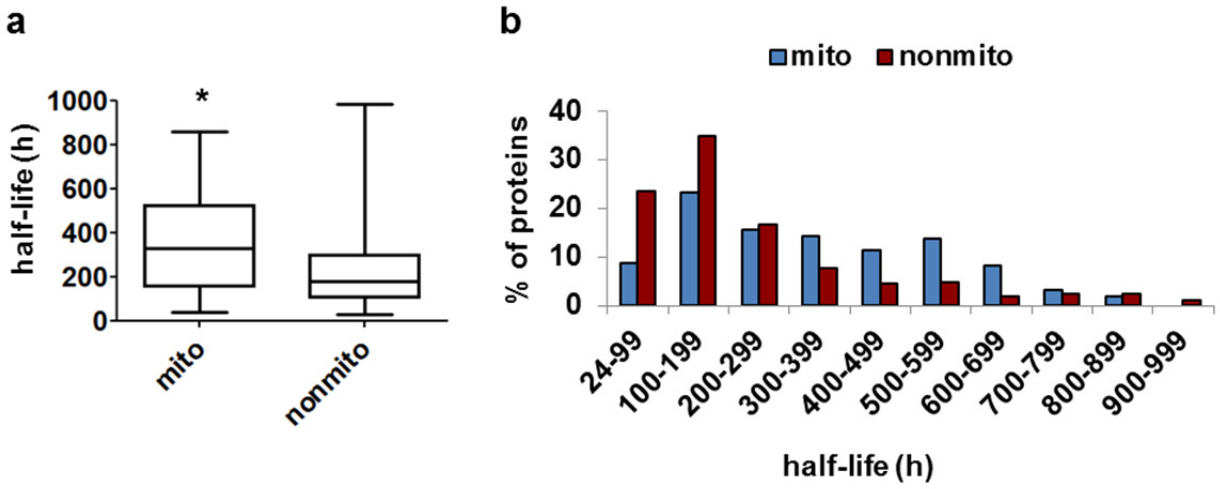

Figure 2.4. Half-lives of *Drosophila* mitochondrial proteins are diverse and tend to be longer than half-lives of nonmitochondrial proteins. (a) Mean half-life in hours of mitochondrial and nonmitochondrial proteins (n = 160 mito, 364 nonmito). Box plots depict the median and the upper and lower quartiles; whiskers represent extreme values. *p = 2.68 x 10^{-7} by Student t test **(b)** Histogram of half-lives for mitochondrial (blue) and nonmitochondrial (red) proteins.

diverse protein half-lives. The mean ER protein half-life was 178.4±217.2 h, for a CV of 1.22. For comparison, the CV for mitochondria was 0.59. Even excluding the three longest-lived ER proteins left the ER with a CV of 0.44. It is possible that some of this variability may be caused by secondary localization of the proteins, but it likely also reflects multiple mechanisms of ER turnover.

Validation

Validating my half-life results was not possible in the classic sense, as I had no gold standard for fly protein half-lives. However, I was able to demonstrate that the measured half-lives were consistent. Analysis of the proteins present in all three WT genotypes revealed that half-life values were highly reproducible, with surprisingly low sensitivity to genetic background (Fig. 2.5a,b).

As another form of indirect validation, I also compared my data to half-lives measured with a related stable isotope labeling technique in mouse brain (136). Half-lives of proteins from fly heads correlated strongly with half-lives of homologous proteins in mouse brain (Fig. 2.5c). This analysis was done using mouse data from Price et al. (136), and my data are also in good agreement with a more recent mouse study, which focused exclusively on turnover of mitochondrial proteins (137). The half-life correlation was especially strong for mitochondrial proteins (Fig. 2.5d). While mitochondrial protein half-lives in fly head were generally shorter than in mouse brain (mean fly/mouse half-life ratio 0.69±0.26), this difference may be explained at least in part by the presence of non-brain tissues in the fly samples; as noted in Chapter 1, mitochondrial half-lives tend to be longer in brain than in other tissues. Nonmitochondrial proteins, by contrast, did not generally have shorter half-lives in fly head than in mouse

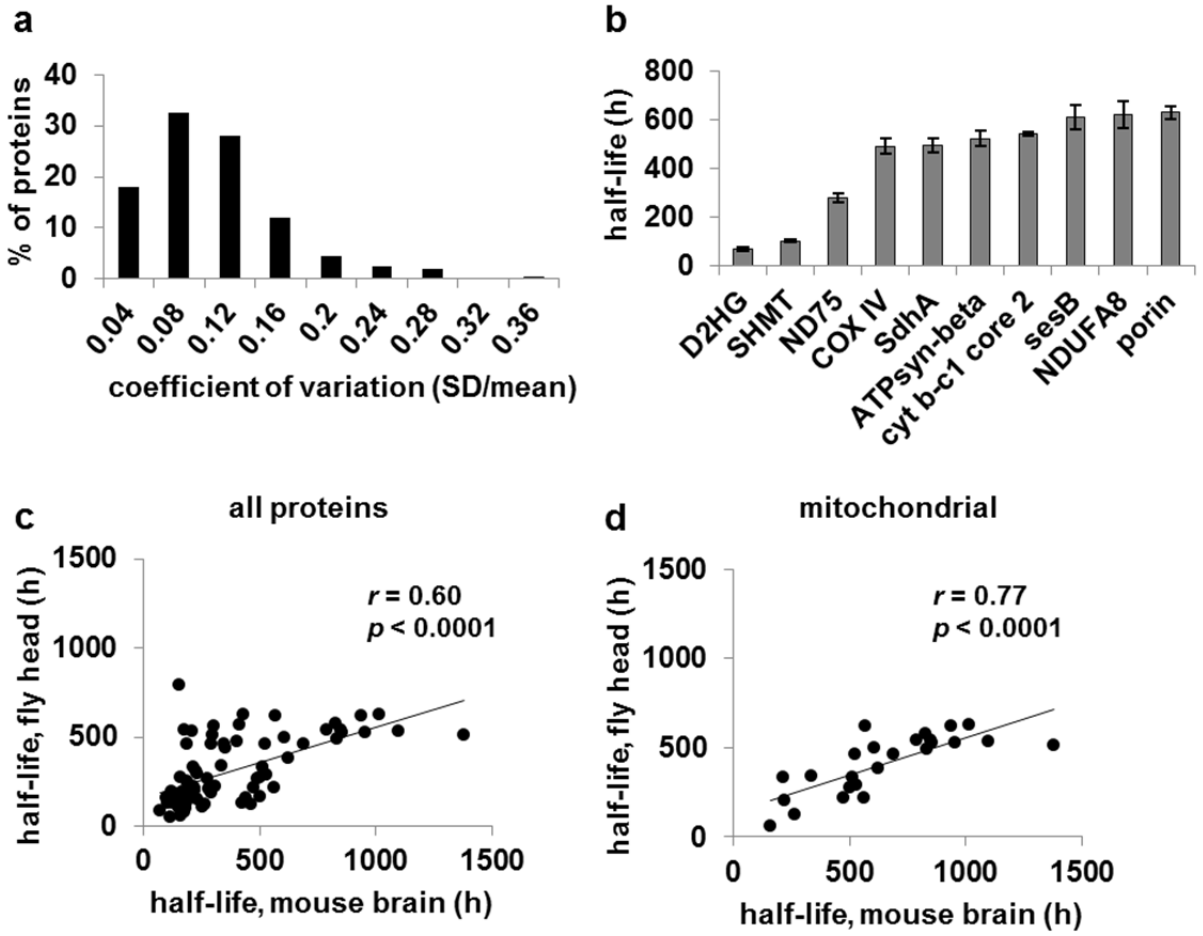

Figure 2.5. Protein half-lives are reproducible across fly genotypes and are evolutionarily conserved. (a) Histogram of the coefficients of variation for the half-lives of proteins (n = 201) detected in flies with three different WT genetic backgrounds. **(b)** The mean half-lives (±SD) of 10 representative *Drosophila* mitochondrial proteins from the analysis in **(a)**. D2HG = D2-hydroxyglutarate dehydrogenase; SHMT = serine hydroxymethyltransferase; ND75 = NADH:ubiquinone reductase 75kD subunit precursor; COX IV = cytochrome C oxidase polypeptide IV; SdhA = succinate dehydrogenase A; ATPsyn-beta = ATP synthase beta subunit; cyt b-1 core 2 = cytochrome *b-c1* complex core protein 2; sesB = stress-sensitive B; NDUFA8 = NADH dehydrogenase (ubiquinone) 1 alpha subcomplex, 8. **(c)** Half-lives of proteins in fly heads vs. their orthologs in mouse brain. All WT fly proteins with orthologs in the data of Price et al. (see text) were included (n = 75). **(d)** Half-lives of mitochondrial proteins in fly heads vs. their orthologs in mouse brain (n = 25).

brain (mean fly/mouse half-life ratio 1.17±0.82). Thus, despite the very different lifespans of flies and mice, protein half-lives showed a surprising degree of evolutionary conservation.

The new assay appeared to be capable of measuring mitochondrial protein half-lives as designed. I therefore applied it to my main experimental question, which will be described in Chapter 3.

MATERIALS AND METHODS

Drosophila strains and culture

Fly stocks were maintained on standard cornmeal-molasses food at 25°C. The wild-type flies used were three groups with intentionally diverse genetic backgrounds: w^{1118}, $PINK1^{rv}$, and *CyOActGFP/+*. Half-lives were measured separately for each group. The $PINK1^{rv}$ allele has been previously described (73). Other strains and alleles were obtained from the Bloomington Stock Center (Bloomington, IN).

In vivo stable isotope labeling of flies

[5,5,5 – $^2H_3$]-leucine (D3-leucine; 99 atom % deuterium) was obtained from Isotec/Sigma-Aldrich (St. Louis, MO). Synthetic complete medium without leucine (C-Leu) was supplemented with glucose and 60 mg/L D3-leucine. A strain of *S. cerevisiae* auxotrophic for leucine (BB14-3A, Brewer Lab, University of Washington (149)) was grown to saturation at 30°, and then spun down, flash-frozen in liquid nitrogen, lyophilized, and stored at -80°C until needed. Groups of 10-50 male flies were selected on the day of eclosion and housed in perforated plastic flasks, which were capped with agar plates smeared with yeast paste. The flies received plain yeast paste for 24 h. They were then provided with D3-leucine–labeled yeast

paste, which was replaced every 2-3 days, and were maintained in humidified containers at 25°C. After 120 h or 240 h of labeling, flies were flash-frozen in liquid nitrogen. Three biological replicates (50-115 heads each) were obtained for each genotype and time point.

All *PINK1* null mutants are male (*PINK1* is an X chromosome gene, and the males are sterile). Male flies were therefore used in all experiments for consistency.

Sample preparation

Frozen flies were vortexed to remove heads, and the isolated heads were homogenized in 0.1% RapiGest solution in 50 mM ammonium bicarbonate (Waters Corporation, Milford, MA) using a Wheaton 0.2-mL micro tissue grinder (Wheaton, Millville, NJ). Homogenates were centrifuged at 4°C at 1600 x *g* for 10 min, and then at 6000 x *g* for 10 min, to remove debris and nuclei. The supernatants were then boiled for 7 min and incubated with DTT (final concentration 5 mM) at 60°C for 30 min. Iodoacetamide was added to a final concentration of 15 mM, and the samples were incubated at room temperature in the dark for 30 min. Trypsin (Promega, Fitchburg, WI) was added at a ratio of 1 μg trypsin per 50 μg protein, and incubated for 1 h at 37°C with shaking. RapiGest was hydrolyzed by adding HCl to a final concentration of 200 mM, followed by incubation at 37°C with shaking for 45 min. The samples were then centrifuged for 10 min at 4°C at 20,000 x *g*, and the supernatant was collected.

Liquid chromatography and mass spectrometry

All mass spectrometry procedures were performed by Gennifer Merrihew of the MacCoss Lab. Fused silica microcapillary columns of 75 μm inner diameter (Polymicro Technologies, Phoenix, AZ) were packed in-house by pressure loading 30 cm of Jupiter 90 Å

C12 material (Phenomenex, Torrance, CA). Kasil (PQ Corporation, Malvern, PA) frit microcapillary column traps of 100 μm inner diameter with a 2-mm Kasil frit were packed with 4 cm of Jupiter 90 Å C12. An equal molar mix of a six-protein bovine digest (Michrom Bioresources, Inc., Auburn, CA) was used to assess quality of the column before and during analysis. Three of these quality control runs were analyzed prior to any sample analysis, and another quality control run was performed after every six sample runs. Two analytical replicates were obtained for each biological replicate. Two micrograms of each sample digest and 200 femtomoles of the six-protein bovine digest were loaded onto the trap and column by the NanoACQUITY UPLC system (Waters Corporation). Buffer solutions used were water, 0.1% formic acid (buffer A), and acetonitrile, 0.1% formic acid (buffer B). The 60-minute gradient of the six-protein bovine digest quality control consisted of 40 minutes of 95% buffer A and 5% buffer B, 1 minute of 68% buffer A and 32% buffer B, 5 minutes of 20% buffer A and 80% buffer B, and 14 minutes of 95% buffer A and 5% buffer B at a flow rate of 0.25 μL/min. The 240-minute gradient for the sample digest consisted of 200 minutes of 95% buffer A and 5% buffer B, 1 minute of 68% buffer A and 32% buffer B, 19 minutes of 20% buffer A and 80% buffer B and 20 minutes of 95% buffer A and 5% buffer B at a flow rate of 0.25 μL/min. Peptides were eluted from the column and electrosprayed directly into an LTQ-Orbitrap mass spectrometer (Thermo Fisher, San Jose, CA) with the application of a distal 3 kV spray voltage. For the six-protein bovine digest quality control analysis, a cycle of one 30,000 resolution full-scan mass spectrum (400-1400 *m/z*) was followed by six selected reaction monitoring (SRM) spectra analyzing 6 peptides and 4-5 fragment ions per peptide at 35% normalized collision energy with a 2 *m/z* isolation window. For the sample digests, a cycle of one 60,000 resolution full-scan mass spectrum (400-1400 *m/z*) was followed by five data-dependent MS/MS spectra at

35% normalized collision energy with a 3 *m/z* isolation window. Application of the mass spectrometer and UPLC solvent gradients were controlled by the Thermo Fisher XCalibur data system.

Analysis of mass spectrometry data

High-resolution MS data were processed by BullsEye to optimize precursor mass information (150). The MS/MS output was searched using SEQUEST (151), with differential modification search of 3.0188325 Da for leucine and a static modification of 57.021461 Da for cysteine, against a FASTA database containing all the protein sequences from FlyBase (10/03/09) plus contaminant proteins. Peptide-spectrum match false discovery rates were determined using Percolator (152) at a threshold of 0.01, and peptides were assembled into protein identifications using an in-house implementation of IDPicker (153). These procedures were also performed by Gennifer Merrihew.

Topograph analysis parameters

The following Topograph quality control cutoffs were applied to all data points (values of percent newly synthesized) for both half-life and abundance analyses:

1) Deconvolution score ≥ 0.95. The deconvolution score reflects the fit of the calculated isotopolog distribution to the observed distribution.
2) Average turnover score (ATS) ≥ 0.98. The ATS reflects the validity of precursor pool enrichment calculations for peptides with two or more leucines. (Peptides with a single leucine are assigned scores of 1.0.)

3) Total area under the curve (AUC) of ≥ 1,000,000 signal units. Data points with AUC values below this threshold generally had an unacceptable signal-to-noise ratio.

For half-life analysis, I also excluded data points more than 2 SD above or below the protein mean for that condition (genotype and time point). As stated above, preliminary observations had demonstrated that most such outliers were caused by artifacts such as peak misidentification.

Topograph's retention time alignment feature was used to identify peptides in replicates in which they were not detected in the MS2 spectra. In a small percentage of cases (5%-7%), Topograph clustered peptides belonging to a single protein into 2-3 nonoverlapping "isoform groups," each of which was treated as a separate protein. Although there were a few proteins in which different isoforms appeared to turn over at notably different rates, isoform groups from a single protein usually had nearly identical half-lives.

Protein half-life calculations

Protein half-lives were calculated using the Topograph software platform, version 1.0 (145). A protein's half-life was computed based on data from all peptides detected. The maximum possible number of percent newly synthesized values for a single peptide was 12 per genotype (3 biological replicates x 2 analytical replicates x 2 time points). Each protein was represented by at least 15 total values of percent newly synthesized per genotype, and therefore by at least two peptides. Peptides that could be the product of more than one gene were excluded from analysis. Data points from all biological replicates were pooled for half-life calculations.

I did not analyze the few proteins with a control half-life ≥ 1000 h, which accumulated too little tracer within the study period to ensure reliable quantification. I also excluded proteins with excessive variability of percent newly synthesized values, defined as follows. I divided the 95% confidence interval (CI) for each half-life (generated by Topograph) by the half-life value itself, creating a measure analogous to coefficient of variation. Proteins with a 95% CI/half-life ratio ≥ 0.3 were excluded from analysis.

Protein classification and annotation

Drosophila protein localization was determined by manual curation using a variety of databases, utilities, and software programs (Table 2.1), as well as primary literature. Decisions were based on the following five information sources:

1. **FlyBase** information (evidence inferred from direct assay, inferred from genetic interaction, or inferred from mutant phenotype).

2. Localization of human, mouse, and rat **orthologs**, where applicable.

I used only information inferred from direct assay for primary localization.

Traceable author statement information was acceptable for mitochondrial sublocalization.

I derived primary localization from an ortholog only when there was one ortholog, or a few with similar localization, and when BLAST matching to *Drosophila* was adequate.

Table 2.1. List of main resources used in protein annotation.

Databases and utilities	Localization predictor software
BLAST EMBL FlyAtlas FlyBase InterPro MGD MitoCarta (mouse) MitoDrome NCBI Gene SGD UniProt	WoLF PSORT MitoProt Predotar SignalP NucPred PTS1 Predictor

3. **Computational localization predictor** information. This included WoLF PSORT for nearly all proteins; MitoProt and Predotar for proteins suspected to be mitochondrial; Predotar and SignalP for proteins suspected to be ER or extracellular; NucPred for suspected nuclear proteins; and PTS1 Predictor for suspected peroxisomal proteins.

Localization predictors were most important when there was a dearth of information from other sources, or conflicting information. They were also useful for detecting split localization (e.g., one isoform cytosolic, one mitochondrial), and served as a double-check on other information sources.

4. **BLAST** information (where necessary to assess the quality of sequence match to an ortholog).

5. Information from **primary literature** where applicable.

Proteins were classified as exclusively mitochondrial (M), mitochondrial with significant other localization (M/N), nonmitochondrial (N), or nonmitochondrial with some mitochondrial localization (N/M). Based on analyses of mean mutation effect and correlations between *Atg7* and *parkin* effect (see Chapter 3), I determined that proteins labeled M/N had similar characteristics to those labeled M, and I therefore combined the two categories as "mitochondrial." There were very few N/M proteins (5 of the 524 total proteins in the WT dataset), and I analyzed them together with the N proteins as "nonmitochondrial."

Comparison to mouse half-lives

Mouse brain half-life data were obtained from Price et al. (2010) (136). Rate constant values (K_0) for mouse brain proteins were converted to half-lives and compared to half-lives of orthologous proteins in the WT fly head data. Orthology to mouse proteins was determined from a variety of resources, primarily FlyBase and NCBI.

Chapter 3: PINK1-Parkin pathway effects on mitochondrial protein turnover

The model of PINK1-Parkin pathway action described in Chapter 1 makes the following predictions:

1. *parkin* or *PINK1* mutations will prolong mitochondrial protein half-lives due to impaired mitophagy.
2. *Atg7* mutations, which impair general autophagy, will prolong mitochondrial protein half-lives to an even greater extent than *parkin* or *PINK1*.
3. *SOD2* mutations, which increase oxidative stress, will not have effects similar to those of *parkin* or *PINK1*, and may shorten mitochondrial protein half-lives.
4. Overexpressing Parkin or PINK1 will shorten mitochondrial protein half-lives due to increased mitophagy.

In this chapter, I report the results of testing all these hypotheses.

FINDINGS

As stated above, I hypothesized that mitochondrial protein half-lives would be prolonged in *parkin* null mutants relative to their controls, due to impaired mitophagy. I also measured half-lives in autophagy-deficient *Atg7* null mutants as a positive control. Atg7 is an essential component of the conventional autophagy machinery, an E1-like enzyme required for activation of Atg8 and Atg12, and thus for autophagosome formation (17, 154). *Atg7* null mutants have shortened lifespans, are hypersensitive to oxidative stress, and develop neuronal protein

aggregates early in adulthood (154). Because Atg5/Atg7-dependent autophagy acts downstream from Parkin (47), and also mediates nonselective forms of mitochondrial degradation (19), I hypothesized that *Atg7* null mutants would have a deficit in mitochondrial protein turnover similar to, but more severe than, that of *parkin* null mutants. To test these hypotheses, I compared the half-lives of 156 mitochondrial proteins from *parkin* mutants and 170 from *Atg7* mutants (147 of which were detected in both datasets) with their half-lives in control flies. For each protein, I divided mutant half-life by control half-life to compute fold change in half-life.

Testing for abundance change artifacts

My initial analyses showed that both *parkin* and *Atg7* mutants had significantly prolonged mitochondrial protein half-lives compared to controls. Before I accepted these results, however, I first tested for the presence of abundance change artifacts. As mentioned in Chapter 2, Topograph half-life computations assume that protein synthesis rate equals degradation rate, and therefore that protein abundance remains constant throughout the experiment (Fig. 3.1). While constant protein abundance is important for the accurate calculation of half-life, the accurate calculation of fold change in half-life between genotypes requires only that any change in protein abundance be the same in both genotypes (Fig. 3.2). If the pattern of abundance over time differs between mutant and control, artifacts can result. The apparent increases in mitochondrial protein half-life in *parkin* and *Atg7* mutants, for instance, could theoretically reflect relative decreases in mitochondrial protein abundance in the mutants over the study period. To address this issue, I compared protein abundance change over the study period in mutants and controls.

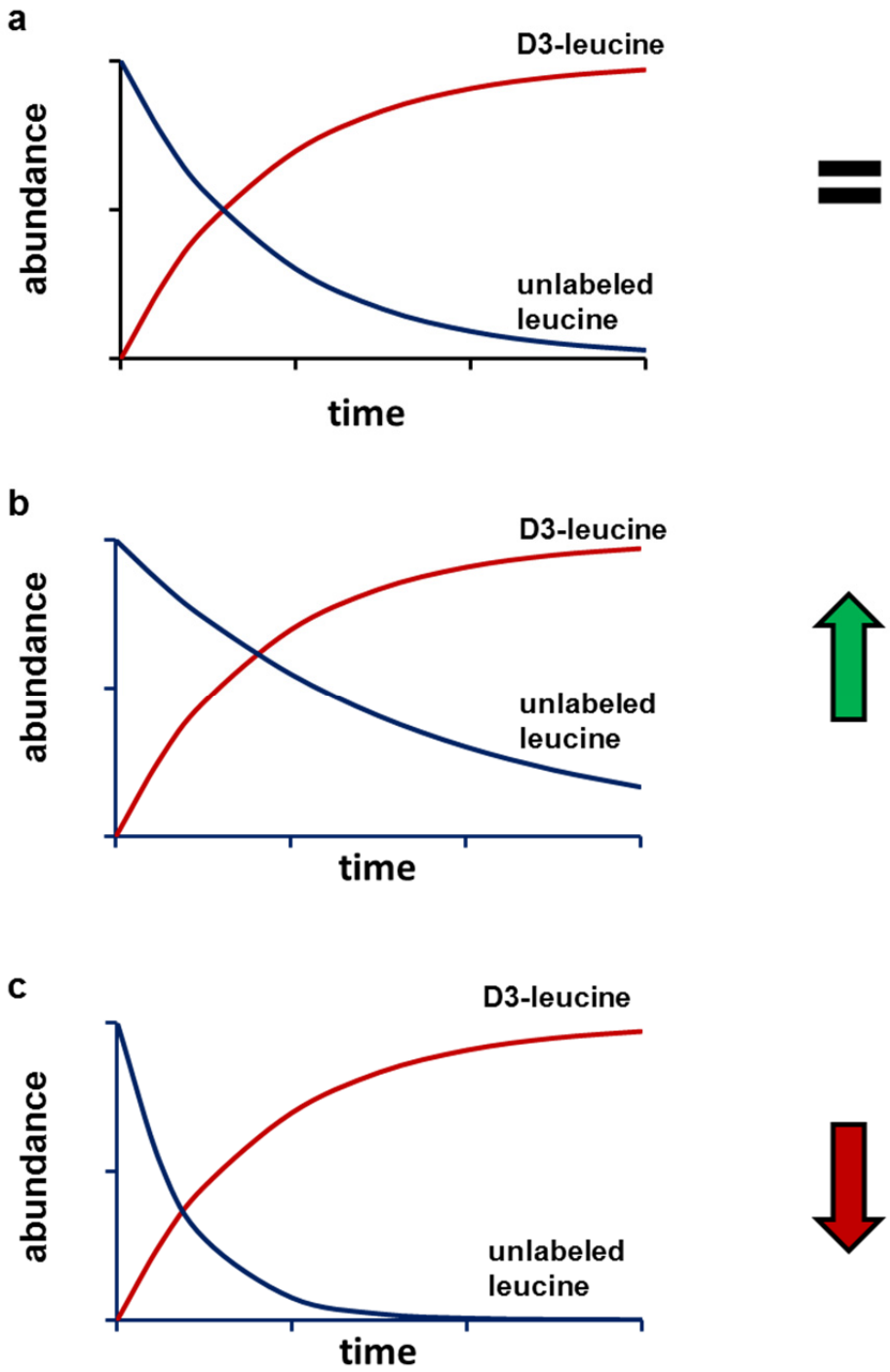

Figure 3.1. Potential effects of abundance change on half-life calculations. Topograph half-life calculations assume steady-state abundance. If abundance of a given protein is constant during the labeling period **(a)**, the calculated percent newly synthesized is equal to the percent degraded. If abundance is increasing **(b)**, degradation is overestimated, and calculated half-lives are artifactually short; if abundance is decreasing **(c)**, degradation is underestimated, and calculated half-lives are too long.

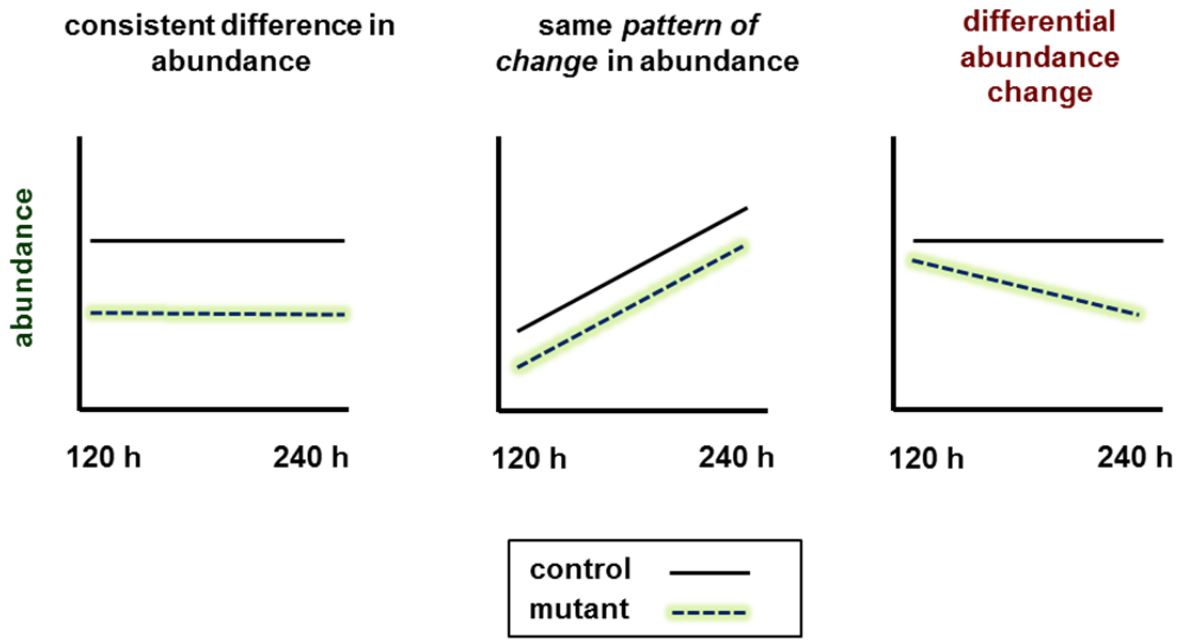

Figure 3.2. Potential effects of differential abundance change on mutant/control half-life comparisons. When comparing half-lives across genotypes, constant protein abundance is not necessary for accuracy, as long as any change in abundance over time occurs equally in both genotypes. If both half-lives have the same degree of bias, then the ratio of the two half-lives will be accurate. If not, there is differential abundance change, and the ratio of half-lives may be distorted.

Topograph, which uses area under the curve measurements to compare the abundance of the various labeled and unlabeled forms of a peptide, can measure total abundance by summing areas under the curve for all forms of a peptide. I compared change over time for each protein between mutants and controls (see Materials and Methods for details). Very few mitochondrial proteins showed significant differential change in abundance over time in mutants compared to controls: *parkin* 3.4% (5 of 149 testable proteins), *Atg7* 3.0% (5/166), *PINK1* 0.7% (1/145), and *SOD2* 0%. Table 3.1 lists all mitochondrial proteins showing differential abundance change.

As another test of abundance change effects, I also looked for a systematic relationship between fold change in half-life and a measure of differential change in abundance (Fig. 3.3a-d). A strong correlation between the two measures would suggest that abundance change was producing a false appearance of difference in half-life between mutant and control. The relationship between fold change in half-life and differential abundance change accounted for < 5% of the total variance in all four datasets (measured as the coefficient of determination, R^2). Furthermore, I found that fold change in half-life often seemed surprisingly insensitive to differential abundance change. As an illustration, ribosomal proteins in the *parkin* dataset displayed the same minimal fold change in half-life over a range of differential abundance change values (Fig. 3.3e). Thus, although differential changes in abundance may contribute slightly to some measured effects on turnover, the turnover changes reported in this chapter do not appear to be artifacts of altered abundance.

Parkin promotes mitophagy *in vivo*

Consistent with my hypotheses, mitochondrial proteins in *parkin* and *Atg7* mutants had significantly prolonged half-lives compared to controls (Fig. 3.4a). Also as hypothesized, lack of

Table 3.1. Mitochondrial proteins showing differential change in abundance over time between mutant and control.

				Atg7 240 h/120 h abundance ratio		*parkin* 240 h/120 h abundance ratio		*PINK1* 240 h/120 h abundance ratio	
CG Number, Isoforms	**Name**	**Description**	**Loc'n**	***Atg7***	**control**	***parkin***	**control**	***PINK1***	**control**
CG10664-PA, PB	-	complex IV; cytochrome C oxidase subunit IV isoform 1	RC	1.04	0.84				
CG11739-PA through PD	-	ortholog SFXN1-3 (mitochondrial transmembrane transporter)	IM	1.34	1.12				
CG12140-PA, PB	-	ortholog ETFDH (electron transfer flavoprotein-ubiquinone oxidoreductase, mitochondrial)	IM (cristae)			0.84	1.12		
CG15261-PA	UK114	ortholog HRSP12	?					0.73	1.05
CG2151-PA, PB, PC	Thioredoxin reductase-1	ortholog TXNRD1-3	mito, cyto	0.93	1.02				
CG2286-PA, PB	NADH:ubiquinone reductase 75kD subunit precursor	complex I, peripheral arm; ortholog NDUFS1	RC	1.00	0.86				
CG3699-PA	-	no orthologs listed; possibly immune	?	0.78	1.06				
CG4581-PA	Thiolase	ortholog HADHB (trifunctional enzyme subunit beta, mitochondrial)	matrix			0.94	1.11		
CG4600-PA	yippee interacting protein 2	ortholog ACAA/ACAT genes; acetyl-CoA C-acyltransferase activity	matrix, IM			0.94	1.16		
CG7834-PA, PB	-	ortholog ETFB (mitochondrial electron transfer flavoprotein beta subunit)	matrix			0.85	1.06		
CG8996-PA, PB	walrus	ortholog ETFA (mito electron transfer flavoprotein alpha subunit)	matrix			0.80	1.19		

Figure 3.3. Difference in half-life between mutant and control is not better explained by differential change in abundance. The fold change in half-life for each mitochondrial protein (mutant/control) is plotted against its differential abundance change index. The differential abundance change index represents a comparison of the ratios representing mutant and control abundance change over time (240 h/120 h). See Materials and Methods for a detailed explanation. **(a-d)** Differential abundance change accounts for < 5% of the variance in fold change in half-life for each of the four datasets. Shared variance is reported as the coefficient of determination (R^2). Number of proteins: *parkin* 156, *Atg7* 170, *PINK1* 147, *SOD2* 106. **(e)** Ribosomal proteins from the *parkin* dataset demonstrate that even substantial differential abundance change is not necessarily reflected in fold change in half-life (n = 43).

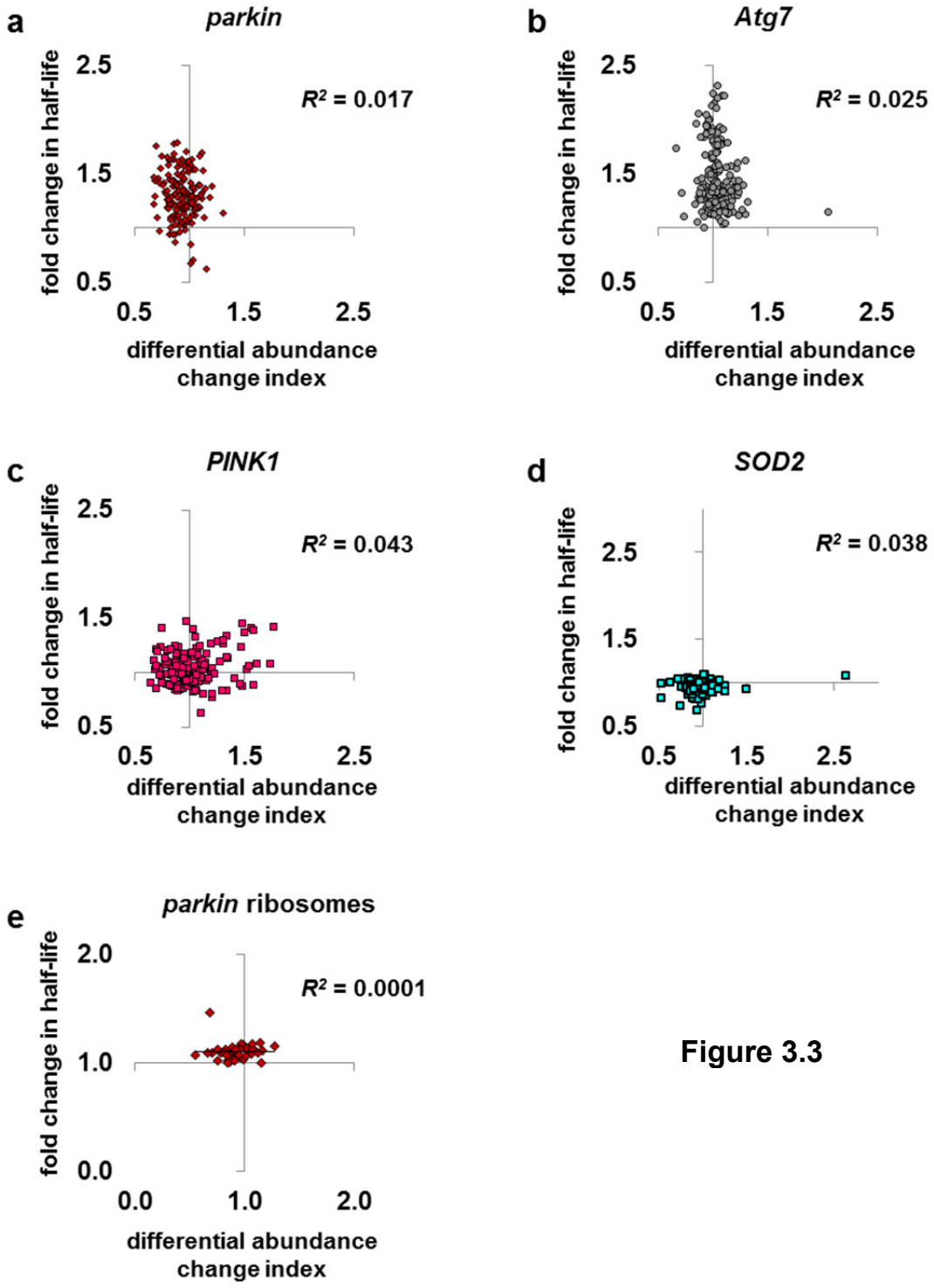
a
parkin
R² = 0.017
fold change in half-life
differential abundance change index
b
Atg7
R² = 0.025
c
PINK1
R² = 0.043
d
SOD2
R² = 0.038
e
parkin ribosomes
R² = 0.0001
0.5
1.5
2.5
0.0
1.0
2.0

Figure 3.3

Figure 3.4. Parkin promotes mitophagy *in vivo*. (a) *parkin* and *Atg7* mutations prolong mitochondrial protein half-life. Box-and-whisker plots of fold change in half-life show median, quartiles, and extreme values. *parkin* mean and SD 1.30±0.22; *Atg7* 1.47±0.30. $^{**}p < 0.005$, mutant vs. control, by nested ANOVA **(b, c)** The effects of *parkin* and *Atg7* mutations on half-life correlate significantly for individual mitochondrial proteins **(b)** but not ribosomal proteins **(c)**. $n = 147$ mitochondrial proteins, 40 ribosomal proteins. All correlations are reported as Pearson *r*. **(d)** SOD2 deficiency produces a nonsignificant acceleration of mitochondrial protein turnover ($p = 0.12$ by nested ANOVA; $n = 106$). **(e, f)** The effects of *parkin* mutation **(e)** or *Atg7* mutation **(f)** on mitochondrial protein half-life do not correlate significantly with those of SOD2 deficiency ($n = 103$ for *parkin*, 103 for *Atg7*).

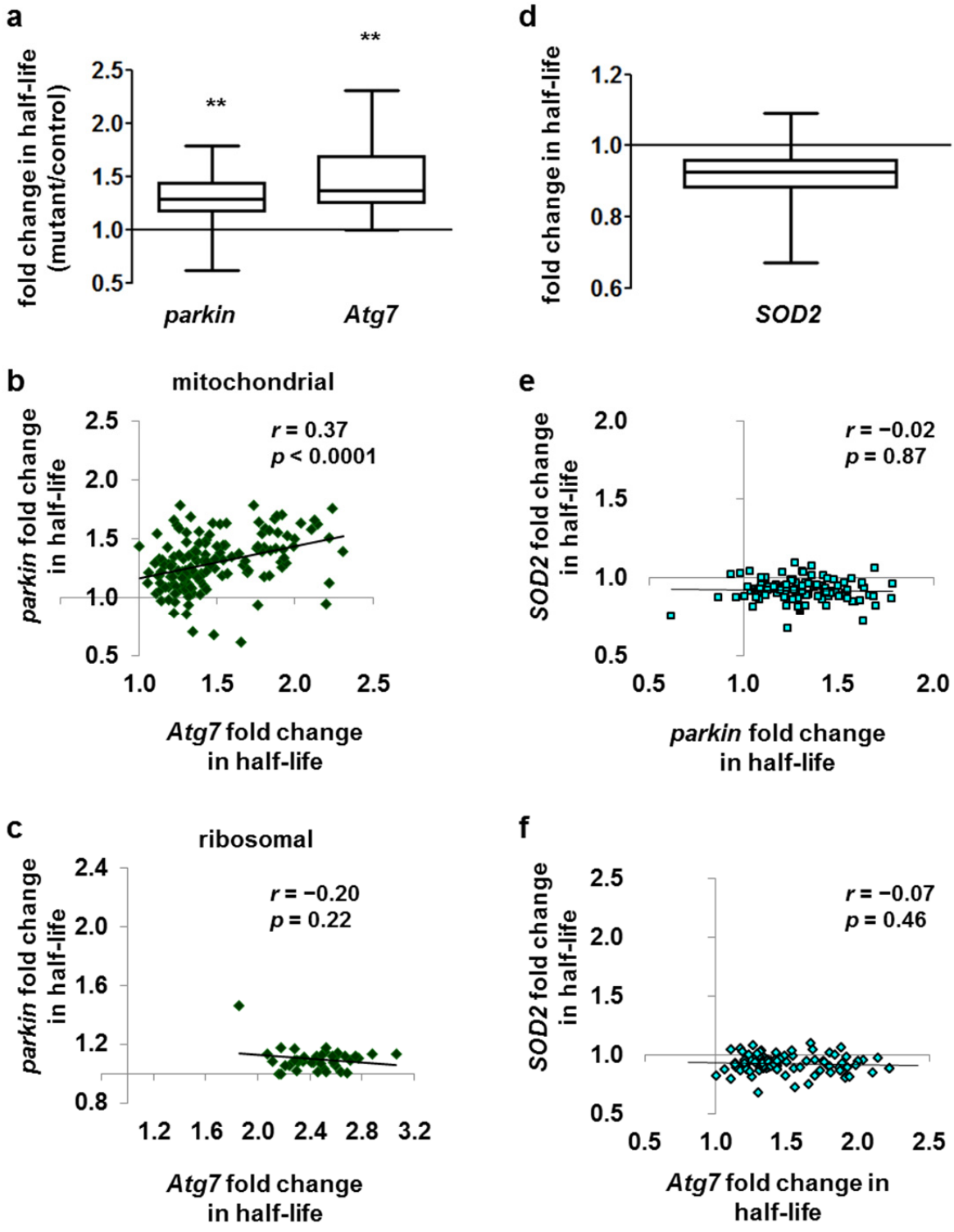
a
fold change in half-life (mutant/control)
2.5
2.0
1.5
1.0
0.5
**
**
parkin
Atg7
d
fold change in half-life
1.2
1.0
0.8
0.6
SOD2
b
mitochondrial
parkin fold change in half-life
r = 0.37
p < 0.0001
2.5
2.0
1.5
1.0
0.5
1.0 1.5 2.0 2.5
Atg7 fold change in half-life
e
SOD2 fold change in half-life
r = −0.02
p = 0.87
2.0
1.5
1.0
0.5
0.5 1.0 1.5 2.0
parkin fold change in half-life
c
ribosomal
parkin fold change in half-life
r = −0.20
p = 0.22
2.4
2.0
1.6
1.2
0.8
1.2 1.6 2.0 2.4 2.8 3.2
Atg7 fold change in half-life
f
SOD2 fold change in half-life
r = −0.07
p = 0.46
2.5
2.0
1.5
1.0
0.5
0.5 1.0 1.5 2.0 2.5
Atg7 fold change in half-life

Figure 3.4

Atg7 had a stronger effect on mitochondrial protein turnover than lack of Parkin (Fig. 3.4a). Furthermore, I found a significant positive correlation between the effects of *parkin* and *Atg7* mutations on the half-lives of the 147 mitochondrial proteins that appeared in both datasets (Fig. 3.4b). This relationship was specific to mitochondrial proteins; there was no such correlation between the effects of *parkin* and *Atg7* mutations on the half-lives of other targets of autophagy, such as ribosomal proteins (148) (Fig. 3.4c). It was possible, however, that the *parkin-Atg7* correlation simply reflected general mitochondrial dysfunction. To explore this possibility, I compared *parkin* and *Atg7* mutants to flies severely deficient in another mitochondrial quality control factor, superoxide dismutase 2 (SOD2). Rather than slowed mitochondrial turnover, the *SOD2* mutants had a slight, nonsignificant increase in mean mitochondrial protein turnover (Fig. 3.4d). *SOD2* effects on half-life did not correlate with the effect of either *parkin* or *Atg7* (Fig. 3.4e,f). Together, these findings support the model that Parkin promotes mitophagy *in vivo*.

Parkin mediates selective turnover of mitochondrial respiratory chain proteins

The turnover of most mitochondrial proteins showed greater dependence on Atg7 than on Parkin, as would be expected if Atg7 acts downstream from Parkin and also mediates nonselective mitochondrial turnover. However, the turnover of 40 mitochondrial proteins showed greater dependence on Parkin than on Atg7. Such proteins potentially represent targets of a Parkin-dependent turnover process that is independent of Atg7. Among these 40 proteins, respiratory chain (RC) components were strikingly overrepresented, as confirmed by chi-squared analysis (10/40 predicted, 19/40 observed, $p = 0.003$). The effect of *parkin* mutation on turnover

exceeded the effect of *Atg7* for fully 53% of all RC proteins detected, compared with only 19% of all other mitochondrial proteins (Fig. 3.5a-c). The RC proteins with greater turnover dependence on Parkin represented all five respiratory complexes, and included a disproportionately large number of membrane-bound subunits (11 of 14 total membrane-bound subunits vs. 8 of 22 subunits not directly anchored to a membrane). Other mitochondrial membrane proteins were not overrepresented, suggesting that Parkin's greater effects on membrane-bound proteins are specific to the RC. In addition, Parkin had a greater mean effect on turnover of membrane-bound RC subunits than on turnover of nonmembrane subunits (Fig. 3.5d). The findings thus suggest that, in addition to its role in mitophagy, Parkin has a selective effect on the turnover of RC proteins.

PINK1 is required for selective RC turnover

Previous work has shown that PINK1 is required for Parkin-mediated mitophagy following treatment of cultured cells with mitochondrial depolarizing agents (8, 48), and genetic studies in *Drosophila* show that *PINK1* null mutants have similar phenotypes to *parkin* null mutants (72, 73). I therefore anticipated that *PINK1* mutants would have mitochondrial protein turnover defects similar to those seen in *parkin* mutants. However, while there was a trend toward increased half-lives of mitochondrial proteins in *PINK1* mutants, this difference did not reach significance ($p = 0.082$ by nested ANOVA; Fig. 3.6a). Further analysis revealed that the RC was the only mitochondrial protein subgroup with a significantly increased mean half-life in *PINK1* mutants (Fig. 3.6a). This increased mean half-life was specific to the RC, and did not occur in non-RC proteins with a *parkin*/*Atg7* ratio > 1 (mean *PINK1* fold change in half-life for

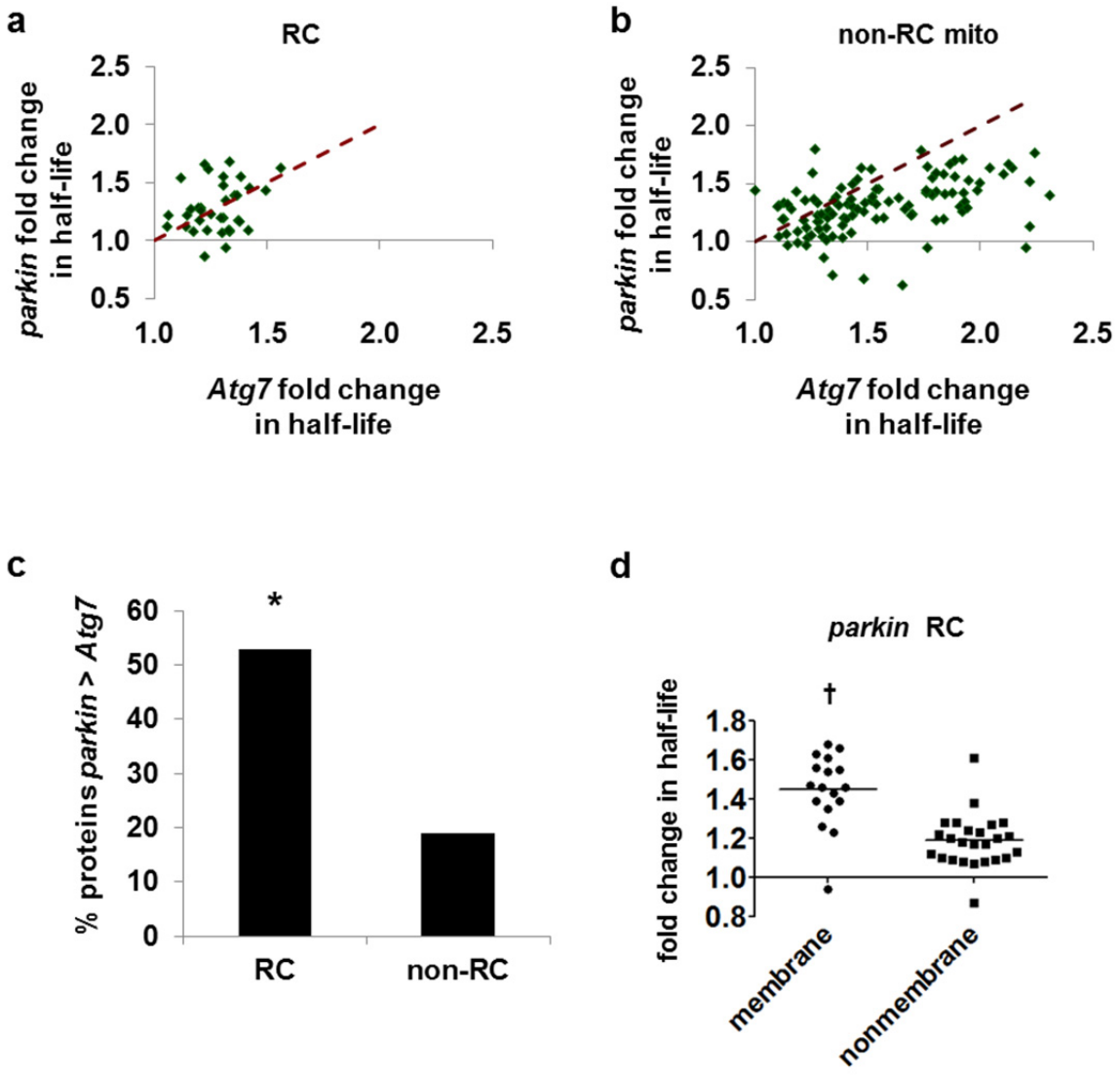

Figure 3.5. Parkin has a selective effect on turnover of respiratory chain (RC) proteins. **(a, b)** Plots comparing the influence of *parkin* and *Atg7* on the half-lives of RC proteins **(a)** and all other mitochondrial proteins **(b)**. Dashed lines indicate equal effect from both mutations; the half-lives of proteins above the dashed line are more greatly influenced by *parkin* mutation than by *Atg7* mutation. **(c)** The percentage of RC and non-RC proteins whose half-lives are more greatly affected by *parkin* than *Atg7* mutation (n = 36 RC proteins, 111 non-RC). The RC is significantly enriched in proteins with greater *parkin* than *Atg7* effect on half-life. *p = 0.003 by χ^2 test **(d)** Mutation in *parkin* has a larger effect on the half-lives of membrane-bound RC subunits than on those of nonmembrane RC subunits (mean fold change 1.45±0.19 vs. 1.19±0.14). Horizontal lines indicate the median. †$p = 4.8 \times 10^{-6}$ by t test

Figure 3.6. *PINK1* null mutants have a selective impairment of RC protein turnover. **(a)** *PINK1* null mutation prolongs the mean half-life of RC proteins but not other mitochondrial proteins. Box-and-whisker plots of fold change in half-life show median, quartiles, and extreme values. Mean fold change: total mito 1.04±0.16, non-RC mito 0.99±0.13, RC 1.17±0.16 (n = 147, 102, and 45 proteins respectively). $^{**}p < 0.0005$, mutant vs. control, by nested ANOVA. **(b)** Mutation in *PINK1* has a larger effect on membrane-bound than on nonmembrane RC subunits (mean fold change 1.24±0.13 vs. 1.11±0.16). Horizontal lines indicate the median. $\dagger p = 0.005$ by t test **(c, d)** The effects of *PINK1* mutation on RC protein half-lives strongly correlate with those of mutation in *parkin* **(c)**, but not with the effects of mutation in *Atg7* **(d)***;* n = 36 for *parkin*, 34 for *Atg7*). **(e)** *parkin* effect on half-life does not correlate significantly with *Atg7* effect for individual RC proteins (n = 36).

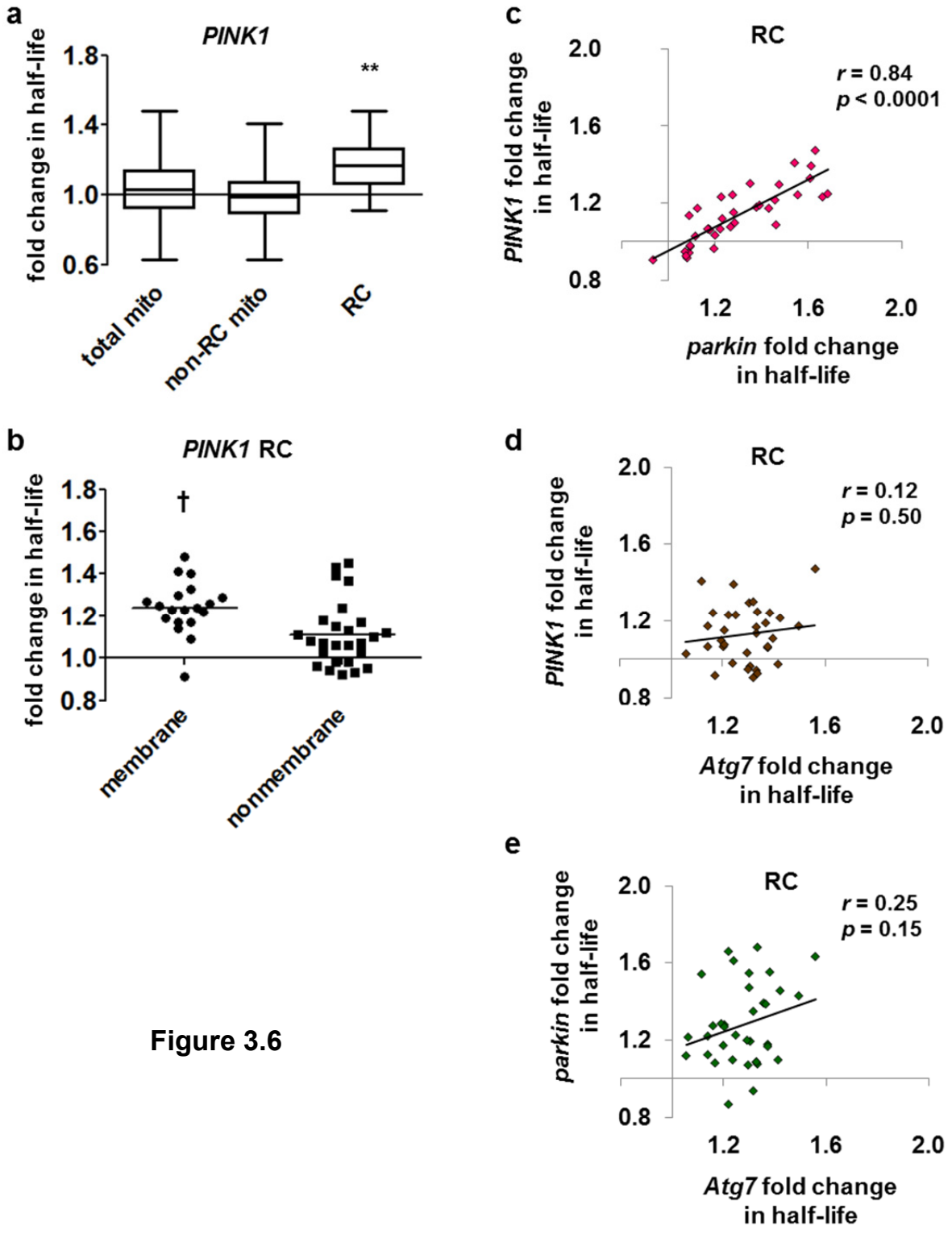
a
PINK1
fold change in half-life
1.8
1.4
1.0
0.6
**
total mito
non-RC mito
RC
b
PINK1 RC
fold change in half-life
1.8
1.6
1.4
1.2
1.0
0.8
†
membrane
nonmembrane
c
RC
PINK1 fold change in half-life
2.0
1.6
1.2
0.8
r = 0.84
p < 0.0001
1.2
1.6
2.0
parkin fold change in half-life
d
RC
PINK1 fold change in half-life
2.0
1.6
1.2
0.8
r = 0.12
p = 0.50
1.2
1.6
2.0
Atg7 fold change in half-life
e
RC
parkin fold change in half-life
2.0
1.6
1.2
0.8
r = 0.25
p = 0.15
1.2
1.6
2.0
Atg7 fold change in half-life

Figure 3.6

this group of non-RC proteins was 1.05±0.12). Like *parkin* mutants, *PINK1* mutants showed greater mean fold change in half-life for membrane-bound than for nonmembrane RC subunits (Fig. 3.6b). The effect of *PINK1* mutation on RC turnover correlated strongly with the effect of *parkin* mutation on the same proteins (Fig. 3.6c), but neither the *PINK1* nor the *parkin* effect on RC correlated with that of *Atg7* (Fig. 3.6d,e). Together, these findings suggest that the PINK1-Parkin pathway promotes selective Atg7-independent turnover of RC proteins.

Compensatory turnover masks a mitophagy deficit in *PINK1* mutants

The apparent lack of impairment in general mitochondrial protein turnover in *PINK1* mutants is surprising given that PINK1 is essential for Parkin-mediated mitophagy *in vitro* (48). However, studies in *Drosophila* indicate that Parkin retains some activity in the absence of PINK1 (72, 73, 79). This residual Parkin activity may be sufficient to support basal mitophagy, which appears to occur at a low rate; the longest-lived mitochondrial proteins in WT flies had half-lives in excess of 30 d. PINK1 may thus be required for mitophagy only under conditions of extreme mitochondrial stress, such as acute ischemia (111) or toxin treatment of cultured cells. Alternatively, because increased autophagy has been described in PINK1-deficient cells and animals (155-157), *PINK1* mutants could have a deficit in mitophagy that is masked by a compensatory increase in another form of protein turnover. While these possibilities are not mutually exclusive, the data appear to support the idea of compensation in *PINK1* mutants. Although *PINK1* mutants show no mean change in turnover of non-RC mitochondrial proteins, the effect of *PINK1* mutation on those proteins correlates well with the effect seen in *parkin* mutants (Fig. 3.7a).

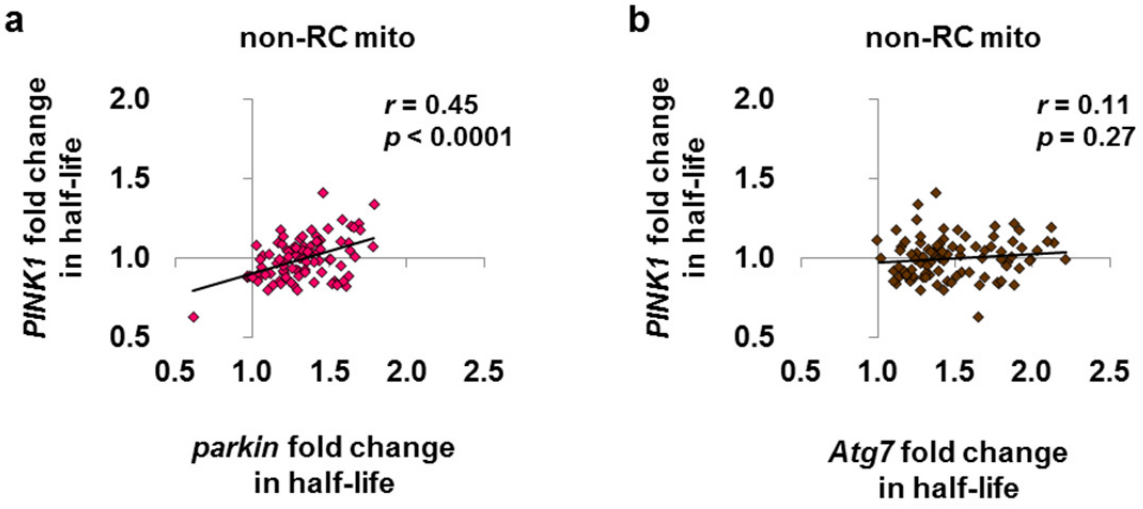

Figure 3.7. Correlation between *PINK1* and *parkin* effects on non-RC mitochondrial turnover suggests a compensated mitophagy deficit. (a) The effects of *PINK1* mutation on the half-lives of non-RC mitochondrial proteins correlate significantly with the effects of *parkin* mutation ($n = 94$). The regression line has a negative y-intercept, suggesting a uniform shift toward faster mitochondrial protein turnover in *PINK1*. **(b)** The effects of *PINK1* mutation on non-RC mitochondrial proteins do not correlate significantly with the effects of *Atg7* mutation ($n = 92$).

There is no comparable correlation between *PINK1* and *Atg7* (Fig. 3.7b). The *PINK1-parkin* correlation appears to reflect a uniform increase in mitochondrial protein turnover in *PINK1* mutants relative to *parkin* mutants, such that the proteins with the smallest turnover impairment in *parkin* mutants actually have slightly increased turnover rates in *PINK1* mutants relative to control. In fact, 41% of mitochondrial proteins had shorter half-lives in *PINK1* mutants than in controls. My findings thus suggest that compensatory degradation masks a mitophagy defect in *PINK1* mutants.

PINK1 **overexpression does not increase mitochondrial turnover** ***in vivo***

I next considered the possible effects of PINK1 and Parkin overexpression on mitochondrial turnover *in vivo*. In a pilot experiment involving a single biological replicate, Parkin overexpression using the strong ubiquitous driver *tubulin-GAL4* failed to alter mitochondrial protein turnover (data not shown). I therefore focused on PINK1 overexpression, which, unlike Parkin overexpression, had already been demonstrated to produce robust phenotypes in *Drosophila*. Vigorous PINK1 overexpression during development is highly toxic, and no flies survive to adulthood when PINK1 is overexpressed with a strong driver such as *Dmef2-GAL4* (74). If overexpressed only in the eye, excess PINK1 produces characteristic morphological abnormalities ("rough eye") (74). In addition, PINK1 overexpression *in vitro* is sufficient to provoke mitophagy even in the absence of depolarization (8, 48, 85). I therefore hypothesized that PINK1 overexpression *in vivo* would cause accelerated mitochondrial turnover.

I used three different strategies to overexpress PINK1, summarized in Table 3.2.

Table 3.2. Summary of PINK1 overexpression study methods.

study	UAS	driver	heat shock?	development temperature	labeling temperature
1a	*UAS-PINK1#3*	*Hsp70-GAL4*	no	25°C	25°C
1b	*UAS-PINK1#3*	*Hsp70-GAL4*	no	25°C	25°C
2	*UAS-PINK1#3*	*elav-GAL4* C155	no	18°C	25°C
3	*UAS-PINK1#2*	*Hsp70-GAL4*	yes, 1 h	25°C	25°C

As mentioned above, strong PINK1 overexpression during development is toxic, so I tested several strategies to find a balance of survivability and strong expression. First, I took advantage of the fact that driving *UAS-PINK1* with the ubiquitous driver *Hsp70-GAL4* results in moderate levels of expression even without heat shock activation. This "leak expression" is approximately 2-3 times greater than endogenous levels of PINK1 (Ruth Thomas, unpublished data). I used this method both at the standard labeling temperature (25°C) and at a higher temperature (29°C), which was intended to increase GAL4 expression and therefore PINK1 expression. Second, I used *elav-GAL4* to drive PINK1 overexpression in neural tissue only, but at high levels. These flies were raised at 18°C to minimize PINK1 expression during development. Third, I used a different *UAS-PINK1* construct from the same source, drove it with *Hsp70-GAL4*, and performed a single one-hour heat shock early in the labeling period to create a pulse of PINK1 expression.

None of these strategies resulted in increased rates of mitochondrial protein turnover. Expressing PINK1 using *Hsp70-GAL4* without heat shock at 25°C caused no significant mean change in either mitochondrial or nonmitochondrial protein turnover (Fig. 3.8a), and the results were the same at 29°C (Fig. 3.8b). *Hsp70-GAL4* PINK1 overexpression plus heat shock caused mild but significant slowing of mitochondrial protein turnover (mean fold change 1.08±0.06, p = 0.0279 by nested ANOVA) without affecting nonmitochondrial protein turnover (Fig. 3.8c). Finally, PINK1 overexpression using *elav-GAL4* produced significant slowing of both mitochondrial and nonmitochondrial protein turnover (Fig. 3.8d). Thus, *in vivo* and with endogenous levels of Parkin, PINK1 overexpression is not sufficient to promote increased mitochondrial turnover.

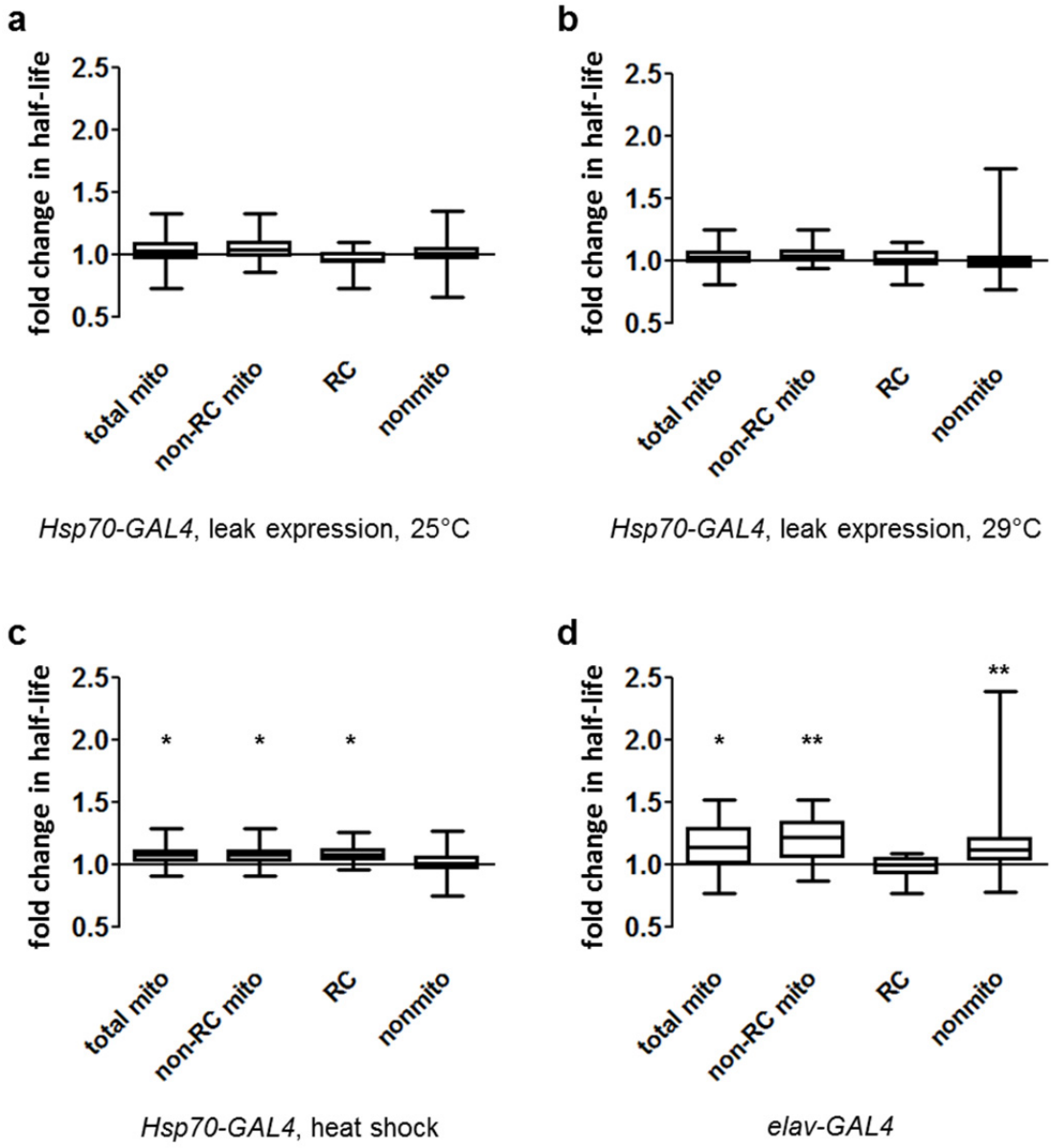

Figure 3.8. *PINK1* overexpression does not accelerate mitochondrial turnover *in vivo.* **(a)** *UAS-PINK1#3* driven with *Hsp70-GAL4*, leak expression at 25°C. Mean fold change for mitochondrial proteins was 1.03±0.09 and for nonmitochondrial proteins 1.01±0.09 ($p = 0.88$ and 0.79; all p values for this figure represent nested ANOVA, overexpressor vs. control). **(b)** *UAS-PINK1#3*, *Hsp70-GAL4*, leak expression at 29°C. Mean fold change 1.03±0.07 mito, 1.00±0.10 nonmito. **(c)** *UAS-PINK1#2*, *Hsp70-GAL4*, single 1-h heat shock 71 h after the start of labeling. Mitochondrial protein turnover was significantly slowed (mean fold change 1.08±0.06, $p = 0.0279$), but nonmitochondrial protein turnover was not (1.01±0.08, $p = 0.30$). **(d)** *UAS-PINK1#3*, *elav-GAL4*. Both mito and nonmito protein turnover were significantly slowed (mean fold change mito 1.15±0.18, nonmito 1.14±0.19). *$p < 0.05$, **$p < 0.005$

DISCUSSION

This chapter offers evidence that the PINK1-Parkin pathway promotes mitophagy *in vivo*, describes an additional role for the pathway in the selective non-mitophagic turnover of RC proteins, and demonstrates that PINK1 overexpression is not sufficient to promote mitophagy *in vivo*.

Mitophagy

The prolongation of mitochondrial protein half-lives in *parkin* and *Atg7*, with effects that correlate between the two genotypes on a protein-by-protein basis, supports the idea that Parkin promotes mitochondrial turnover through autophagy. The evidence is, of course, correlational in nature. Increasing mitophagy and determining whether lack of Parkin prevents the increase would be a more rigorous test; however, as noted above, it proved far more difficult than anticipated to accelerate mitochondrial turnover. I will test other mitophagy-accelerating strategies, such as hyperoxic stress, in future.

An alternate explanation of the results is impaired turnover of proteins before mitochondrial import, rather than impaired turnover of mitochondria. If this were true, I would expect mitochondrially encoded proteins to be less affected than nuclearly encoded mitochondrial proteins. While I detected very few mitochondrially encoded proteins, their turnover was affected in the same manner as that of comparable nuclearly encoded proteins. For instance, the mitochondrially encoded ortholog of COX2 (mt:CoII) had a fold change in half-life of 1.55 in *parkin* and 1.30 in *Atg7*, consistent with the respective dataset means of 1.45 and 1.31 for membrane-bound RC proteins. Similarly, mt:ATPase8 had a fold change of 1.40 in *PINK1*,

compared to the mean of 1.24 for membrane-bound RC. While this type of comparison cannot be made for non-RC proteins, it is worth noting that many mitochondrial proteins are cotranslationally imported (158) and therefore could not be turned over before reaching the mitochondria.

The wide range of *parkin* and *Atg7* effects on individual proteins suggests that a high percentage of mitochondrial turnover may take place selectively rather than by mitophagy. Various forms of compensatory turnover are almost certainly taking place in the mutants, but considering the range of mitochondrial protein half-lives in WT flies, the variable effects of *parkin* and *Atg7* mutations raise the suspicion that mitophagy may not be the primary means of mitochondrial protein turnover in fly heads.

The question of whether *PINK1* is necessary for mitophagy, discussed above, is intriguing. What causes the putative compensatory increase in turnover? Is the compensation unique to *PINK1*, or does a similar process also lessen the severity of turnover defects in *parkin* mutants? If *PINK1* mutants do experience compensatory turnover through increased general autophagy, I would expect to see effects of this increase on turnover of nonmitochondrial proteins as well. I will address this issue in Chapter 5.

Selective RC turnover

The finding of selective PINK1/Parkin effect on RC turnover was entirely unanticipated. However, loss of PINK1 and/or Parkin activity has previously been reported to cause RC deficits, particularly in complex I (159, 160), and complex I dysfunction has repeatedly been implicated in the pathogenesis of PD (161). My findings suggest that selective impairment of RC

protein turnover could conceivably explain the RC deficits seen in both familial and sporadic PD patients. Impaired turnover could, for example, lead to the accumulation of misfolded RC proteins, previously noted in *PINK1* and *parkin* mutant flies (162). Complex I, the largest and most intricate of the RC complexes, may be the most vulnerable to dysfunction under such conditions.

The mechanism of selective RC turnover is at this point entirely unknown. However, recent work suggests at least two possible models (Fig. 3.9). One model involves chaperone-mediated extraction of mitochondrial proteins, as described by Margineantu et al. (14). Another possible mechanism is mitochondria-derived vesicles, which have been shown to transport selected mitochondrial cargo to the lysosome in an autophagy-independent manner (163). Such vesicles have been shown to transport a membrane-bound complex IV subunit and to contain inner mitochondrial membrane (164), thus offering a potential explanation for the greater effect of *PINK1* and *parkin* mutations on membrane-bound RC components. (Another possible explanation is greater accessibility of nonmembrane subunits to a compensatory turnover mechanism.) Mitochondrial "buds" have also been documented in human T lymphocytes stressed with galectin-1 (165). The mitochondrial fission factor Drp1 was recruited to the surface of nascent buds; given the powerful rescue of *parkin* mutants by Drp1 overexpression, this is of interest.

PINK1 overexpression

I initially expected to stimulate mitophagy by increasing PINK1 levels, and was surprised when repeated experiments did not produce this effect. In hindsight, perhaps I should not have

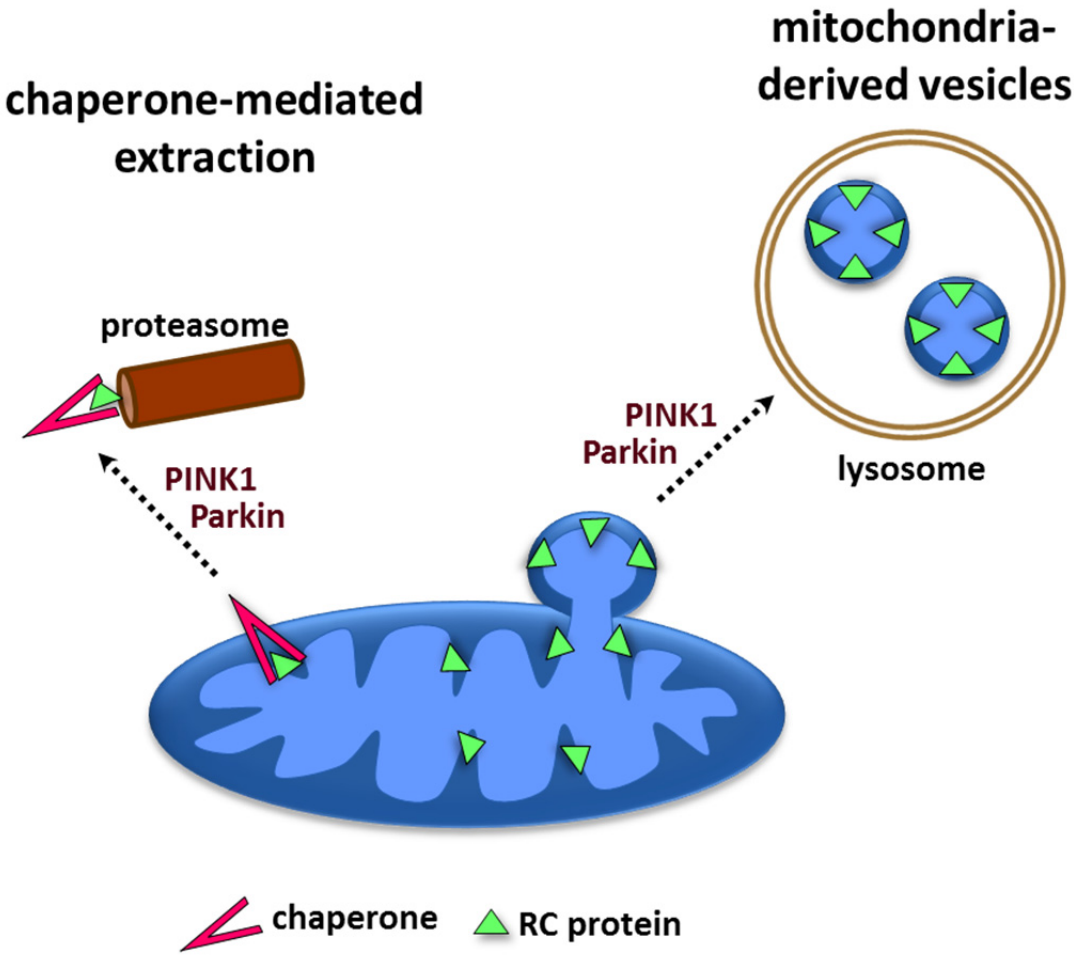

Figure 3.9. Possible mechanisms of selective RC turnover. 1) Chaperone-mediated extraction and proteasomal degradation. 2) Transport to the lysosome via mitochondria-derived vesicles.

been so surprised. All three reports of mitophagy stimulated by PINK1 overexpression alone involved simultaneous overexpression of Parkin (8, 48, 85). It is possible that even *in vitro*, increased PINK1 would not be sufficient to cause mitophagy without increased abundance of its downstream effector. The surplus of PINK1 compared to Parkin might also explain the mild impairment of mitochondrial turnover in the two experiments producing higher levels of PINK1 expression (studies 2 and 3). As ectopically expressed PINK1 is known to recruit Parkin (85), excessive amounts of PINK1 in the cytosol might conceivably sequester Parkin and prevent it from reaching mitochondria. Given that PINK1 is degraded in the mitochondrial matrix by Lon protease (Ruth Thomas, unpublished data), excess PINK1 could interfere with degradation of other Lon substrates. Similarly, large quantities of cytosolic PINK1 could overload the proteasome. Finally, there may be additional signals necessary for mitophagy induction *in vivo.*

MATERIALS AND METHODS

Drosophila strains and culture

Fly stocks were maintained on standard cornmeal-molasses food at 25°C. The $park^{25}$, $park^{rvA}$, $PINK1^{B9}$, $PINK1^{rv}$, $Atg7^{d4}$, $Atg7^{d77}$, $SOD2^{n283}$, and $SOD2^{wk}$ alleles have been previously described (68, 73, 154, 166, 167). $PINK1^{rv}$ and $park^{rvA}$ are the precise excision (revertant) controls for $PINK1^{B9}$ and $park^{25}$ respectively. The *UAS-PINK1*, *Hsp70-GAL4*, and *elav-GAL4* constructs have also been previously described (73, 168, 169). Other strains and alleles were obtained from the Bloomington Stock Center (Bloomington, IN). Detailed fly genotypes are listed in Table 3.3.

Table 3.3. Detailed fly genotypes.

Dataset	Experimental	Control	Comments
parkin	*If/CyO* ; $park^{25}/park^{25}$	*If/CyO* ; $park^{25}/park^{rvA}$	
Atg7	$Atg7^{d4}/Atg7^{d77}$	$Atg7^{d4}$/*CyOGFP* and $Atg7^{d77}$/*CyOGFP*	sibling controls
PINK1	$PINK1^{B9}$/Y	$PINK1^{rv}$/Y	
SOD2	$SOD2^{n283}/SOD2^{wk}$	*CyOActGFP/+*	sibling controls
Hsp70-GAL4 (no heat shock)	*UAS-PINK1#3*/*Hsp70-GAL4*	*UAS-PINK1#3/CyO* and *Hsp70-GAL4/CyO*	sibling controls
elav-GAL4	*elav-GAL4* ; *UAS-PINK1#3/+*	*elav-GAL4* ; *CyO/+*	sibling controls
Hsp70-GAL4 (heat shock)	*UAS-PINK1#2/Hsp70-GAL4*	*UAS-PINK1#2/CyO* and *Hsp70-GAL4/CyO*	sibling controls

Stable isotope labeling

Labeling was performed as in Chapter 2, with the following exceptions: the PINK1 overexpression experiments were performed at the temperatures designated in Table 3.2. For PINK1 overexpression study 3, a single one-hour heat shock was performed 71 h after the start of labeling. The agar plates with D3-leucine yeast paste were removed from the labeling flasks and replaced with plain agar plates. The flasks were placed in a 37°C incubator for 1 h, after which the flies were provided with fresh D3-leucine yeast and returned to 25°C for the remainder of the labeling period.

Sample preparation and mass spectrometry

Samples were prepared and mass spectrometry was performed as described in Chapter 2.

Protein half-life calculations

Half-life means for mitochondrial proteins were compared across genotypes using one-way nested ANOVA (biological replicates nested under genotypes). For significance testing, a separate half-life was computed for each biological replicate.

Protein abundance measurement

I used Topograph to calculate total abundance for each mitochondrial protein. Abundance was measured for individual peptides because the range of absolute peptide abundances within a protein can be large. Abundance values were normalized by dividing by the sum of all

abundance values in that biological replicate. These summed abundance values were not excessively variable across replicates (coefficient of variation 0.19 in the *Atg7* dataset).

For each peptide, I computed mean abundance at 240 h and 120 h and used the 240 h/120 h abundance ratio as a measure of change. I then grouped the peptide results by protein and performed paired sample *t* tests comparing abundance ratios in mutant and control flies. Significant differences in mean abundance ratio between genotypes were considered to reflect significantly different patterns of abundance over time. The *p* values were adjusted for multiple comparisons using the Benjamini-Hochberg step-up false discovery rate–controlling procedure with a false discovery rate of 5% (170).

There was no significant difference between mutant and control in abundance pattern over time for any mitochondrial protein in the *SOD2* dataset. In the *PINK1* dataset, 0.7% of mitochondrial proteins (1 of 145 proteins for which significance could be tested) showed a different abundance pattern over time in mutant and control. In the *parkin* dataset, 3.4% of mitochondrial proteins (5 of 149) showed different abundance patterns. Four of these were matrix proteins and one was a non-RC protein of the inner mitochondrial membrane (IM). In the *Atg7* dataset, 3.0% of mitochondrial proteins (5 of 166) showed different abundance patterns (2 sublocalization unknown, 1 IM, 2 RC). Abundance analyses were not performed for the PINK1 overexpression datasets.

As an additional test, I created an index of differential abundance change and compared fold change in half-life to differential abundance change for individual proteins (see Fig. 3.3). The differential abundance change index is calculated for each protein as follows:

$$\frac{\text{mean mutant abundance, 240 h}}{\text{mean mutant abundance, 120 h}}$$

$$\frac{\text{mean control abundance, 240 h}}{\text{mean control abundance, 120 h}}$$

If abundance of a protein decreased 20% in mutants but remained constant in controls, that would yield 0.80/1.00, a differential abundance change score of 0.80. The same score could result if abundance increased in both genotypes, but increased less in mutant than in control: 1.12/1.40 = 0.80.

A limitation of this method is the fact that I did not have "0 h" abundance data (data from unlabeled flies processed at the same time as the labeled flies). Such data would have enabled me to test for abundance change between 0 and 120 h as well as between 120 and 240 h. As mentioned in Chapter 2, I did not include unlabeled flies in my studies due to mass spectrometer time limitations. While I cannot rule out effects from differential abundance change between 0 and 120 h, I do not think it likely that such potential effects had major influence on the half-life findings. On informal sampling, fold change in half-life for a given protein did not alter substantially when half-lives were calculated using only the presumed 0-h values (0% D3-leucine) and the 120-h values (data not shown). It is thus unlikely that differential abundance changes occurring only between 0 and 120 h had a major impact on the half-life results.

Chapter 4: Tissue heterogeneity in mitochondrial protein turnover

The protein composition of mitochondria varies considerably across tissues in mammals (9), and RNA data suggest that mitochondrial composition varies across tissues in *Drosophila* as well (171). While analyzing my protein turnover data, I found evidence consistent with heterogeneous composition of *Drosophila* mitochondria in different tissues, and investigation of this serendipitous finding yielded additional insights into mitochondrial protein turnover.

FINDINGS

Patterns of *parkin* and *Atg7* effect suggest that mitophagy rates differ across tissues

When I began analyzing half-life data, I expected that *Atg7* and *parkin* mutations would produce the strongest effects on mitochondrial proteins with long half-lives. In accordance with a model proposed by Dr. Pallanck, I assumed that longer-lived proteins were turned over almost exclusively by mitophagy, and that shorter-lived proteins had shorter half-lives because much of their turnover depended on non-mitophagic mechanisms (Fig. 4.1a). Because the dependence of half-life on mitophagy rate would therefore be greatest for the longest-lived mitochondrial proteins, I expected *parkin* and *Atg7* fold change in half-life to increase as control half-life increased (Fig. 4.1b).

The data did not fit the predicted pattern. Instead, *Atg7* and *parkin* had their greatest effects on a group of relatively short-lived proteins (control half-lives under 250 h), and more uniform effects on other proteins. This pattern was most striking in *Atg7* (Fig. 4.2a), but present

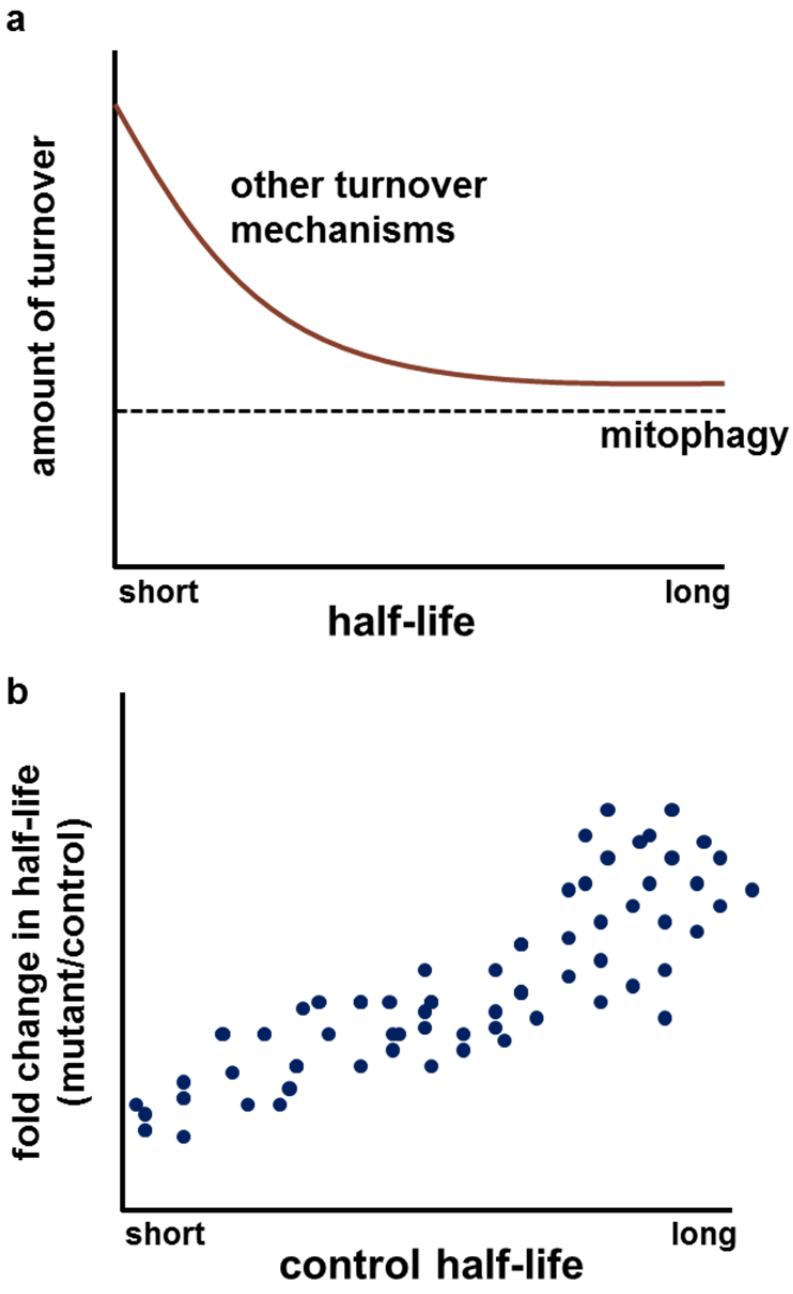

Figure 4.1. Model: *parkin* and *Atg7* will have greater effects on turnover of longer-lived mitochondrial proteins. This prediction presumes that short-lived mitochondrial proteins are short-lived only because they are turned over by nonautophagic mechanisms as well as by mitophagy. If so, the *absolute* effect of a decrease in mitophagy should be the same for all mitochondrial proteins **(a)**; however, the *relative* effect, as reflected by fold change in half-life, should be greatest on long-lived proteins **(b)**.

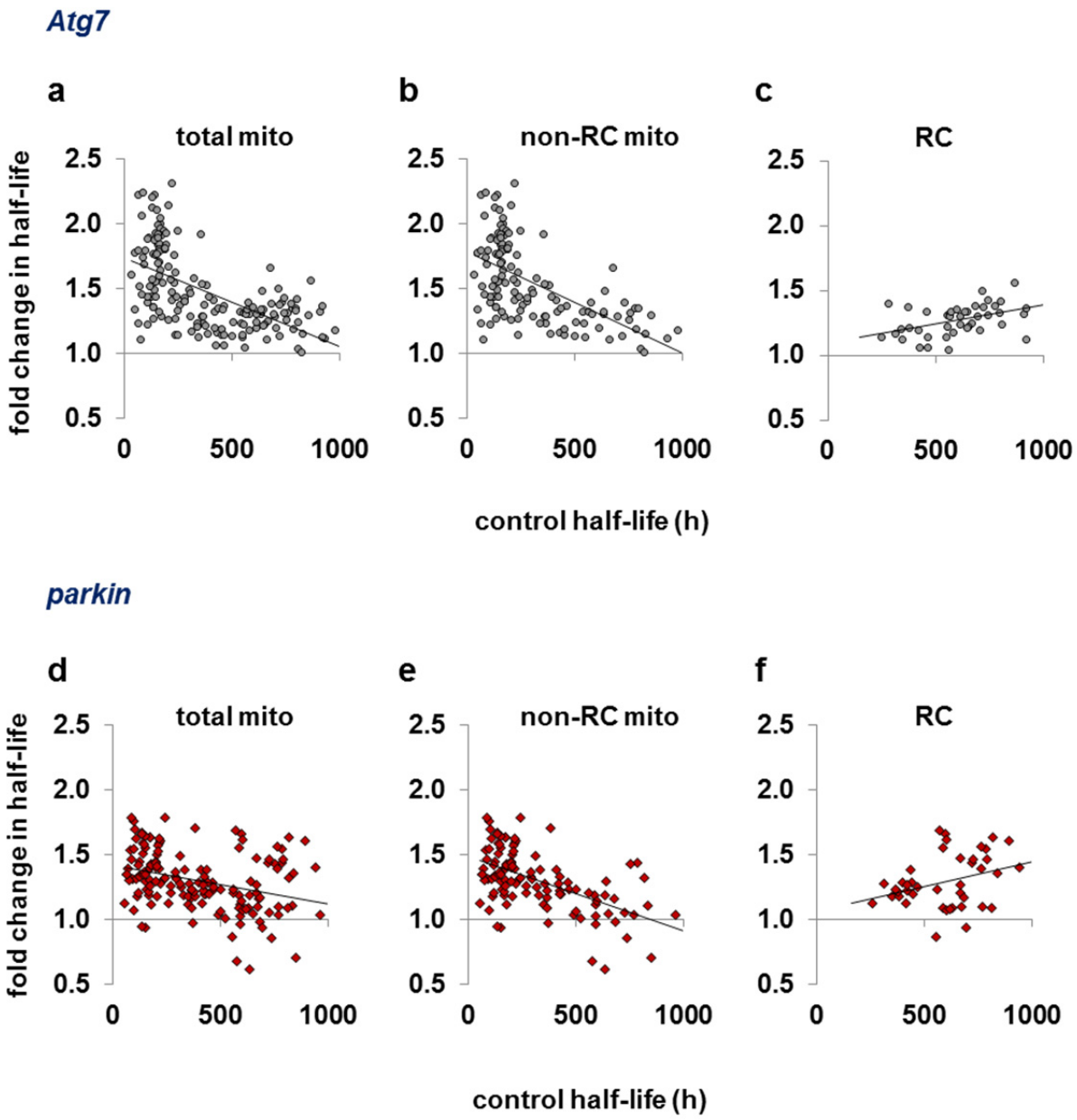

Figure 4.2. *parkin* and *Atg7* have greater effects on shorter-lived mitochondrial proteins. Fold change in half-life correlates negatively with control half-life for mitochondrial proteins overall **(a, d)** and non-RC mitochondrial proteins **(b, e)**. The correlation between fold change and control half-life is *positive* for RC **(c, f)** in both mutants. All correlations are significant (Pearson r, $p < 0.05$).

in *parkin* as well (Fig. 4.2d). When I analyzed the data in more detail, the picture became even more puzzling. Non-RC mitochondrial proteins showed the same pattern as mitochondrial proteins overall: strongest mutation effect on some but not all short-lived proteins (Fig. 4.2b,e). Only RC proteins showed a mild tendency toward the original prediction of greater effect with increasing half-life (Fig. 4.2c,f). I was unable to interpret this complex pattern until a 1987 paper offered a potential explanation.

The Grisolía group (172) found that the difference in half-life of two proteins in liver mitochondria could be explained by their differential expression in two types of hepatocytes. One protein was short-lived; this protein was enriched in "light hepatocytes," which were demonstrated to have a high autophagy rate. The other protein was long-lived, and was enriched in "heavy hepatocytes," which had a much lower autophagy rate. This paper reminded me that fly heads are complex mixtures of tissues, and that, as mentioned in Chapter 1, mammalian studies have found dramatically slower mitochondrial turnover rates in brain than in other tissues. I therefore hypothesized that differential tissue expression, combined with tissue-specific mitochondrial turnover rates, might explain the correlation between half-life and *Atg7/parkin* effect in my data. This hypothesis contains two separate assumptions:

1) The protein composition of fly mitochondria varies across the tissues of the head.
2) The mitophagy rate differs substantially between at least two head tissues.

Expression of mitochondrial proteins in brain varies substantially from protein to protein

I used FlyAtlas (171) to test the first assumption, gathering data on tissue expression of nuclear genes encoding the mitochondrial proteins in my datasets. I focused first on brain expression, normalizing the RNA values for isolated brain to those for whole heads. Thus, genes encoding proteins with high normalized brain expression (NBE) had high expression in brain compared to other tissues of the head, while those with low NBE were expressed primarily in head tissues other than the brain. Mitochondrial proteins showed substantial variation in NBE (Fig. 4.3), with values ranging from 0.02 to over 2.5. Notably, RC proteins had comparatively consistent brain expression, as might be expected given their central role in mitochondrial functioning.

Mitochondrial turnover appears to be slower in brain than in other tissues of the fly head

I next tested the hypothesis that the mitochondrial turnover rate varied across tissues of the fly head. I predicted that mitochondrial turnover would be slow in brain, and that proteins with strong brain expression would therefore have longer control half-lives. When I plotted control half-life against normalized brain expression, the proteins fell into two distinct groups (Fig. 4.4a). All mitochondrial proteins with NBE < 0.5 had control half-lives < 225 h, while only 12% of proteins with NBE ≥ 0.5 had comparably short half-lives (*Atg7* dataset). Even within the group of proteins with low brain expression, there was a positive association between brain expression and control half-life (Fig. 4.4b). Proteins with NBE ≥ 0.5, on the other hand, had a very broad range of control half-lives, and there was no significant relationship between NBE and half-life within the group (Fig. 4.4c). The distinctness of the grouping for mitochondrial

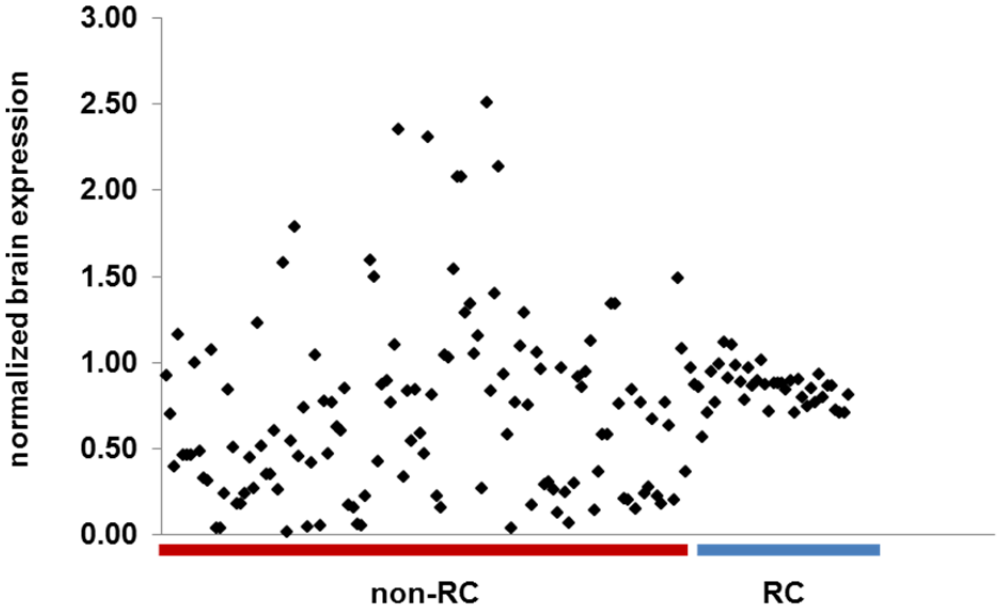

Figure 4.3. Mitochondrial proteins from fly heads show a wide range of variation in brain expression. Expression data from FlyAtlas for nuclear genes encoding mitochondrial proteins from the *Atg7* dataset. Normalized brain expression for a gene is the RNA value for isolated brain divided by the value measured in whole head.

Figure 4.4. Mitochondrial proteins with low brain expression have short half-lives.
(a) Control half-lives of mitochondrial proteins compared to their normalized brain expression (n = 165). Controls from the *Atg7* dataset, which had the largest number of mitochondrial proteins, were used; *parkin* and *PINK1* controls produced the same pattern (data not shown).
(b, c) Mitochondrial proteins with NBE < 0.5 **(b)** show a positive correlation between NBE and control half-life, but proteins with NBE ≥ 0.5 **(c)** do not (n = 55 and 110).
(d) Cytoplasmic proteins show a monotonic positive correlation between NBE and control half-life (n = 126).

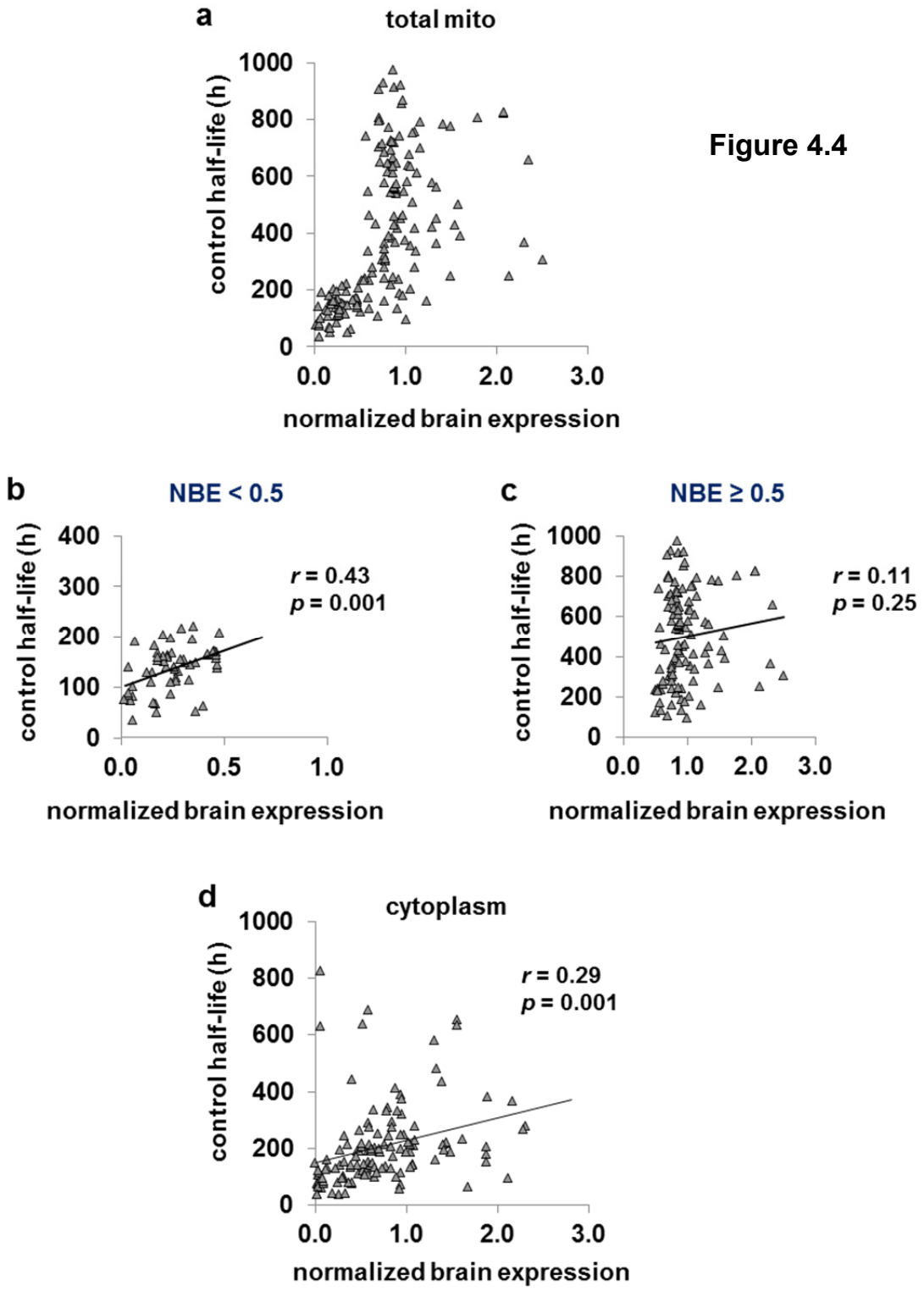
a
total mito
control half-life (h)
1000
800
600
400
200
0
0.0
1.0
2.0
3.0
normalized brain expression
b
NBE < 0.5
control half-life (h)
400
300
200
100
0
r = 0.43
p = 0.001
0.0
0.5
1.0
normalized brain expression
c
NBE ≥ 0.5
control half-life (h)
1000
800
600
400
200
0
r = 0.11
p = 0.25
0.0
1.0
2.0
3.0
normalized brain expression
d
cytoplasm
control half-life (h)
1000
800
600
400
200
0
r = 0.29
p = 0.001
0.0
1.0
2.0
3.0
normalized brain expression

Figure 4.4

proteins suggested that separate populations of mitochondria were undergoing turnover at different rates. Cytoplasmic proteins, by contrast, demonstrated a positive, monotonic correlation between NBE and half-life (Fig. 4.4d).

The data suggested, not surprisingly, that mitochondrial turnover rates were slower in brain than in other tissues of the head. FlyAtlas contains data for two head tissues other than brain: eye and fat body. Neither eye expression nor fat body expression had as sharply defined a relationship to control half-life as brain, but both had significant, nonmonotonic relationships with control half-life. Proteins with very low eye expression or high fat body expression generally had short half-lives (Fig. 4.5a,b). A detailed combinatorial analysis of the effects of tissue expression on half-life is beyond the scope of this discussion. However, a simple analysis suggests that mitochondrial turnover rates in fat body are likely substantially higher than those in brain or eye. Mitochondrial proteins with short half-lives (< 225 h) had significantly lower expression in brain and eye, and significantly higher expression in fat body, compared to longer-lived proteins (Fig. 4.5c).

Atg7 and *parkin* have greater effects on turnover of proteins with low brain expression

The idea that different tissues have different baseline mitochondrial protein turnover rates raises a related question. Do all tissues accomplish mitochondrial turnover primarily through mitophagy, or do other turnover mechanisms assume different degrees of importance in different tissues? If the proportion of mitochondrial protein turnover that occurs through mitophagy is equal in two tissues, then a given decrease in autophagy should cause an equal fold change in half-life regardless of the initial mitophagy rate. However, impairment of autophagy should

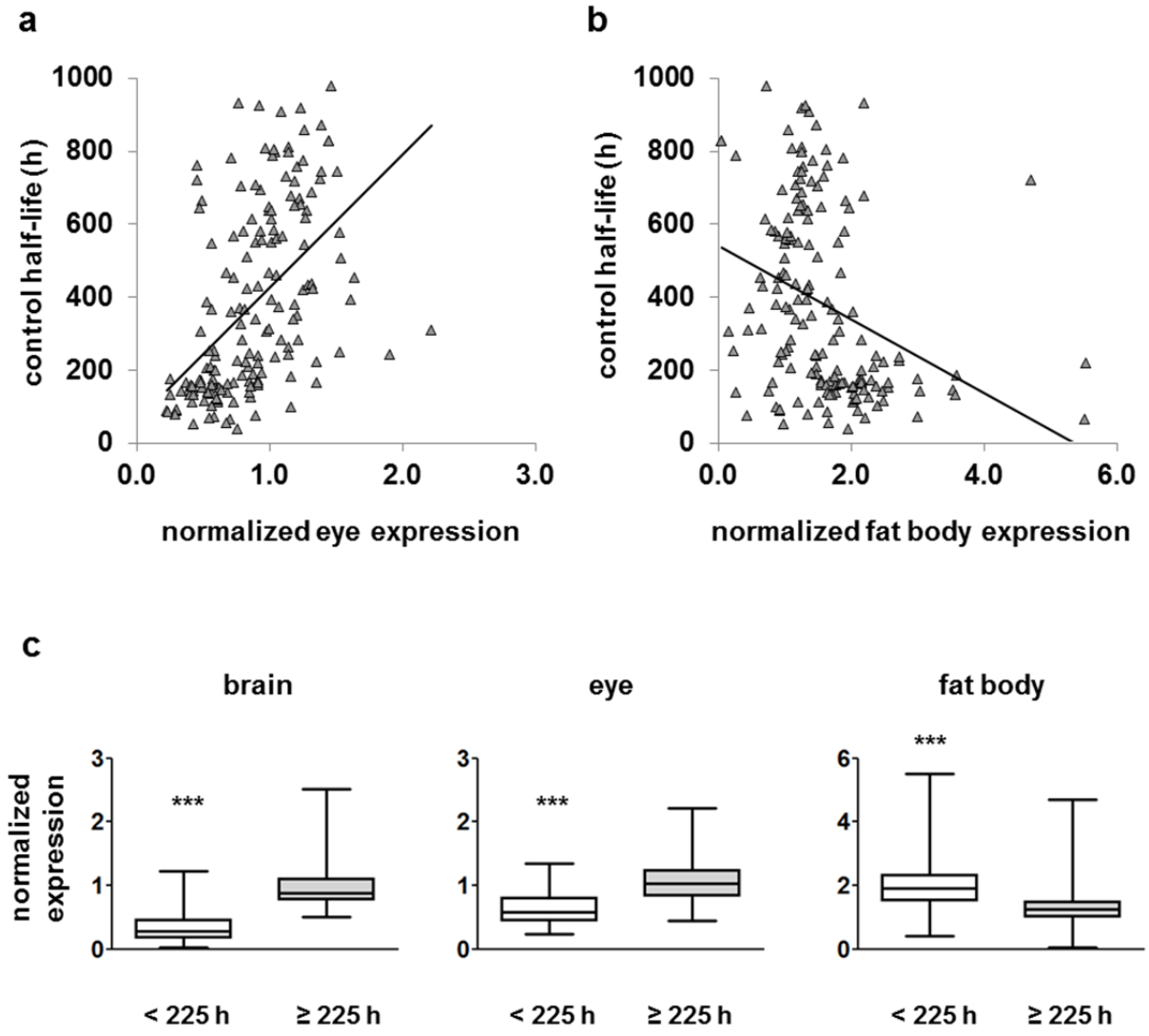

Figure 4.5. Short half-life in mitochondrial proteins is associated with lower expression in brain and eye, but higher expression in fat body. (a, b) Mitochondrial proteins with low normalized eye expression **(a)** or high normalized fat body expression **(b)** have short control half-lives. **(c)** Mitochondrial proteins with half-lives < 225 h have low expression in brain and eye, and high expression in fat body, compared to longer-lived proteins (n = 68 short-lived, 97 longer-lived). Mean normalized brain expression was 0.37±0.28 in short-lived proteins and 1.01±0.41 in longer-lived proteins. Mean normalized eye expression was 0.63±0.25 vs. 1.05±0.32, and mean normalized fat body expression was 2.01±0.91 vs. 1.28±0.60. ***$p < 0.0001$ by t test, short- vs. long-lived. Control half-life values, as in Fig. 4.4, are taken from the *Atg7* dataset.

cause a greater fold change in half-life in tissues that accomplish a high proportion of turnover through mitophagy, compared with tissues that rely more heavily on other mitochondrial turnover mechanisms.

To test whether the proportion of turnover through mitophagy differed across tissues, I examined the relationship of *Atg7* effect on half-life to normalized brain expression. Mean fold change in half-life in *Atg7* mutants was significantly greater for proteins with brain expression < 0.5 than for those with higher brain expression (Fig. 4.6a), and there was a strong negative correlation between brain expression and *Atg7* effect on half-life (Fig. 4.6b). This negative correlation was driven exclusively by non-RC proteins (Fig. 4.6c). As mentioned above, the RC proteins had a narrow range of brain expression values (all > 0.5), and RC proteins showed no relationship between expression and *Atg7* effect (Fig. 4.6d). There was also no correlation between *Atg7* effect and brain expression for cytoplasmic proteins (Fig. 4.6e). Thus, while the proportion of mitochondrial turnover accomplished through mitophagy appears to be low in brain, the proportion of cytoplasmic turnover accomplished through autophagy does not.

The same patterns of relationship between brain expression and mutation effect occurred in *parkin*, though to a lesser degree. Mean *parkin* fold change in half-life was significantly greater in proteins with NBE ≤ 0.5 (Fig. 4.7a), and there was a significant negative correlation between NBE and *parkin* effect on overall mitochondrial protein turnover (Fig. 4.7b,c). As with *Atg7*, neither RC mitochondrial proteins nor cytoplasmic proteins showed a relationship between brain expression and mutation effect (Fig. 4.7d,e). The greater effect of *parkin* in tissues with a high proportion of turnover through mitophagy lends further support to the idea that Parkin promotes mitophagy. No such relationship between mutation effect and brain expression

Figure 4.6. *Atg7* has greater effects on mitochondrial proteins with low brain expression. **(a)** Mean *Atg7* fold change in half-life is greater in mitochondrial proteins with NBE < 0.5 (mean 1.76±0.29, $n = 55$) than in proteins with NBE ≥ 0.5 (mean 1.34±0.19, $n = 110$). ***$p = 6.2 \times 10^{-22}$ by *t* test **(b, c)** *Atg7* effect on half-life in mitochondrial proteins overall **(b)** and non-RC mitochondrial proteins **(c)** has a strong negative correlation with brain expression ($n = 165$ total mito, 126 non-RC). **(d, e)** *Atg7* effect on half-life does not correlate with brain expression for RC proteins **(d)** or cytoplasmic proteins **(e)**. $n = 39$ RC, 126 cyto.

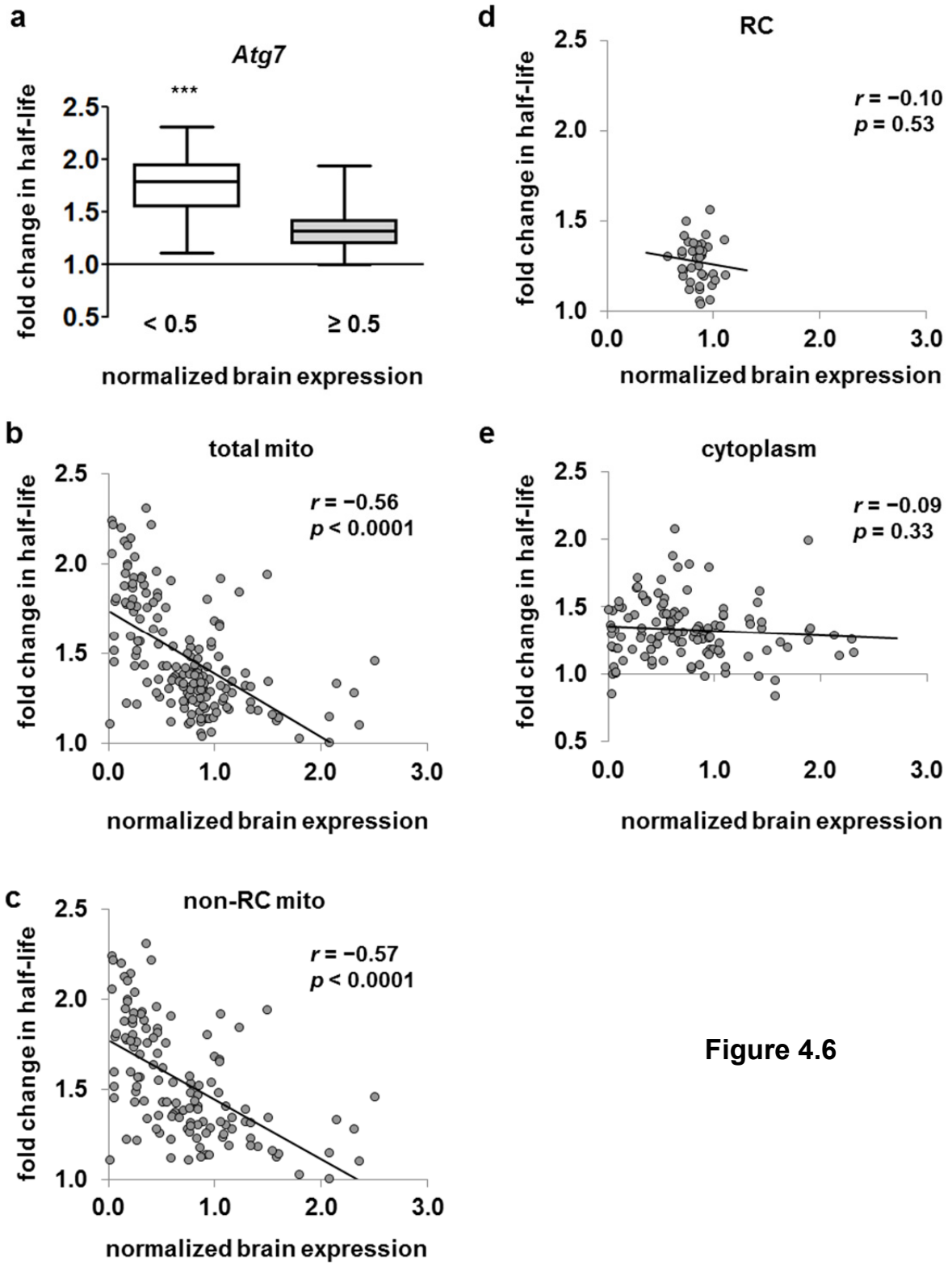
a
Atg7
***
fold change in half-life
2.5
2.0
1.5
1.0
0.5
< 0.5
≥ 0.5
normalized brain expression
b
total mito
r = −0.56
p < 0.0001
fold change in half-life
normalized brain expression
c
non-RC mito
r = −0.57
p < 0.0001
fold change in half-life
normalized brain expression
d
RC
r = −0.10
p = 0.53
fold change in half-life
normalized brain expression
e
cytoplasm
r = −0.09
p = 0.33
fold change in half-life
normalized brain expression
0.0
1.0
2.0
3.0

Figure 4.6

Figure 4.7. *parkin* has greater effects on mitochondrial proteins with low brain expression. **(a)** Mean *parkin* fold change in half-life is greater in proteins with NBE < 0.5 (mean 1.41±0.20, $n = 47$) than in proteins with NBE ≥ 0.5 (mean 1.25±0.21, $n = 107$). ***$p = 1.6 \times 10^{-5}$ **(b, c)** There was a significant negative correlation between NBE and *parkin* effect on overall mitochondrial protein turnover **(b)** and non-RC mito turnover **(c)**. **(d, e)** *parkin* effect on half-life does not correlate with brain expression for RC proteins **(d)** or cytoplasmic proteins **(e)**. $n = 154$ mito, 114 non-RC mito, 40 RC, 101 cyto. **(f)** Mitochondrial proteins in *PINK1* mutants show no relationship between brain expression and mutation effect ($n = 146$).

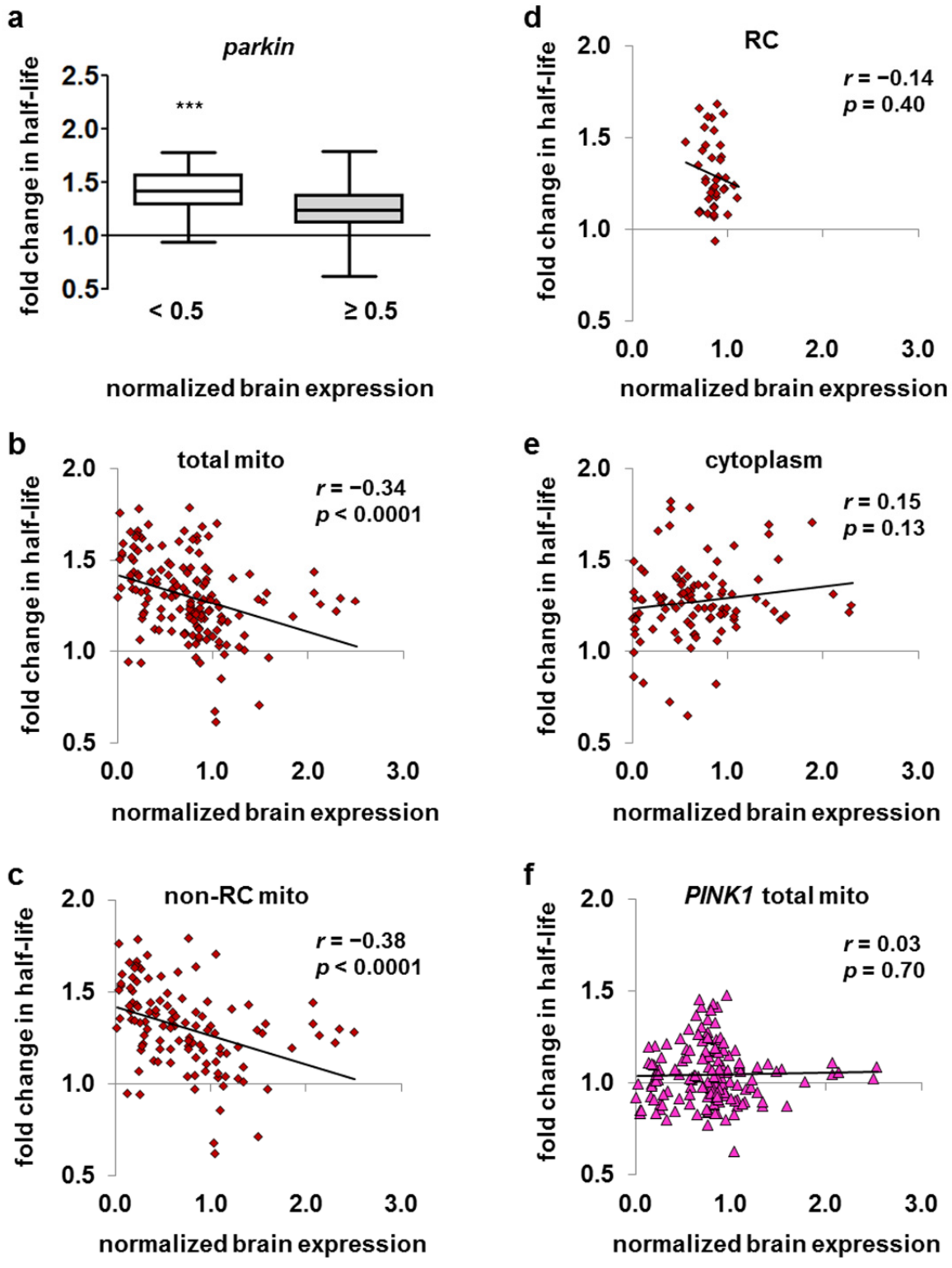
a
parkin
***
fold change in half-life
2.5
2.0
1.5
1.0
0.5
< 0.5
≥ 0.5
normalized brain expression
b
total mito
r = −0.34
p < 0.0001
fold change in half-life
2.0
1.5
1.0
0.5
0.0
1.0
2.0
3.0
normalized brain expression
c
non-RC mito
r = −0.38
p < 0.0001
fold change in half-life
normalized brain expression
d
RC
r = −0.14
p = 0.40
fold change in half-life
normalized brain expression
e
cytoplasm
r = 0.15
p = 0.13
fold change in half-life
normalized brain expression
f
PINK1 total mito
r = 0.03
p = 0.70
fold change in half-life
normalized brain expression

Figure 4.7

appeared in the *PINK1* data (Fig. 4.7f), consistent with the idea of a compensated mitophagy deficit in *PINK1*.

DISCUSSION

In a perfectly homogeneous sample, the effect of *Atg7* would probably follow our original model: greater mutation effect on longer-lived proteins. However, the heterogeneity of both mitochondrial composition and mitophagy rates across tissues makes it impossible for me to discern such a relationship. Even if I were to use brains rather than heads, there would still be considerable heterogeneity across cell types; the paper that alerted me to this issue compared two different types of liver cells.

It is tempting to point out the positive correlation between control half-life and *Atg7* or *parkin* effect in RC components as an example of the predicted autophagy-dependent pattern appearing in a homogeneously expressed group of proteins. However, even leaving aside the findings of selective RC turnover in Chapter 3, the pattern of effect in RC is probably better explained in ways other than the original hypothesis. RC components do not have truly uniform tissue expression, and *Atg7* effect on turnover of RC components correlates strongly with fat body expression ($r = 0.56$, $p = 0.0002$).

While tissue heterogeneity has prevented me from testing our original theory, analysis based on differential tissue expression has provided other useful information.

Total mitochondrial turnover is slow in brain

My findings suggest that, like mammals, *Drosophila* have different mitochondrial protein turnover rates in different tissues, with a particularly slow rate in brain. Low brain expression is the strongest predictor of short half-life in mitochondrial proteins from fly heads. As I noted in Chapter 3, even based solely on the half-lives of the longest-lived mitochondrial proteins, the physiological rate of mitochondrial turnover in fly heads appears to be low. If this rate is a weighted average of the rate in each tissue, and other tissues have faster mitochondrial turnover, then the turnover rate in brain must be slow indeed. In another similarity to mammals, a low rate of mitochondrial turnover in brain does not mean that general autophagy is sluggish in brain. Indeed, in mammals, general autophagy in brain has been shown to be vigorous and rapid (173). Similarly, while there is a positive correlation between NBE and half-life for cytoplasmic proteins, the cytoplasmic proteins with NBE $\geq$ 0.5 turn over much more quickly than the mitochondrial proteins in the same range of NBE (mean control half-life 271.9±146.4 cyto, 502.5±229.6 mito, $p = 1.1 \times 10^{-25}$ by *t* test).

The proportion of mitochondrial turnover accomplished through mitophagy is low in brain

Not only is overall mitochondrial turnover slow in fly brain, but relatively little of that turnover appears to occur through mitophagy. The extreme scatter in the half-lives of proteins with NBE $\geq$ 0.5 is a strong indication that the proportion of mitophagy vs. other turnover is low; if mitophagy were the predominant turnover mechanism, the rate of mitophagy would form a "ceiling" on the range of half-lives. This appears to be the case for the proteins with NBE < 0.5, none of which exceeds 225 h in control half-life. In addition, the effects of *Atg7* suggest that

mitophagy is responsible for less turnover in brain than in other tissues. Mean fold change in *Atg7* mutants for proteins with moderate to high brain expression is dramatically lower than the fold change for proteins with low brain expression. The turnover of brain mitochondria is thus less dependent on autophagy than is turnover of fat body mitochondria. An alternative explanation is that compensatory turnover mechanisms are more active and/or effective in brain.

Mitophagy rate is low in brain: implications

If we accept that overall mitochondrial turnover is slow in fly brain, and that mitophagic turnover is a low percentage of that turnover, then the absolute baseline mitophagy rate in fly brain must be low. This picture of mitochondrial turnover in brain contradicts the widespread and frequently unstated assumption that most mitochondrial turnover occurs through autophagy (174). It also clashes with current ideas about the PINK1-Parkin pathway's physiological role. A large number of journal articles and reviews have explicitly proposed failure of mitophagy as an explanation for the role of *PINK1* and *parkin* mutations in familial parkinsonism, and as a possible pathogenetic mechanism in sporadic Parkinson disease (e.g., (8, 38, 48, 175)). If mitophagy is not the primary mechanism for mitochondrial turnover in brain, then perhaps it is less critical to neuronal survival and health than more selective mechanisms of mitochondrial turnover. The evidence of *PINK1* flies suggests that impairment of protein-selective turnover alone can be sufficient to cause neurodegeneration.

MATERIALS AND METHODS

FlyAtlas expression data were obtained either through FlyBase or directly from FlyAtlas (171). For genes with more than one possible matching probeset, BLAST was used to choose one probeset, optimizing sequence coverage and matching, specificity, and number of isoforms matched. In some cases, no one probeset was clearly best, and/or all had poor numbers of Affymetrix "present calls." No expression values were recorded for such proteins. No values were available for mitochondrially encoded proteins. Brain, eye, and fat body values were all normalized to the value for whole head.

Note that FlyAtlas fat body values were measured from abdominal fat. Lacking specific data on head fat, I have made the assumption that expression patterns are reasonably similar in head fat. This may or may not be warranted.

Analyses of tissue expression effects on control half-life were performed using controls from the *Atg7* dataset because that dataset had the largest number of detected mitochondrial proteins. However, essentially identical results were obtained with *parkin* and *PINK1* controls (data not shown).

Chapter 5: PINK1-Parkin pathway effects on nonmitochondrial protein turnover

While my primary interest in *PINK1* and *parkin* mutants was the mitochondrial functions of PINK1 and Parkin, I also examined the effects of these mutations on nonmitochondrial proteins. As mentioned in Chapter 1, most of the many proposed substrates of Parkin are nonmitochondrial, and Parkin resides primarily in the cytoplasm. Parkin might thus play a role in nonmitochondrial protein turnover quite independent of its mitochondrial function, with or without involvement of PINK1.

FINDINGS

Testing for abundance change artifacts

As with mitochondrial proteins, there was little evidence for half-life artifacts caused by differential abundance change in nonmitochondrial proteins. In all four mutant/control datasets, shared variance between fold change in half-life and differential abundance change was < 3% (Fig. 5.1). No nonmitochondrial proteins in the *SOD2* dataset showed differential change in abundance. In the *parkin* dataset, 1.6% of nonmitochondrial proteins showed differential abundance change (6 of 372 testable); *PINK1*, 1.0% (3/306); and *Atg7*, 6.5% (28/432). The *Atg7* dataset had very low inter-replicate variability, and many of the statistically significant differences between *Atg7* and control are so small that they are of uncertain biological significance. For a complete list of nonmitochondrial proteins with significant differential abundance changes, see Tables 5.1-5.3. I will discuss differential abundance change

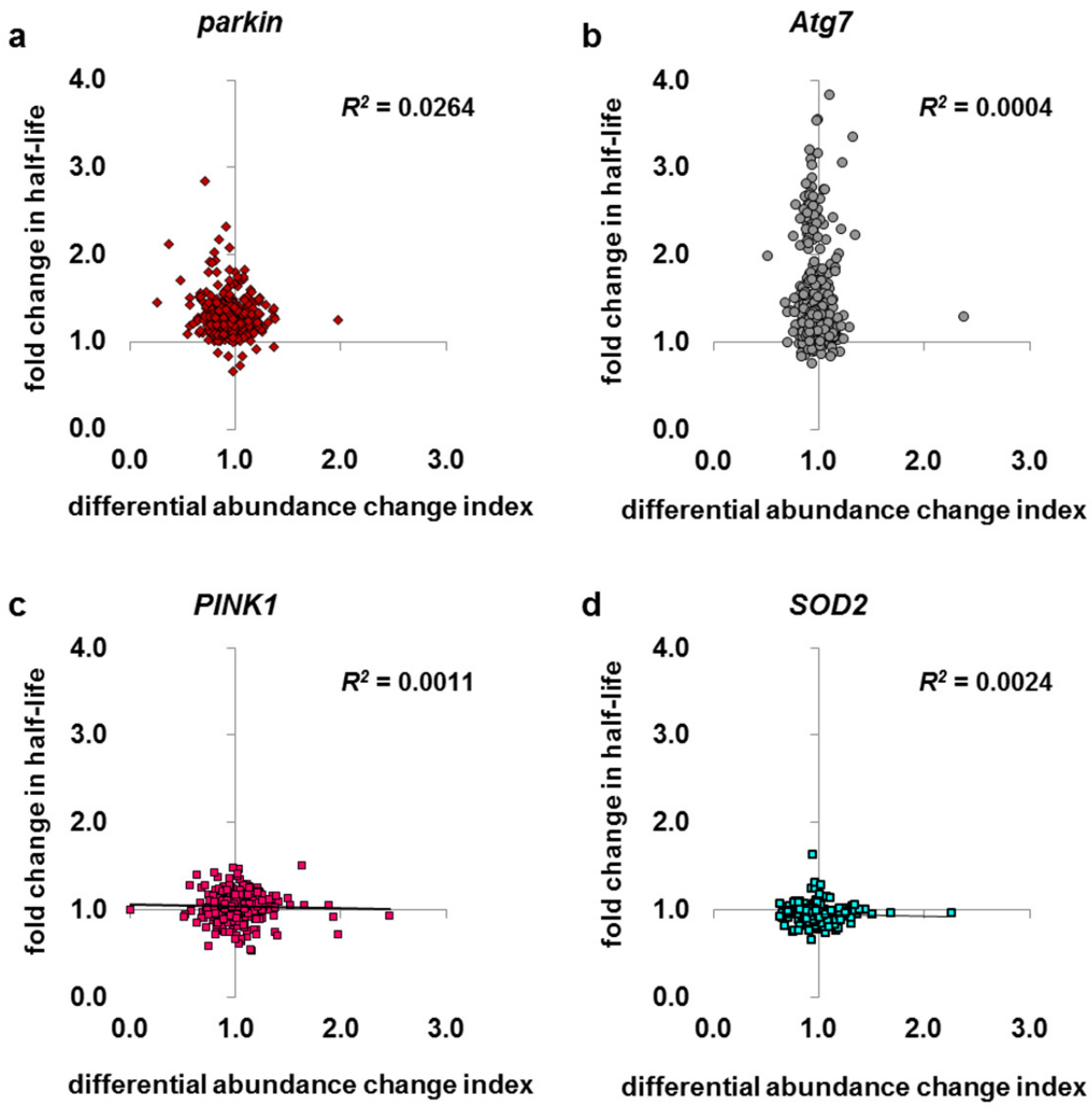

Figure 5.1. Differential abundance change does not appear to play a major role in mutation effects on nonmitochondrial protein half-life. Fold change in half-life vs. differential abundance change index for nonmitochondrial proteins in the *parkin*, *Atg7*, *PINK1*, and *SOD2* datasets. See Chapter 3, Materials and Methods, for a full explanation of the differential abundance change index. Note that, to avoid scale inconsistency, a single extreme outlier on the *x*-axis of the *Atg7* graph (coordinates 8.18, 1.35) is not displayed.

Table 5.1. Nonmitochondrial proteins with differential change in abundance over time between mutant and control (Part 1).

				Atg7 240 h/120 h abundance ratio		*parkin* 240 h/120 h abundance ratio		*PINK1* 240 h/120 h abundance ratio	
CG Number, Isoforms	**Name**	**Description**	**Loc'n**	***Atg7***	**control**	***parkin***	**control**	***PINK1***	**control**
CG4067-PA through -PE	pugilist	ortholog MTHFD1, MTHFD1L, MIS1 (folic acid metabolism)	cyto	0.85	0.99				
CG3989-PA	ade5	ortholog PAICS (purine biosynthesis)	cyto			0.84	1.38		
CG4104-PA	Trehalose-6-phosphate synthase 1	ortholog worm tps-1, -2 and yeast TPS1	cyto	0.70	0.80				
CG4265-PA, PB	Ubiquitin carboxy-terminal hydrolase	ortholog UCHL1, 3, 4	cyto, ?nucl	0.82	0.87				
CG32031-PA through -PF	Arginine kinase	creatine kinase family ortholog	cyto, extr			0.89	1.14		
CG3523-PA, PB	-	ortholog FASN (fatty acid synthase	cyto, LP, ?nucl	0.92	1.05				
CG9042-PA, PB, PC	Glycerol 3 phosphate dehydrogenase	ortholog GPD1, GPD1L	cyto, sarc	0.84	0.98				
CG12030-PA, PB	UDP-galactose 4'-epimerase	ortholog GALE, GAL10	cyto	0.76	0.89				
CG5362-PA	Malate dehydrogenase 1	ortholog MDH1	cyto	0.91	0.97				
CG7070-PA, PB	pyruvate kinase	ortholog PKM, PKLR	cyto	0.97	1.04				
CG11089-PA through PE	-	ortholog ADE17, ATIC (purine biosynthesis)	cyto, PM	0.83	0.94				
CG4696-PA, PB	Muscle protein 20	ortholog TAGLN2, -3 (actin binding)	cysk	0.91	1.08				
CG1977-PA	alpha-spectrin	ortholog SPTA1, SPTAN1	cysk, PM, etc.			0.87	1.05		

Table 5.2. Nonmitochondrial proteins with differential change in abundance over time between mutant and control (Part 2).

				Atg7 240 h/120 h abundance ratio		*parkin* 240 h/120 h abundance ratio		*PINK1* 240 h/120 h abundance ratio	
CG Number, Isoforms	**Name**	**Description**	**Loc'n**	***Atg7***	**control**	***parkin***	**control**	***PINK1***	**control**
CG13057-PA	retinin	no orthologs; cornea-specific	extr (corneal cuticle)	0.91	0.80				
CG6186-PA	Transferrin 1	no orthologs; immune/defense, iron transport	extr	0.95	1.23				
CG1668-PA, PB	Odorant-binding protein 19d	no orthologs	extr	0.97	1.40				
CG7592-PA	Odorant-binding protein 99b	no orthologs	extr					0.72	1.13
CG1469-PA,PB, PC	Ferritin 2 light chain orthologue	no orthologs; iron storage, immune	extr, intr. ferritin complex					0.68	1.20
CG11064-PA	Retinoid- and fatty acid-binding glycoprotein	ortholog vit-2; an apolipophorin	extr, endo. vesicle	0.75	0.97	0.82	1.00		
CG2233-PA	-	no orthologs	extr	2.53	1.07				
CG6917-PA	Esterase 6	ortholog K07C11.4; pheromone biosynthesis	extr	0.77	0.87				
CG1803-PA through PD	regucalcin	ortholog regucalcin; immune	extr	1.18	1.03				
CG5670-PA through PI	Na pump α subunit	ortholog ATP1- genes, ATP4A	PM, nucl, septate junction	0.98	0.85				
CG3620-PA through PE	no receptor potential A	ortholog PLCB1-4	rhab	0.97	0.86				
CG5125-PA, PB	neither inactivation nor afterpotential C	no orthologs; deactivation of rhodopsin signaling	rhab, cyto, cysk	0.90	1.04				

Table 5.3. Nonmitochondrial proteins with differential change in abundance over time between mutant and control (Part 3).

				Atg7 240 h/120 h abundance ratio		*parkin* 240 h/120 h abundance ratio		*PINK1* 240 h/120 h abundance ratio	
CG Number, Isoforms	**Name**	**Description**	**Loc'n**	***Atg7***	**control**	***parkin***	**control**	***PINK1***	**control**
CG8732-PA through PI	Acyl-CoA synthetase long-chain	ortholog ACSL3, ACSL4	ER, cytoplasm	1.16	1.01				
CG6988-PA	Protein disulfide isomerase	ortholog P4HB, PDIA2, PDILT; protein folding	ER, cyto, extr	0.97	1.05				
CG11796-PA, PB	-	ortholog HPD; degrades tyrosine	ER, Golgi	1.25	1.07				
CG32444-PA	-	ortholog GALM; aldose 1-epimerase activity	?	0.81	0.99				
CG10863-PA	-	ortholog aldo/keto reductases	?	0.96	1.12				
CG7322-PA	-	ortholog DCXR (?uronate cycle)	?	0.78	0.96				
CG7077-PA	retinol dehydrogenase B	ortholog DHRS11; rhodopsin biosynthesis	?	0.96	1.06				
CG6287-PA	-	ortholog phosphoglycerate dehydrogenase (PHGDH)	?	0.86	1.07				
CG6871-PA	catalase	ortholog CAT	ubiquitous					0.91	1.20

Localization abbreviations:

cyto = cytosol/cytoplasm, cysk = cytoskeleton, ER = endoplasmic reticulum, extr= extracellular, LP = lipid particle, nucl = nucleus, PM = plasma membrane, rhab = rhabdomere, sarc = sarcomere

intr. ferritin complex = intracellular ferritin complex
endo. vesicle = endocytic vesicle

further in cases where it appears relevant to an unusual finding about a particular protein group.

parkin effects on nonmitochondrial protein turnover

Lack of Parkin causes a moderate, significant impairment in turnover of most types of nonmitochondrial proteins (fold change in half-life ~1.25-1.30; Fig. 5.2). Ribosomal proteins were the only category of the 11 tested that did not show statistically significant change in half-life in *parkin* mutants vs. controls. The mean ribosomal protein fold change was 1.10±0.07, significantly lower than fold change for other nonmitochondrial protein groups (*t* test vs. all nonmitochondrial proteins, $p = 2.56 \times 10^{-8}$).

Conversely, *parkin* had an unusually strong effect on extracellular proteins (1.53±0.39; *t* test vs. all nonmitochondrial proteins, $p = 2.50 \times 10^{-10}$). Surprisingly, this effect was significantly larger than the mean *parkin* effect on turnover of mitochondrial proteins (*t* test, $p = 1.26 \times 10^{-6}$). There is a potential mild contribution of differential abundance change to the strong effect of *parkin* on extracellular proteins (11% of variance; Fig. 5.3); however, such a contribution does not appear sufficient to explain the full effect of *parkin* on this class of proteins.

Parkin has already been implicated in regulation of the endocytic/endosomal degradation pathway, which is responsible for turnover of most extracellular proteins (19). Specifically, Parkin regulates endocytic turnover of the epidermal growth factor receptor (EGFR) through monoubiquitination of the adaptor protein Eps15 (176). The effects of *parkin* mutation on extracellular region proteins were highly heterogeneous; fold change values for individual

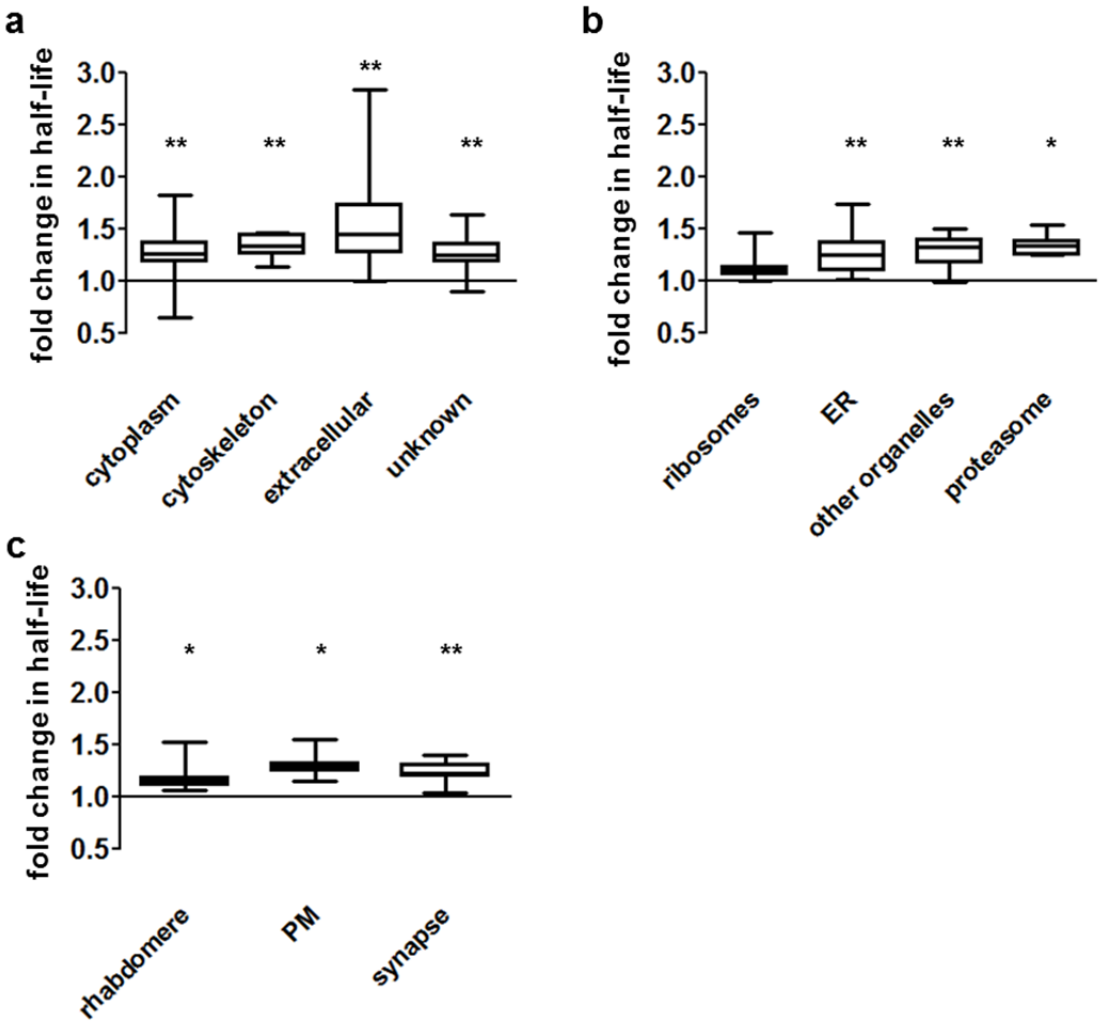

Figure 5.2. *parkin* effects on turnover of nonmitochondrial proteins. (a-c) Box plots depict median and upper and lower quartiles; whiskers represent extreme values. Proteins per category: cytoplasm 103, cytoskeleton 10, extracellular region 39, localization unknown 62, ribosomes 46, ER 16, other organelles (lysosome, nucleus, peroxisome) 16, proteasome 8, rhabdomere 14, PM 29, synapse 21. $*p < 0.05$, $**p < 0.005$

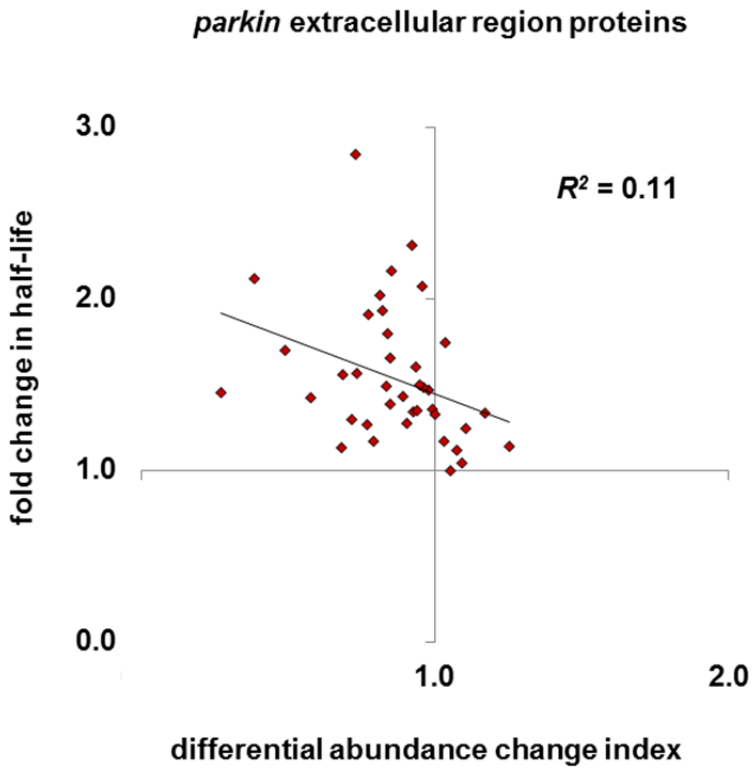

Figure 5.3. Differential abundance change may contribute modestly to the effects of *parkin* on extracellular region proteins. While the amount of shared variance is not large, the association between fold change in half-life and differential abundance change is negative. That is, proteins with a greater relative decrease in abundance in mutants tend to have larger fold change in half-life, raising the question of whether some of the apparent fold change might in fact be due to differential abundance change.

proteins ranged from 0.99 to 2.83. This is not entirely surprising, as extracellular cargo is taken up and trafficked via multiple pathways, with multiple separate regulatory mechanisms (177).

Parkin may also regulate aspects of endosomal turnover downstream of endocytosis; *parkin* mutants had impaired turnover of plasma membrane (PM) and synaptic proteins, many of which are also turned over via the endosomal route (19, 178). The effects of *parkin* mutation on these protein categories were much more moderate than the effects on extracellular proteins, but also much more consistent (1.30±0.09 for PM, 1.24±0.08 for synapse).

Atg7 effects on nonmitochondrial protein turnover

Like *parkin*, *Atg7* caused significant mean slowing of protein turnover in most nonmitochondrial protein categories (9 of 11; Fig. 5.4a-c). Only cytoskeleton (mean fold change 1.09±0.11) and rhabdomere (mean fold change 1.06±0.22) were not significantly affected. In the case of the rhabdomere, fold change in half-life may have been influenced by differential abundance change (R^2 = 0.32; Fig. 5.4d). The significance of this finding, and of the surprising number of rhabdomeric proteins with apparently accelerated turnover in *Atg7* mutants, is not clear.

By far, the strongest effects of *Atg7* were on ribosomes, ER, and peroxisomes (Fig. 5.4; mean fold change for peroxisomes 3.19±0.46, n = 3). Thus, while *parkin* has a greater effect on mitochondria than on other organellar targets of autophagy, the reverse is true for *Atg7* (Fig. 5.5). And while ER and ribosomes have similar mean effects in *Atg7*, ribosomal proteins are the only group without significant mean fold change in half-life in *parkin*.

parkin and *Atg7* effects on nonmitochondrial protein groups were frequently of comparable magnitude to the effects on mitochondrial proteins, an unexpected finding. However,

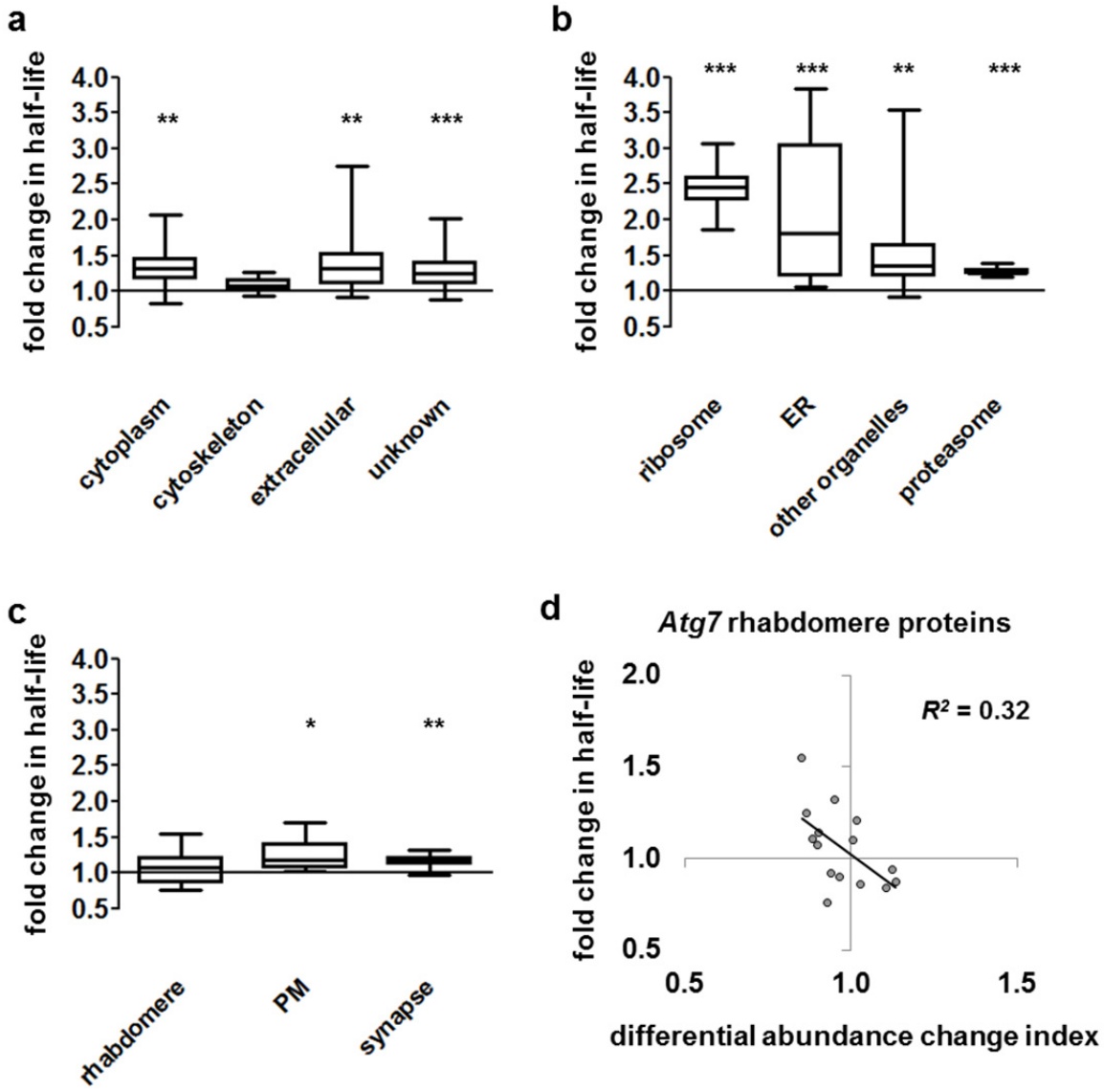

Figure 5.4. *Atg7* effects on turnover of nonmitochondrial proteins. (a-c) Fold change in half-life for 11 groups of nonmitochondrial proteins. Proteins per category: cytoplasm 127, cytoskeleton 10, extracellular region 33, localization unknown 78, ribosomes 47, ER 22, other organelles 19, proteasome 11, rhabdomere 15, PM 35, synapse 21. $*p < 0.05$, $**p < 0.005$, $***p < 0.0001$ **(d)** Rhabdomere proteins show a strong negative relationship between differential abundance change and fold change in half-life.

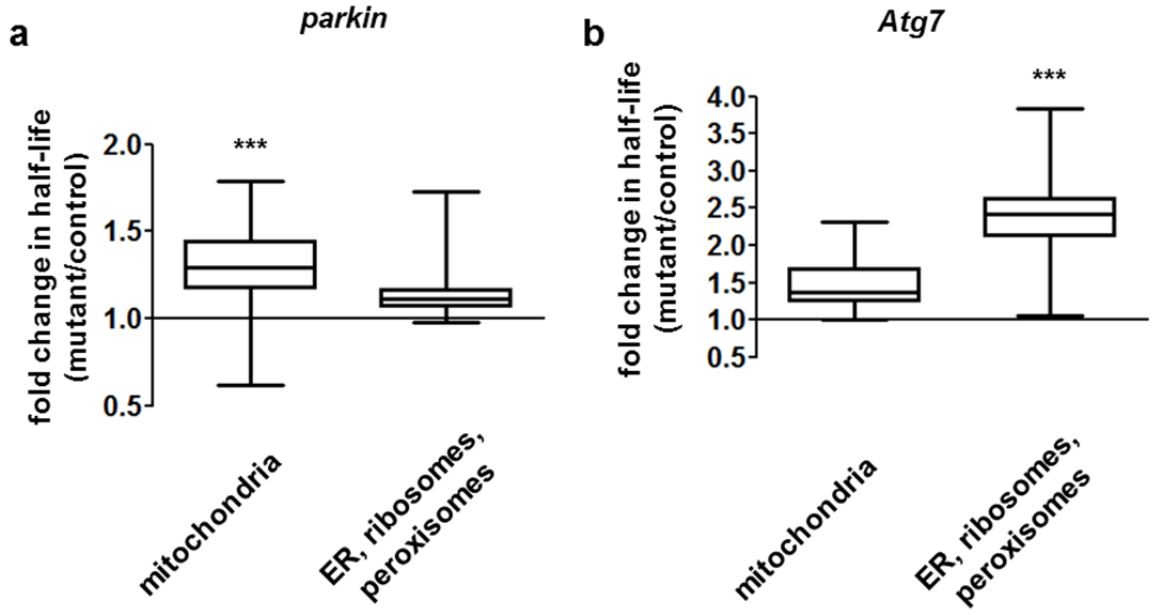

Figure 5.5. *parkin* has stronger effects on mitochondrial proteins than on proteins from other targets of autophagy; the converse is true of *Atg7*. Mean fold change in half-life for *parkin* **(a)**: mitochondria 1.30±0.22, ER/ribosomes/peroxisomes 1.14±0.14; for *Atg7* **(b)**: mitochondria 1.47±0.30, ER/ribosomes/peroxisomes 2.34±0.59. ***$p < 0.0001$

there was no significant correlation between *parkin* and *Atg7* effects for any of the 11 categories of nonmitochondrial proteins tested (Fig. 5.6). This suggested that the effects on *parkin* on nonmitochondrial proteins were distinct from the mitochondrial effects and were not mediated by *Atg7*. I will return to this subject in Chapter 6.

PINK1 effects on nonmitochondrial protein turnover

In general, *PINK1* had a far smaller mean effect on nonmitochondrial protein turnover than either *parkin* or *Atg7* (overall mean fold change for *PINK1* nonmitochondrial proteins: 1.04±0.15). Only three nonmitochondrial protein categories showed significant, though modest, half-life change in *PINK1* mutants: cytoskeleton, rhabdomere, and synapse (Fig. 5.7). Of note, *PINK1* mutants did not share *parkin* mutants' impairment in extracellular protein turnover. The mean fold change in half-life for extracellular region proteins was 1.04±0.21, and the highest fold change for an individual protein was 1.46. Furthermore, there was no correlation of *PINK1* and *parkin* effect for extracellular proteins (Fig. 5.8). Also, while mean synaptic protein turnover was significantly slower in *PINK1* than in control, the mean fold change was only 1.12±0.08. Parkin's potential role or roles in endosomal turnover may thus be independent of *PINK1*.

The only protein category that showed a significant positive correlation between the effects of *PINK1* and *parkin* was cytoplasmic proteins (Fig. 5.8). This correlation ($r = 0.48$) was as strong as the *PINK1-parkin* correlation for mitochondrial proteins ($r = 0.45$). *PINK1* and *parkin* may thus cooperate in turnover of some cytosolic proteins, possibly through the ubiquitin-proteasome system.

As in the case of mitochondrial proteins, the *PINK1-parkin* correlation for cytoplasmic proteins existed despite the fact that mean cytoplasmic protein turnover was significantly slowed

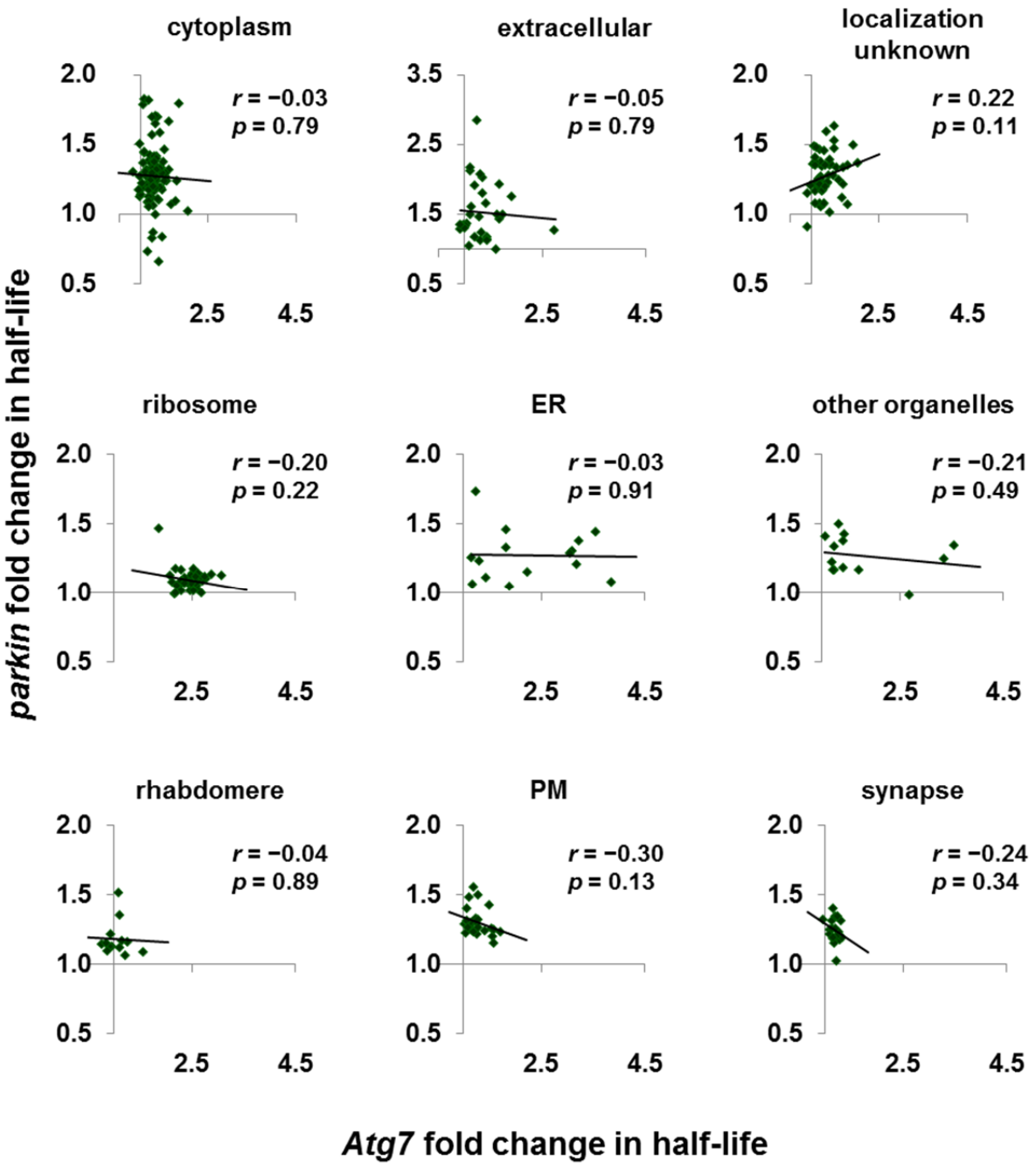

Figure 5.6. The effects of *parkin* and *Atg7* on nonmitochondrial protein turnover show no correlation. Proteins per category: cytoplasm 96, extracellular region 30, localization unknown 56, ribosome 40, ER 15, other organelles 13, rhabdomere 13, PM 26, synapse 18. All p values > 0.05.

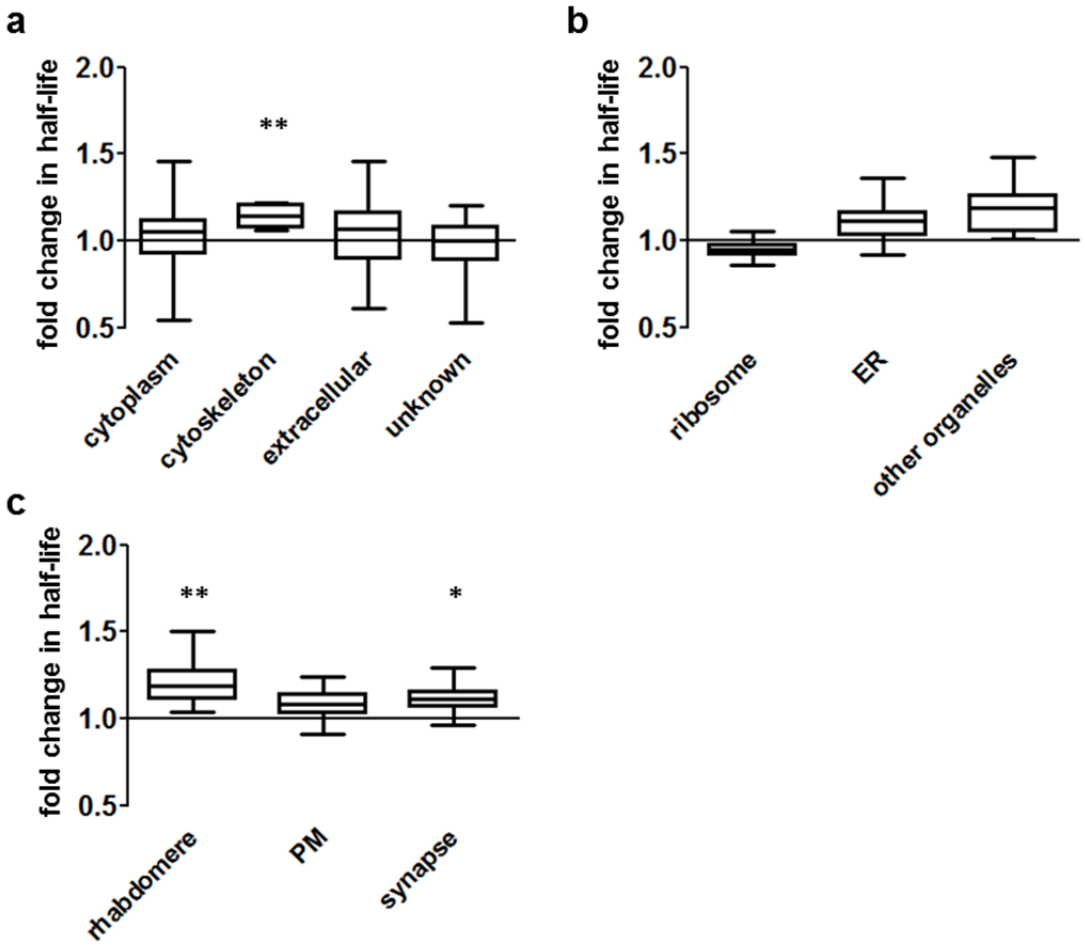

Figure 5.7. *PINK1* effects on turnover of nonmitochondrial proteins. (a-c) Fold change in half-life for 10 groups of nonmitochondrial proteins. Proteins per category: cytoplasm 88, cytoskeleton 8, extracellular region 25, localization unknown 47, ribosomes 39, ER 14, other organelles 9, rhabdomere 15, PM 26, synapse 21. *$p < 0.05$, **$p < 0.005$

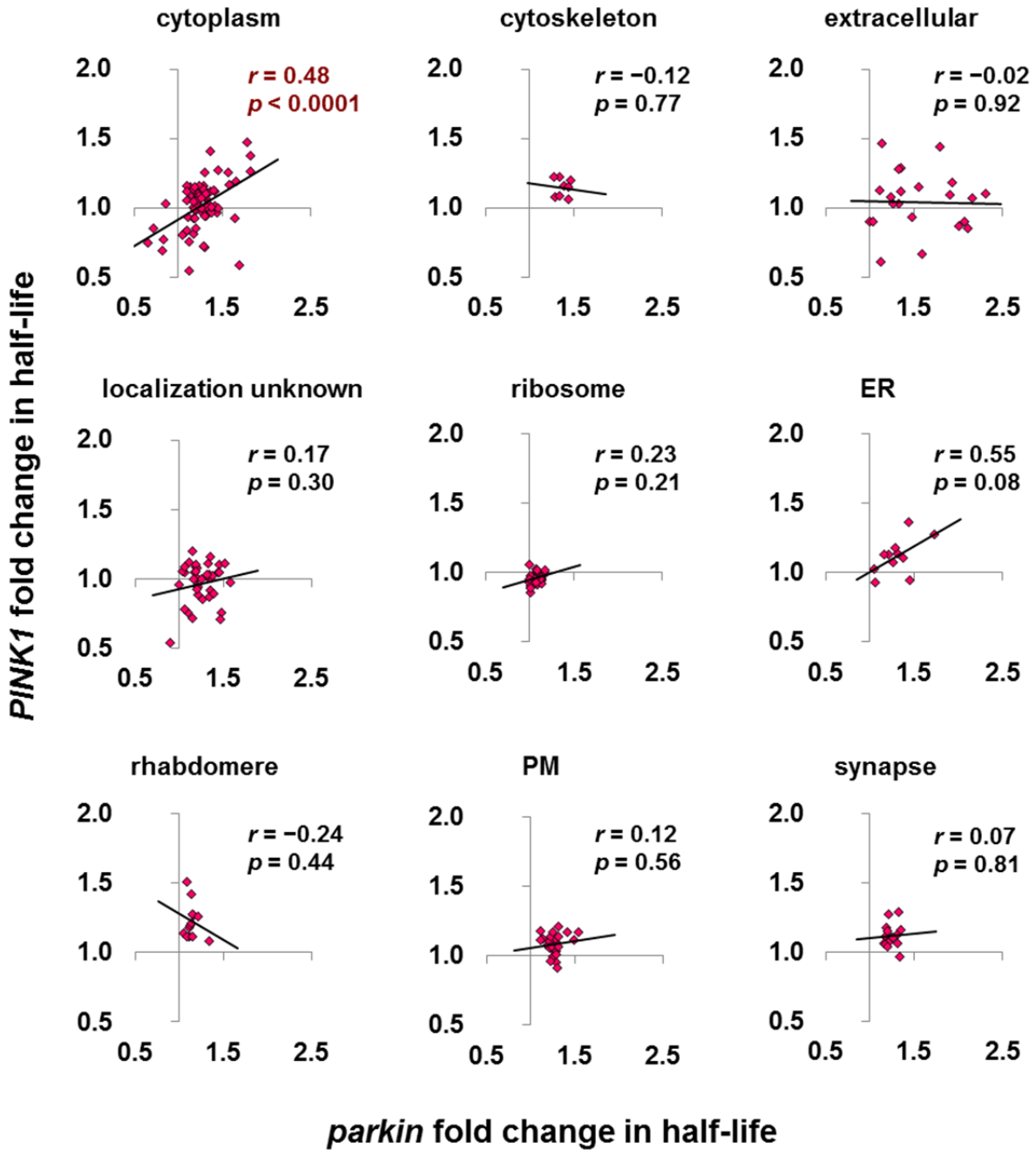

Figure 5.8. The effects of *parkin* and *PINK1* correlate for cytoplasmic proteins but not other nonmitochondrial proteins. Proteins per category: cytoplasm 75, cytoskeleton 8, extracellular region 22, localization unknown 40, ribosomes 31, ER 11, rhabdomere 13, PM 25, synapse 16.

in *parkin* mutants but not in *PINK1* mutants. This is consistent with the idea, discussed in Chapter 3, that general autophagy may be increased in *PINK1* mutants. I examined the nonmitochondrial protein data for more evidence on this question. I found that a large number of nonmitochondrial proteins turn over more quickly in *PINK1* than in control flies. Forty-two percent of cytoplasmic proteins and 87% of ribosomal proteins have a fold change in half-life < 1 in *PINK1*. By contrast, only 15% and 5% of proteins from the PM and synapse, which are not considered major targets of autophagy, have accelerated turnover in *PINK1* mutants. The evidence is not unmixed; 36% of extracellular proteins show fold change < 1 in *PINK1*, and only 14% of ER proteins have accelerated turnover. However, as noted in previous chapters, the ER has a very wide range of control protein half-lives, and also wide protein-to-protein variation in the effects of *Atg7*, suggesting turnover by multiple processes. The data are thus reasonably consistent with increased general autophagy in *PINK1* mutants.

SOD2 effects on nonmitochondrial protein turnover

Only one protein category showed a significant change between *SOD2* mutants and controls: nonmitochondrial proteins of unknown localization (Fig. 5.9). As this is almost certainly a heterogeneous group, and the *p* value was 0.0138, the biological significance of this finding is open to question. However, the *SOD2* dataset was of comparatively poor quality, with low numbers of proteins identified and high inter-replicate variability. Because 77% of nonmitochondrial proteins (and 87% of mitochondrial proteins) had fold change values < 1, the increases in nonmitochondrial protein turnover might well be significant if the study were repeated. These mild increases might be mediated by increased protein damage due to leakage of mitochondrial ROS, or by direct ROS-mediated stimulation of autophagy (179).

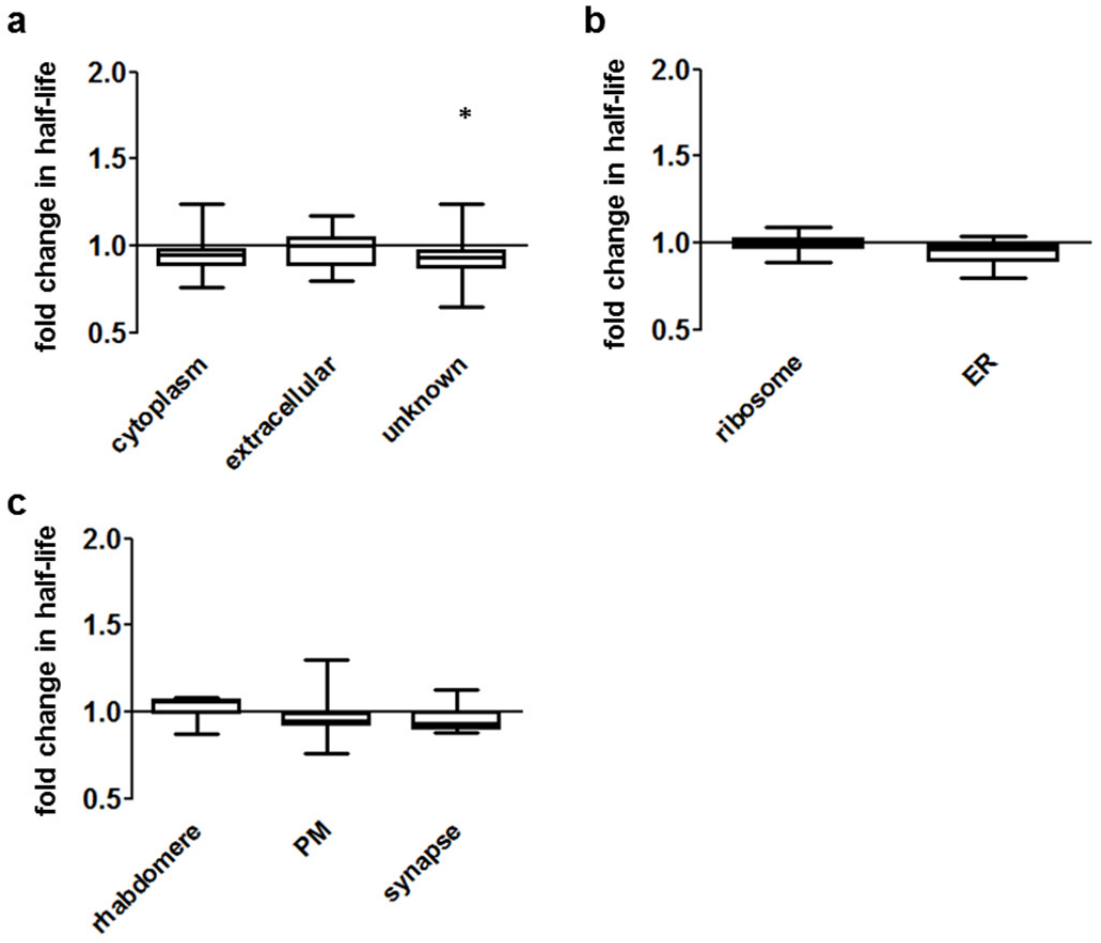

Figure 5.9. *SOD2* effects on turnover of nonmitochondrial proteins. (a-c) Fold change in half-life for 9 groups of nonmitochondrial proteins. Proteins per category: cytoplasm 66, extracellular region 13, localization unknown 35, ribosomes 19, ER 9, rhabdomere 9, PM 17, synapse 10. $*p < 0.05$

DISCUSSION

parkin and *PINK1*

When I began my research, I expected *parkin* mutants to show an isolated effect on mitochondrial protein turnover, with perhaps mild secondary effects on turnover of other proteins. I considered the nonmitochondrial proteins only as a useful negative control for the mitochondrial proteins. In retrospect, this idea was naïve, given the number of roles already posited for Parkin in the cytoplasm. In addition, mitochondria are so fundamental to cellular functioning that it would be difficult to disrupt them without causing substantial changes in other parts of the cell. Nevertheless, I was puzzled by the widespread and relatively consistent effects of *parkin* across nonmitochondrial protein categories, and by the similarity of the effect magnitudes between mitochondrial and nonmitochondrial proteins. The lack of correlations between *parkin* and *Atg7* effects for nonmitochondrial proteins suggested that the effects of *parkin* on nonmitochondrial proteins were mediated differently from its effects on mitochondrial proteins. In addition, if *parkin* effects on mitochondrial turnover were due to a defect in general autophagy, I would expect *parkin* to cause an *Atg7*-like pattern of turnover slowdown, with greater effects on ribosomal and ER proteins than on mitochondrial proteins. I was nevertheless left with the question of why *parkin* had relatively similar effects on turnover of so many disparate types of proteins. With the exception of ribosomal proteins, the nonmitochondrial category mean fold change values ranged from 1.18 to 1.34, though proteins in some categories were turned over primarily by the proteasome, in other categories by autophagy, and in still others by the endosomal degradation pathway.

I considered the possibility that decreased ATP production, caused by mitochondrial dysfunction, was impairing multiple types of turnover. There could be some decrease in ATP

levels in *parkin* mutant heads; *parkin* larvae have markedly decreased ATP in hemolymph (180), and fibroblasts from human *parkin* homozygotes also have subnormal ATP levels (181). Decreased ATP has also been reported in adult *PINK1* null flies (72, 73) and PINK1-deficient cells (182, 183), however, and nonmitochondrial protein turnover in *PINK1* mutant heads does not show broad, substantial impairment. In young *parkin* mutants, the degree of mitochondrial dysfunction in head tissues may not be sufficient to cause major impairment of cellular functions. Previous work in this laboratory found no gross brain defects and no abnormal TUNEL staining in adult *parkin* mutant brains, and the mutants' age-related neuron loss is restricted to DA neurons (80). Finally, if lack of ATP were the major factor in *parkin* mutants' nonmitochondrial protein turnover impairment, I would expect ribosomal turnover to be significantly impaired as well.

Another possible explanation for the widespread effects of *parkin* on nonmitochondrial proteins is impairment of the proteasome. Parkin has been reported to interact directly with the proteasome and to be required for full proteasome function (184-186), and excessive ROS from mitochondrial dysfunction can impair proteasomal function (187). Certainly, the proteasomal impairment might explain the deficit in cytoplasmic protein turnover; however, it is not as appealing an explanation for the comparable deficit in PM protein turnover. At this time, no single effect of *parkin* mutation appears to offer a good explanation for all the observed deficits. Instead, absence of Parkin seems to cause separate effects (direct or indirect) on proteasomal, autophagic, and endosomal turnover.

If selective RC turnover occurs through mitochondrial vesicles, one might speculate that Parkin plays a broad role in vesicle trafficking that would affect mitochondrial as well as

endocytic vesicles. However, this seems unlikely given the lack of evidence for endosomal pathway impairment in *PINK1* mutants, which share the RC turnover deficit.

Atg7

The fact that *Atg7* affects mitochondrial protein turnover less than turnover of other organellar proteins reinforces the idea that much mitochondrial protein turnover probably occurs through selective processes. In addition, mitochondria likely have a greater ability than other organelles to compensate for loss of autophagic turnover. For instance, the elaborate system of mitochondrial resident proteases does not have a parallel in other organelles. It is also possible that alternative autophagy can more efficiently compensate for lack of Atg7-dependent autophagy in turnover of mitochondria than in turnover of other organelles. Alternative autophagy has already been demonstrated to be involved in Nix-mediated mitophagy (22). Studies using *Drosophila* with mutations in components of the alternative autophagy pathway may help resolve this question.

MATERIALS AND METHODS

Nonmitochondrial proteins were categorized by their primary localization. Categories containing < 8 proteins in a given dataset were not analyzed. As noted in figure legends, "other organelles" refers to proteins from the lysosome, nucleus, and peroxisome. Abundance analyses were performed as in Chapter 3.

Proteins designated "extracellular" in this chapter were localized to the extracellular region and/or extracellular space. The two or three extracellular matrix proteins, which may turn over by different mechanisms than soluble extracellular proteins, were excluded. Proteins

designated “synaptic” are largely membrane bound, but include cytosolic proteins that operate primarily within the synapse.

Chapter 6: Heterozygous effects of *parkin* and *Atg7* mutations

For *parkin* and *Atg7* experiments, I used heterozygote controls to minimize genetic background effects, assuming that the heterozygotes would have essentially wild-type protein turnover. However, as I analyzed the data, I noticed that the half-lives of some mitochondrial proteins in the *parkin* and *Atg7* control groups seemed unusually long. The $park^{25}$ allele has previously been demonstrated to have some heterozygous effect: a single copy of $park^{25}$ almost completely suppresses the eye abnormalities caused by PINK1 overexpression (Ruth Thomas, unpublished data). I hypothesized that *parkin* and/or *Atg7* mutations might affect protein turnover even in heterozygotes, and that I might therefore be underestimating the effects of the homozygous mutations on mitochondrial protein turnover.

FINDINGS

parkin and *Atg7* have heterozygous effects on mitochondrial protein half-lives

I compared protein half-lives in heterozygote controls for *parkin* and *Atg7* to half-lives from the composite WT control data used in Chapter 1. This dataset is obviously not an ideal control, as mutant and control data should come from the same mass spectrometry run, and genetic background is not comparable. However, as the WT dataset includes data from three separate genotypes, genetic background differences should at least partially "average out."

Because the WT dataset was a composite dataset, it was not feasible to do significance testing with nested ANOVA, which requires a consistent number of individual half-life values for each protein. I therefore used paired sample *t* tests, but set a significance level of 0.005 to approximate the greater stringency of ANOVA.

Mitochondrial half-lives in *parkin* heterozygotes were significantly longer than in WT flies (Fig. 6.1a), with a mean heterozygote/WT half-life ratio of 1.16±0.15. While both RC and non-RC proteins were significantly affected (Fig. 6.1a), the effect on RC proteins was much stronger. RC proteins had a mean heterozygote/WT ratio of 1.26±0.12, compared to 1.12±0.14 for non-RC mitochondrial proteins. The difference between RC and non-RC was significant (*t* test, $p = 2.1 \times 10^{-7}$). I repeated these analyses for the *Atg7* heterozygotes, and found a strikingly similar pattern. Mitochondrial protein half-lives were again significantly longer in *Atg7* heterozygotes than in WT flies, with the strongest effects on RC proteins (Fig. 6.1b). The heterozygote/WT half-life ratios were 1.17±0.14 for all mitochondrial proteins, 1.29±0.15 for RC, and 1.13±0.12 for non-RC.

I next compared the fold change in half-life for *parkin* and *Atg7* homozygotes vs. the original heterozygote controls to the fold change vs. WT controls. As hypothesized, the fold change in half-life was significantly greater for both null mutants when compared to WT controls (Fig. 6.1c,d). The mean fold changes in half-life reported in Chapter 3 for all mitochondrial proteins were 1.30±0.22 for *parkin* and 1.47±0.30 for *Atg7*; the fold changes computed using WT controls were 1.52±0.21 and 1.69±0.28 ($p < 1 \times 10^{-19}$ for both genotypes). Furthermore, the pattern of effects on mitochondrial protein subgroups changed. In *parkin* nulls vs. heterozygote controls, non-RC and RC proteins had comparable mean fold change values (Fig. 6.1c). When I calculated fold change using WT controls, however, RC proteins showed significantly greater change in half-life than non-RC proteins (Fig. 6.1c). In *Atg7* nulls, by contrast, RC proteins showed a smaller fold change than non-RC proteins when the homozygotes were compared to heterozygote controls (Fig. 6.1d). When the homozygotes were compared to WT controls, there was no significant difference in mean fold change between RC and non-RC proteins ($p = 0.31$).

Figure 6.1. *parkin* and *Atg7* mutations affect mitochondrial protein half-lives even when present only in a single copy. (a, b) Mitochondrial protein half-lives in *parkin* heterozygotes **(a)** and *Atg7* heterozygotes **(b)** were significantly longer than in WT flies; the effect was largest on RC proteins. Mean half-life values for total mito, non-RC mito, and RC (n = 137, 96, and 41) were all significantly different between heterozygous mutants and WT controls by paired t test, $p < 0.005$ (see note in text on significance testing). Comparisons between mitochondrial subgroups: $^{**}p < 0.005$, $^{***}p < 0.0001$ by unpaired t test. **(c)** In *parkin* nulls vs. heterozygote controls, RC proteins do not differ significantly in mean fold change from non-RC proteins (RC 1.29±0.21, non-RC 1.31±0.21, $p = 0.62$). In *parkin* nulls vs. WT controls, however, RC proteins show significantly greater fold change (RC 1.63±0.21, non-RC 1.47±0.21, $p = 0.0036$). n = 41 RC, 96 non-RC. **(d)** In *Atg7* nulls, with heterozygote controls, RC proteins had a smaller fold change than non-RC proteins (1.28±0.11 vs. 1.52±0.30, $p = 5.5 \times 10^{-6}$). With WT controls, there is no significant difference between RC and non-RC (1.65±0.23 vs. 1.70±0.30, $p = 0.31$). n = 38 RC, 99 non-RC.

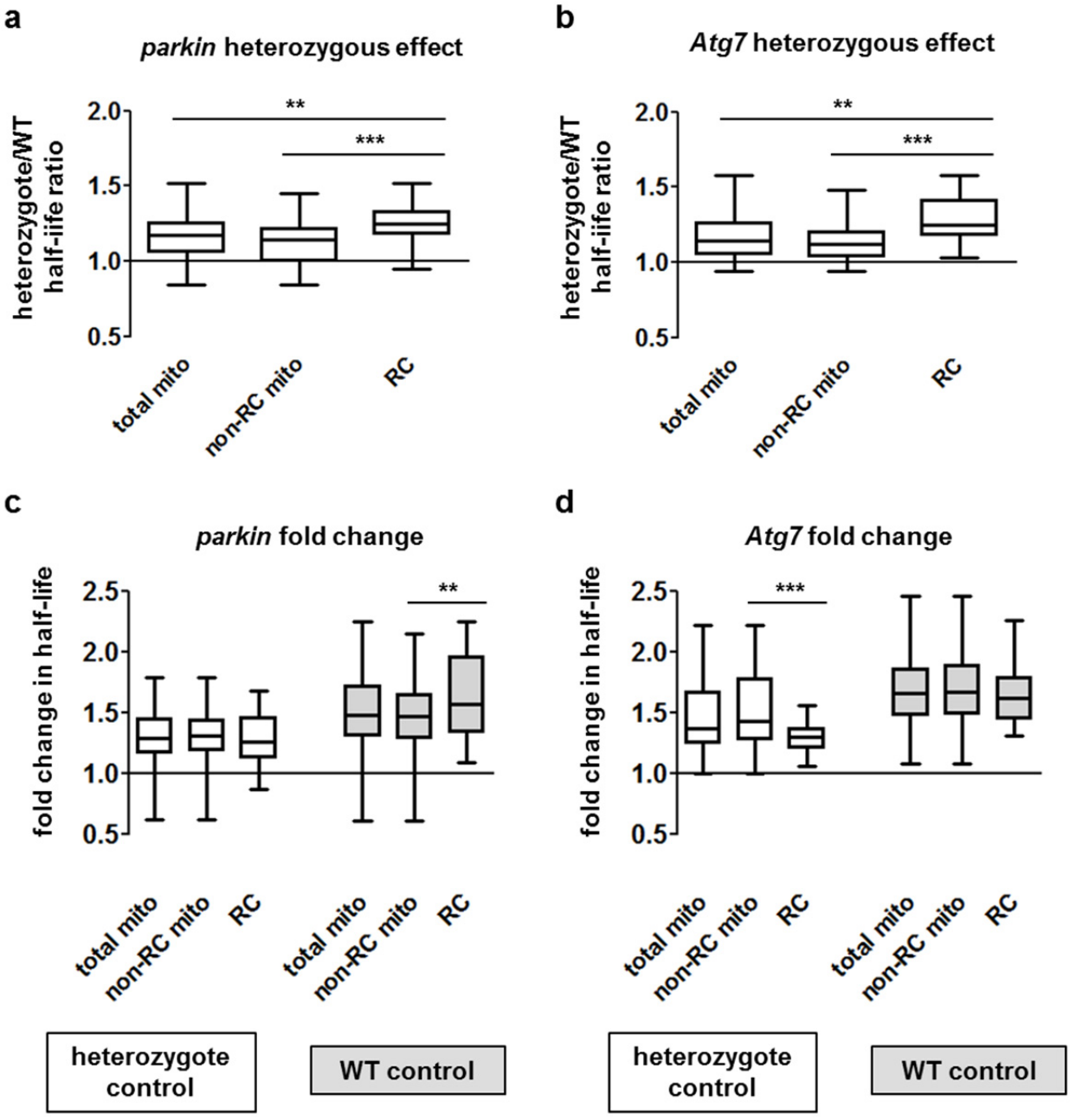
a
parkin heterozygous effect
heterozygote/WT half-life ratio
2.0
1.5
1.0
0.5
**
***
total mito
non-RC mito
RC
b
Atg7 heterozygous effect
heterozygote/WT half-life ratio
2.0
1.5
1.0
0.5
**
***
total mito
non-RC mito
RC
c
parkin fold change
fold change in half-life
2.5
2.0
1.5
1.0
0.5
**
total mito
non-RC mito
RC
total mito
non-RC mito
RC
heterozygote control
WT control
d
Atg7 fold change
fold change in half-life
2.5
2.0
1.5
1.0
0.5
***
total mito
non-RC mito
RC
total mito
non-RC mito
RC
heterozygote control
WT control

Figure 6.1

Thus, with heterozygote controls, *parkin* mutations appeared to have comparable effects on RC and non-RC mitochondrial proteins, and *Atg7* mutations appeared to have weaker effects on RC than on non-RC proteins. Using WT controls, however, *parkin* mutations appear to have greater mean effect on RC turnover, and *Atg7* mutations appear to have comparable effects between RC and non-RC mitochondrial proteins. The results with WT controls make better intuitive sense than the results with heterozygote controls; given the fact that *parkin* clearly had a selective effect on the RC, it seemed strange that the mean fold change for RC proteins was not greater than that for non-RC proteins (even non-RC proteins of comparable half-life).

RC proteins show a significant *parkin-Atg7* correlation when WT controls are used

I retested the correlation between *Atg7* and *parkin* using the WT controls for both mutants. The correlation for mitochondrial proteins overall was nearly identical to the correlation reported in Chapter 3 (Fig. 6.2a); for non-RC mitochondrial proteins, it was somewhat reduced though still clearly significant ($r = 0.34$ vs. WT, 0.42 vs. heterozygotes; Fig. 6.2b). On the other hand, RC proteins, which had not shown a significant *Atg7-parkin* correlation with heterozygote controls, now showed a strong correlation ($r = 0.53$; Fig. 6.2c). As the results for non-RC mitochondrial proteins demonstrated, comparing both null mutants to a single control did not necessarily produce stronger correlations. Thus, heterozygous effects of *parkin* and *Atg7* on the RC appear to have interacted in a manner that specifically obscured a correlation.

Importantly, the selective effect of *parkin* on RC proteins was still clearly present when I used WT controls (Fig. 6.2c). Of the 36 RC proteins available for comparison, 17 showed greater effect from *parkin* than from *Atg7* (47%, comparable to the 53% reported in Chapter 3). The overrepresentation of RC subunits among proteins with greater effect from *parkin* than *Atg7*

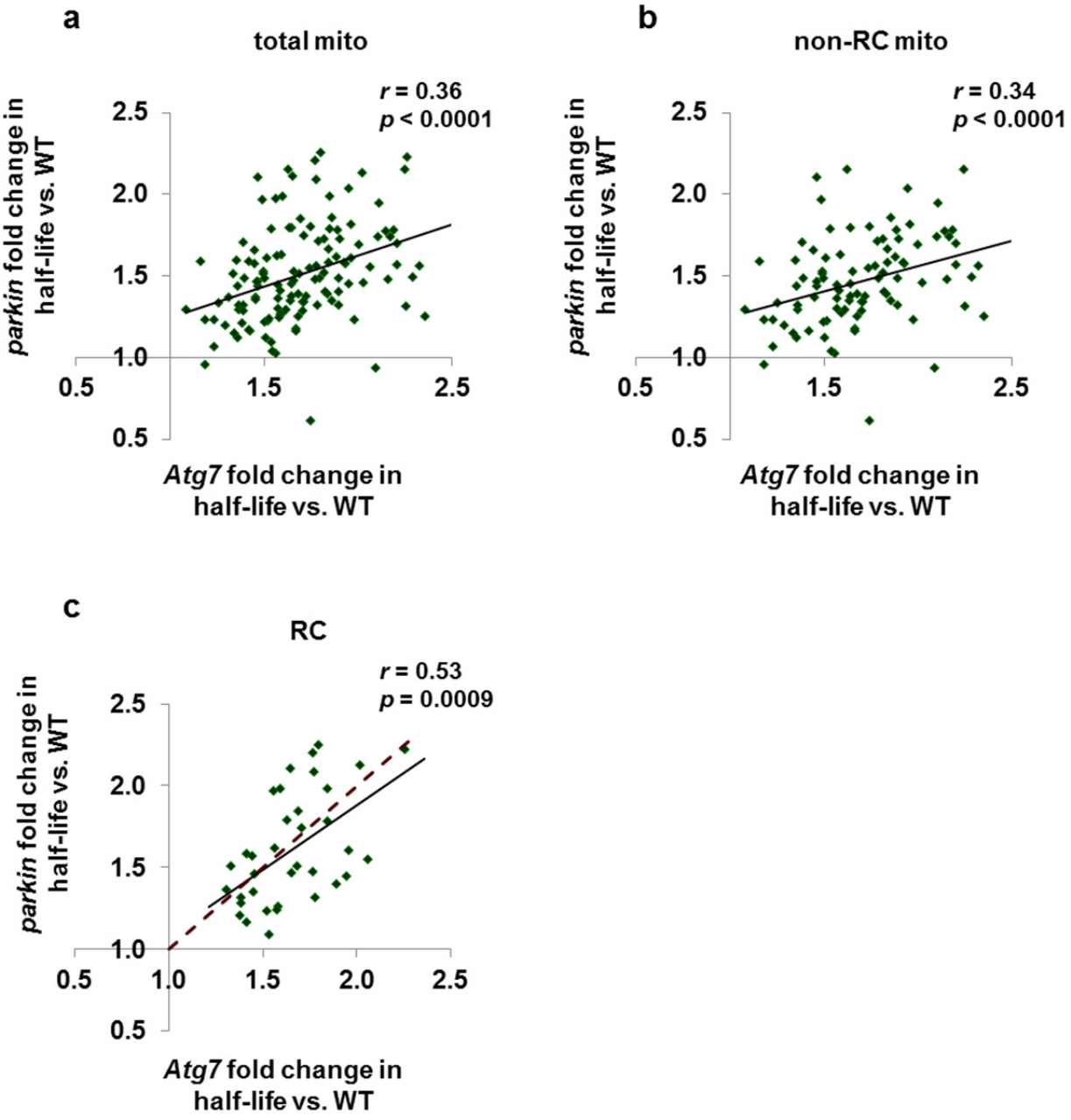

Figure 6.2. Mitochondrial protein correlations for *Atg7* vs. *parkin* when comparing both mutants to a WT control. (a-c) *parkin* and *Atg7* effects on individual proteins correlated significantly for mitochondrial proteins overall **(a)**, non-RC mitochondrial proteins **(b)**, and RC proteins **(c)**; n = 130, 94, and 36 proteins respectively. **(c)** Selective *parkin* effect on the RC is still evident when using WT controls. The dashed red line indicates equal effect from both mutations. The half-lives of proteins above the dashed line are more greatly influenced by *parkin* than by *Atg7*.

remained statistically significant with WT controls (37 total proteins *parkin* > *Atg7;* 10 RC predicted, 17 detected; $\chi^2 = 0.019$).

The *parkin*-*Atg7* correlation for RC with WT controls, as well as the RC-selective heterozygous effect of *Atg7,* suggested that the selective turnover of RC components by Parkin might be partially mediated by autophagy. I therefore tested whether the effect of *Atg7* null mutations on RC proteins was greater for membrane-bound subunits, as was the case for *parkin*. *Atg7* did have a slightly greater effect on membrane-bound subunits (Fig. 6.3). However, the difference was barely significant when using heterozygous controls and just missed significance when using WT controls. The heterozygous effect itself was the same for membrane and nonmembrane subunits (heterozygote vs. WT half-life ratio 1.30±0.18 membrane, 1.28±0.12 nonmembrane, $p = 0.70$). Thus, the heterozygous effect of *Atg7* is equal for membrane and nonmembrane RC proteins, but the homozygous effect is slightly biased toward membrane proteins. The significance of this finding is as yet unclear to me. Nevertheless, the strong heterozygous effect itself suggests that *Atg7* makes some contribution to selective RC turnover.

parkin and *Atg7* have mild heterozygous effects on nonmitochondrial proteins

I next tested whether *parkin* and *Atg7* also had heterozygous effects on nonmitochondrial proteins. *parkin* mutation had mild heterozygous effects on a number of nonmitochondrial protein groups (overall average: 1.08±0.18). Four of 10 groups had significant difference in half-life between heterozygote and control at the $p < 0.005$ level: cytoplasm, localization unknown, PM, and synapse (Fig. 6.4).

The *Atg7* heterozygous effects on nonmitochondrial proteins were slightly larger (overall mean: 1.11±0.15), and differences for 5 of 8 testable groups reached significance (Fig. 6.5). The

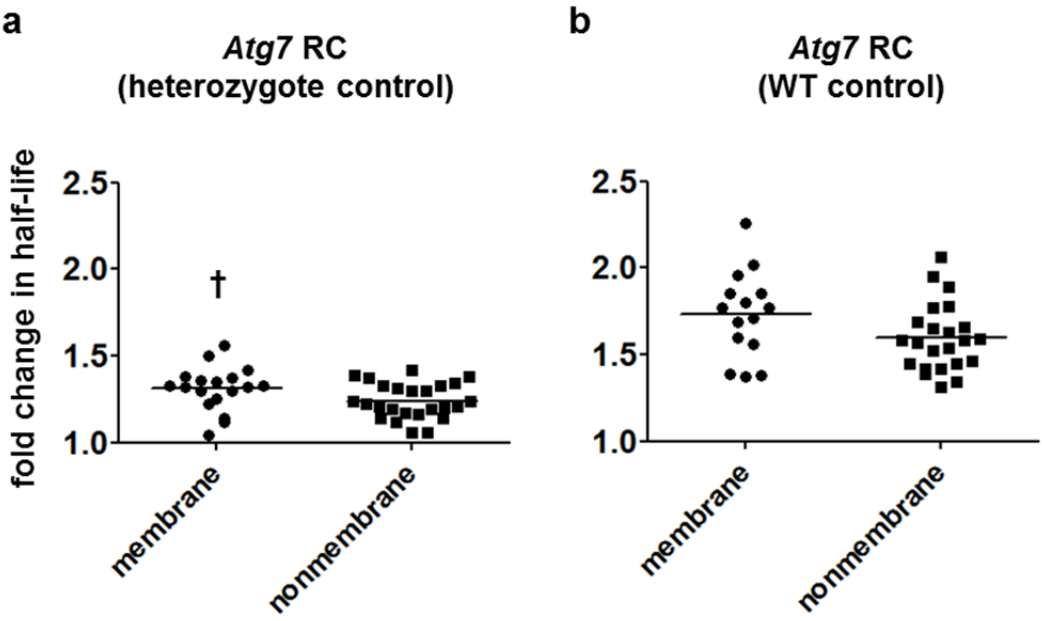

Figure 6.3. *Atg7* has a slightly greater effect on turnover of membrane-bound than nonmembrane RC subunits. With heterozygote controls **(a)**, the difference is just significant ($p = 0.0489$); with WT controls **(b)**, it just misses significance ($p = 0.0645$). Mean fold change values with heterozygote controls: 1.31±0.13 membrane ($n = 18$) and 1.24±0.10 nonmembrane ($n = 25$). Mean fold change values with WT controls: 1.73±0.25 membrane ($n = 15$) and 1.60±0.20 nonmembrane ($n = 23$).

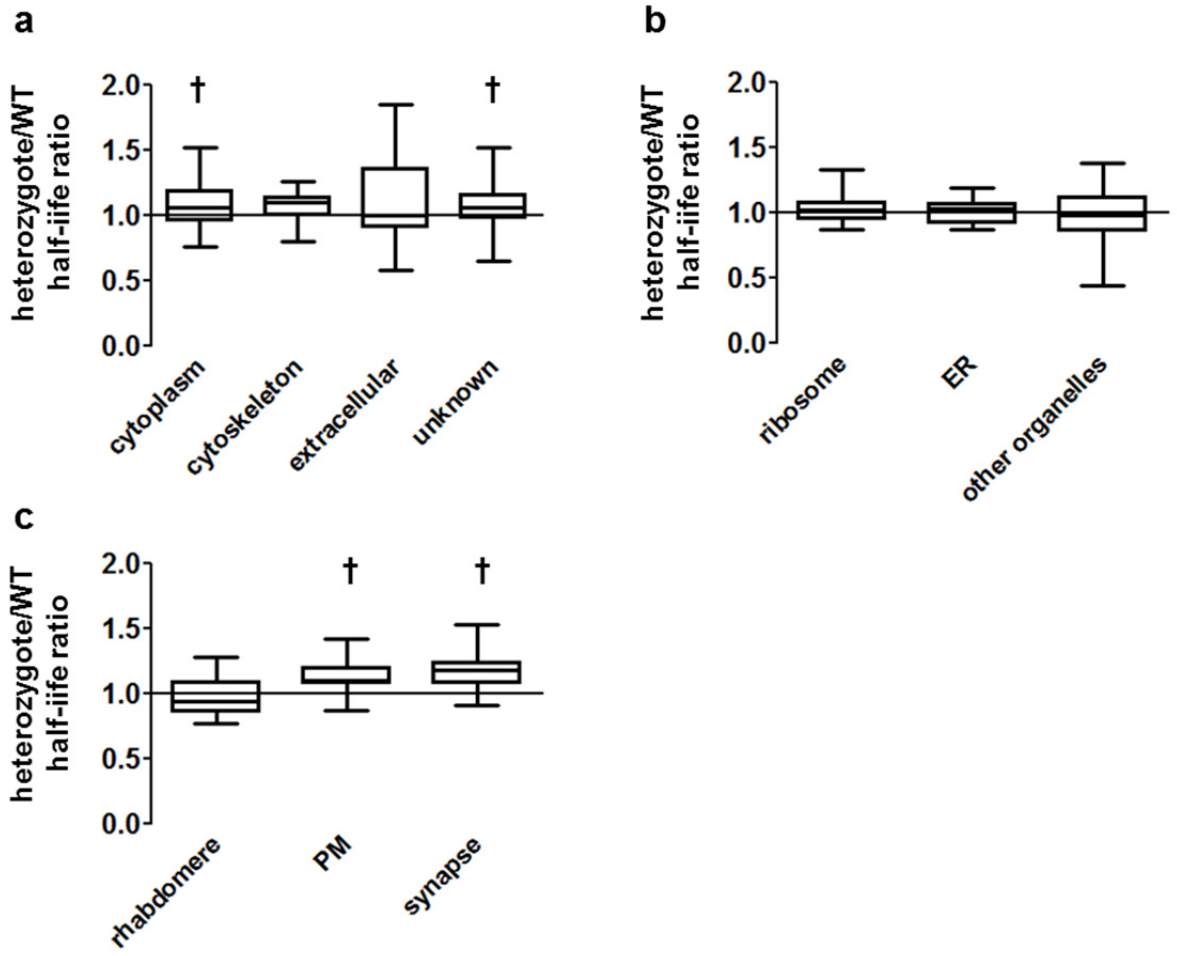

Figure 6.4. Heterozygous effects of *parkin* on nonmitochondrial proteins. (a-c) Mean *parkin* heterozygote/WT half-life ratios for nonmitochondrial protein groups; 4 of 10 groups show a significant difference in half-life between heterozygote and WT. Number of proteins: cytoplasm 83, cytoskeleton 10, extracellular region 26, localization unknown 44, ribosome 34, ER 14, other organelles (lysosome and nucleus) 9, rhabdomere 13, PM 25, synapse 17. †$p < 0.005$ by paired *t* test

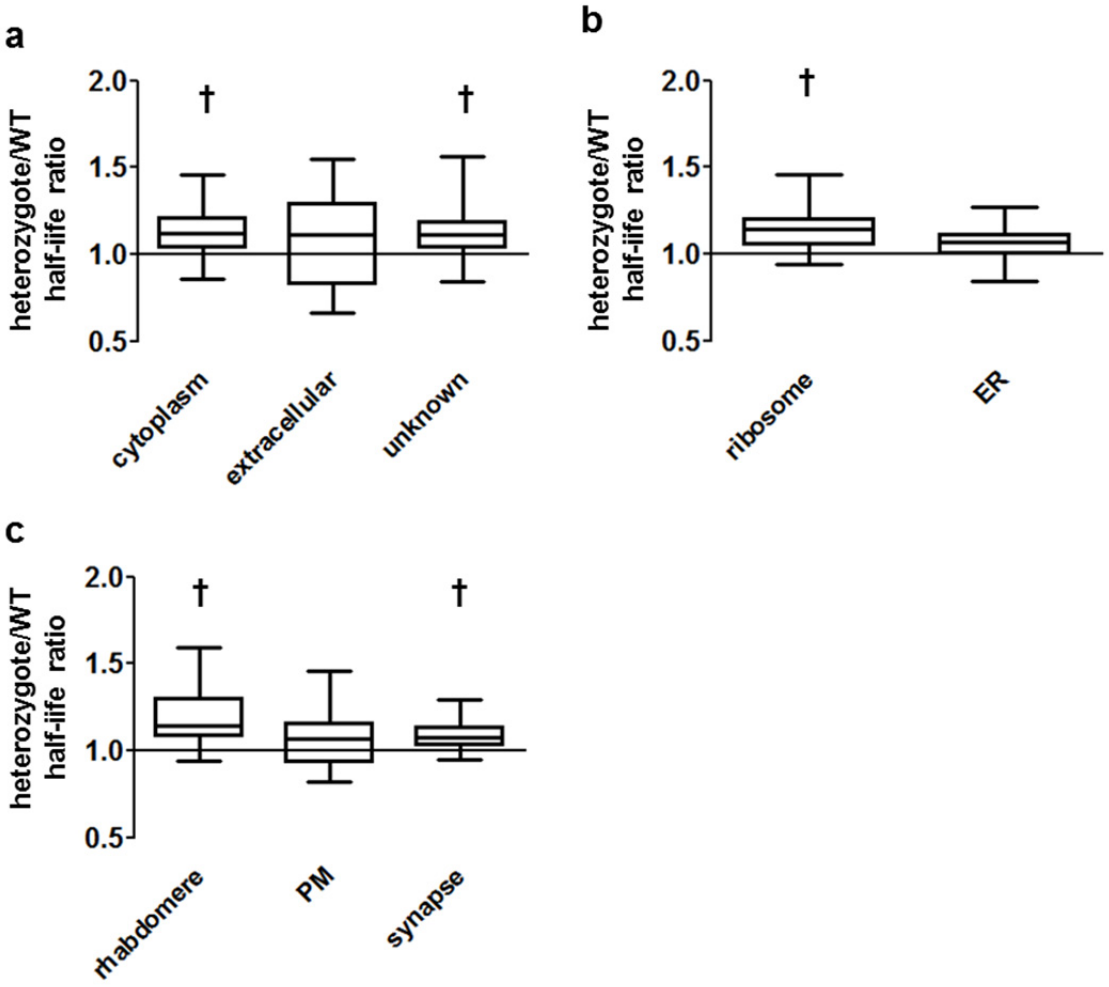

Figure 6.5. Heterozygous effects of *Atg7* on nonmitochondrial proteins. (a-c) Mean *Atg7* heterozygote/WT half-life ratios for nonmitochondrial protein groups; 5 of 8 groups show a significant difference in half-life between heterozygote and WT. Number of proteins: cytoplasm 87, extracellular region 23, localization unknown 48, ribosome 36, ER 15, rhabdomere 12, PM 24, synapse 18. †$p < 0.005$ by paired *t* test

groups with significant heterozygous effects in *Atg7* were cytoplasm, localization unknown, ribosome, rhabdomere, and synapse. Given the strong effects of *Atg7* null mutation on ribosomal proteins, I was surprised that the *Atg7* heterozygous effect on ribosomal proteins, though significant, was considerably smaller than its heterozygous effect on mitochondrial RC proteins (ribosome 1.15±0.12, RC 1.29±0.15). The heterozygous effect of *Atg7* thus differs strikingly from its homozygous effect. Regardless of control group, *Atg7* nulls show far greater slowdown in ribosomal turnover than in mitochondrial turnover. Perhaps there are compensatory mechanisms for ribosomal turnover that are evoked only when impairment of autophagy is severe.

parkin and *Atg7* effects vs. WT controls correlate significantly for several nonmitochondrial protein groups

Far more striking than the mean heterozygous effects of *parkin* and *Atg7* was the appearance of significant *parkin*-*Atg7* correlations when using WT controls. As noted in Chapter 5, no nonmitochondrial protein group showed a significant *parkin*-*Atg7* correlation when the null mutants were compared to their heterozygote controls (see Fig. 5.6). When fold change in half-life was calculated with WT controls, however, 6 of 8 categories showed significant *parkin*-*Atg7* correlations (Fig. 6.6). Some of these correlations were marginally significant (cytoplasm, localization unknown) or largely dependent on an outlier (extracellular). However, the correlations for ribosome, plasma membrane, and synapse were all ≥ 0.57—that is, stronger than the correlation for RC mitochondrial proteins. This was particularly surprising because the absolute magnitude of *parkin* turnover effects on ribosomal proteins remained weak with WT controls (1.13±0.14), whereas the *Atg7* turnover effects were very strong (2.78±0.42). The

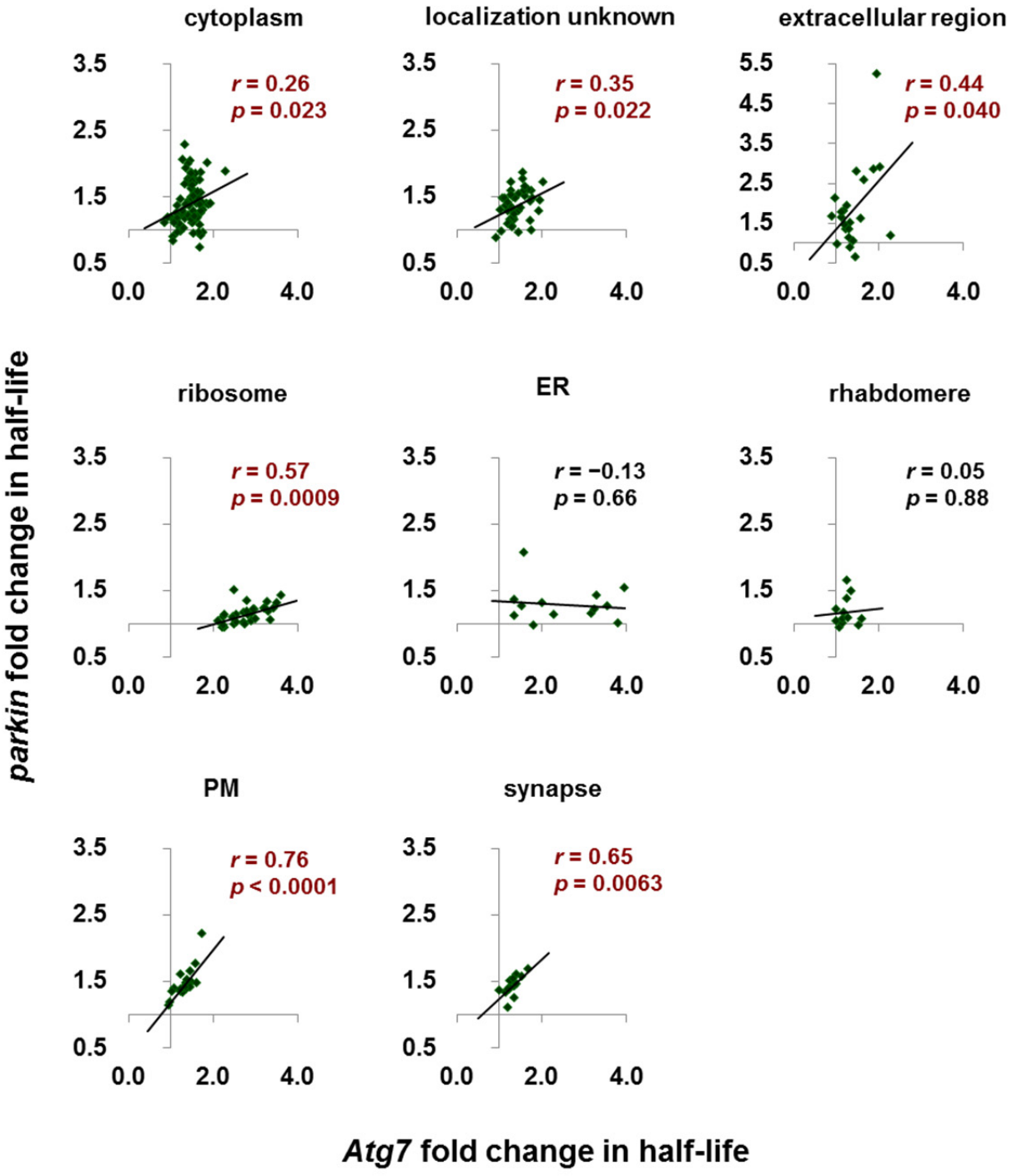

Figure 6.6. Significant *parkin-Atg7* correlations are evident for several nonmitochondrial protein groups when mutants are compared to WT controls. Six of 8 groups show significant correlations. Number of proteins: cytoplasm 78, extracellular region 22, localization unknown 42, ribosome 31, ER 13, rhabdomere 12, PM 23, synapse 16.

effects of *parkin* and *Atg7* on proteins of the plasma membrane and synapse were far more comparable (PM mean fold change 1.45±0.20 for *parkin* null mutants, 1.34±0.20 for *Atg7*), but the correlation was just as puzzling. Making sense of these correlations requires a plausible explanation of how *parkin* mutants could have a mild defect in general autophagy and *Atg7* mutants could have a moderate defect in endosomal turnover. I will speculate on this subject in the Discussion section.

Several groups of nonmitochondrial proteins are more affected by *parkin* than by *Atg7*

Comparing the relative effects of the mutations on the different categories offers more support for the idea of a primary endosomal degradation defect in *parkin* mutants. There were three categories of proteins in which *parkin* produced significantly greater fold change in half-life (homozygote vs. WT) than did *Atg7*. These categories were extracellular region, PM, and synapse—all predominantly turned over by the endosomal pathway. The mean *parkin*/*Atg7* ratios were 1.31±0.55 for extracellular region proteins, 1.09±0.11 for PM proteins, and 1.10±0.11 for synaptic proteins (p = 0.037, 0.0015, and 0.0012 respectively by paired t test).

Use of WT controls causes little change in *PINK1-parkin* correlations

I retested the correlations between *PINK1* and *parkin* using WT controls for *parkin*. (As previously mentioned, *PINK1* controls are revertants and are essentially WT.) The overall mitochondrial correlation, already strong, increased to 0.61; the correlation for non-RC mitochondrial proteins changed little, and the RC correlation decreased slightly from 0.84 to 0.74 (Fig. 6.7). For nonmitochondrial proteins, using WT controls for *parkin* had little impact on the pattern of results. The only substantial difference was that the *PINK1-parkin* correlation for ER,

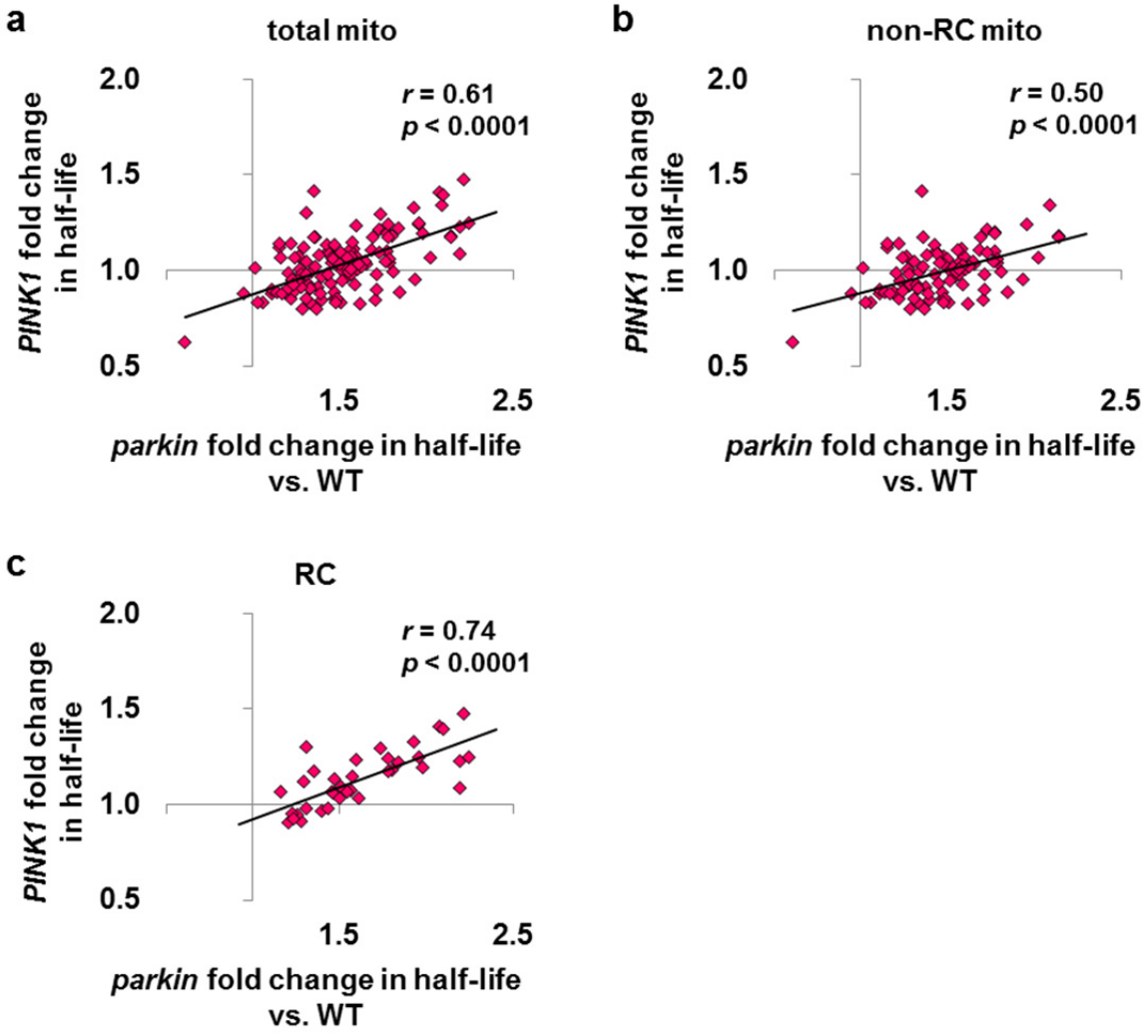

Figure 6.7. *PINK1-parkin* correlations for mitochondrial proteins are not substantially altered by using WT controls for *parkin*. **(a)** The *PINK1-parkin* correlation for all mitochondrial proteins is 0.61 with WT controls, 0.50 with *parkin* heterozygote controls (n = 129). **(b)** Non-RC mitochondrial proteins: r = 0.50 with WT controls, 0.47 with heterozygotes (n = 93). **(c)** RC proteins: r = 0.74 with WT controls, 0.84 with heterozygotes (n = 36). Proteins not present in the WT dataset were omitted when calculating correlations for heterozygote controls.

which had been nearly significant with heterozygote controls, reached significance (Fig. 6.8). The similarity of the correlations obtained with WT and heterozygote controls offers further support for the idea that the difference between WT and heterozygote controls in *parkin-Atg7* correlations was specifically due to interaction of *parkin* and *Atg7* heterozygous effects.

DISCUSSION

My test for heterozygous effects of *parkin* and *Atg7* was intended to resolve a simple question, but the findings have had unexpected, substantial consequences for my interpretation of the data. They forced me to reconsider the evidence that Parkin promotes mitophagy, and also to reevaluate the role of *Atg7* in selective RC turnover. Finally, the WT control group findings shed new light on the possible effects of *parkin* and *Atg7* on endosomal turnover.

Evidence that Parkin promotes mitophagy: reevaluation

The appearance of correlations between *parkin* and *Atg7* effect for turnover of nonmitochondrial protein groups made me ask myself whether I had sufficient evidence to claim that Parkin promotes mitophagy. As mentioned in Chapter 3, I had originally intended to test the question in a more direct, experimental fashion: I would accelerate mitochondrial turnover by overexpressing PINK1, then determine whether an *Atg7* null background blocked PINK1-induced increases in mitochondrial turnover. Because this experiment proved impossible, my case for Parkin-induced mitophagy rested on the correlation between *parkin* and *Atg7* effect in mitochondria, and the lack of similar correlations for other protein groups. In the nonmitochondrial protein results obtained using WT controls, I found strong *parkin-Atg7* correlations that did *not* appear to indicate the presence of a Parkin-Atg7 pathway relationship

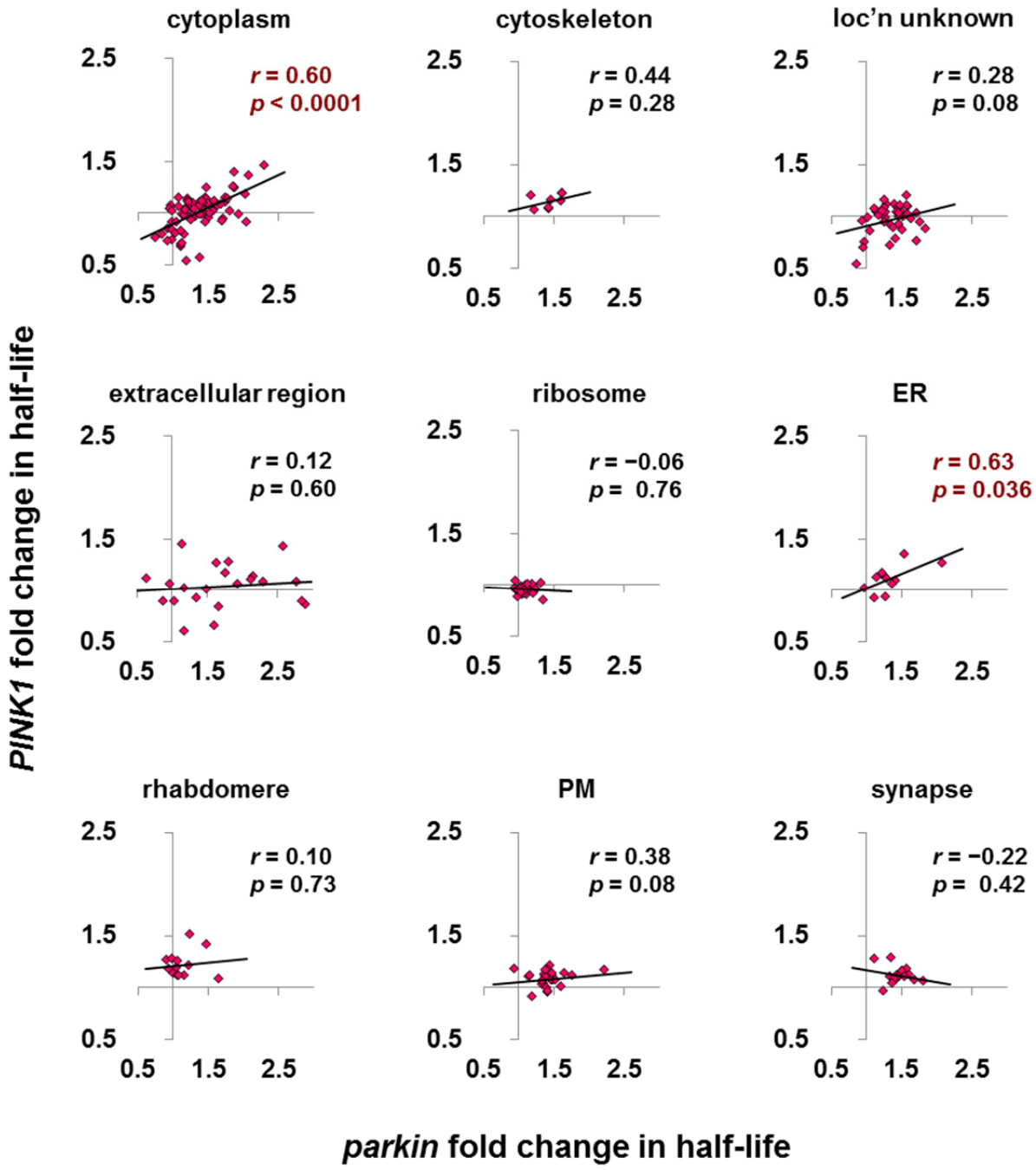

Figure 6.8. *PINK1-parkin* correlations for nonmitochondrial proteins are not substantially altered by using WT controls for *parkin*. When using heterozygote *parkin* controls, the only nonmitochondrial protein group with a significant *PINK1-parkin* correlation was cytoplasm. With WT controls, there is also a significant correlation for ER; this correlation was nearly significant (0.077) with heterozygote controls. Number of proteins: cytoplasm 77, cytoskeleton 8, extracellular region 22, localization unknown 40, ribosome 31, ER 11, rhabdomere 13, PM 23, synapse 16.

during normal turnover. For instance, it does not seem likely that Parkin usually acts upstream of Atg7 to facilitate autophagic turnover of PM or synaptic proteins, although I obviously cannot rule this out completely. I also do not think that the correlation for ribosomal proteins indicates a normal role of Parkin in ribosomal turnover. The magnitude of the effect is so much smaller in *parkin* than in *Atg7* that it seems more indicative of a possible secondary defect in general autophagy in *parkin* mutants.

These findings inevitably led me to question how much weight I could place on the *parkin-Atg7* correlation for mitochondrial proteins. It is worth noting, however, that the correlations for all mitochondrial proteins and non-RC mitochondrial proteins are the only *parkin-Atg7* correlations to appear with both heterozygote and WT controls. Also, as noted in the previous chapter, mitochondrial protein turnover deficits in *parkin* homozygotes are unlikely to be the result of a secondary defect in general autophagy. As for the possibility that *Atg7* and *parkin* both affect some other process affecting mitochondrial turnover, I cannot rule it out based on the existing findings. However, given the wealth of data indicating that mitochondria are turned over by autophagy, the simplest explanation remains that the *parkin-Atg7* correlation represents the coordinated activity of Parkin and Atg7 in mitophagy.

Role of Atg7 in selective RC turnover

The WT control analyses also raise the question of to what extent, and by what mechanism, Atg7 is involved in Parkin-stimulated selective RC turnover. Both the strong heterozygous effect of *Atg7* on RC protein turnover and the *parkin-Atg7* correlation for RC proteins when using WT controls suggest that Atg7 has a substantial influence on this selective turnover. The slightly greater effect of *Atg7* mutation on membrane-bound RC subunits points in

the same direction. This evidence suggests that the selective RC turnover occurs through two or more processes, at least one dependent on *Atg7*. Alternatively, the findings might arise through a secondary effect of autophagy impairment, rather than through involvement of *Atg7* in the normal RC turnover process.

Effects of *parkin* and *Atg7* mutations on the endosomal pathway

In Chapter 5, I suggested that Parkin plays a significant role in endocytic/endosomal turnover. Findings in the current chapter support this idea, particularly the finding that the three nonmitochondrial protein groups with greater effect from *parkin* than *Atg7* are primarily turned over by endosomal degradation. This finding only reaches significance when the null mutants are compared to WT controls, but the same trend occurs when comparing the nulls to heterozygous controls.

Another indirect piece of support for the idea of Parkin as a modulator of endosomal turnover comes from some of the surprising nonmitochondrial protein correlations that appear with the use of WT controls. I mention above that the *parkin*-*Atg7* correlation for ribosomal proteins could be explained by a mild secondary deficit in general autophagy in *parkin* nulls. Such a deficit in general autophagy would very likely be present if *parkin* mutants have an impairment of endosomal turnover, as abnormalities in the endosomal degradation pathway are known to impair autophagic turnover. Inhibition or absence of endosomal pathway components such as Rab5, Rab7, or ESCRT complexes can lead to reduced autophagic flux (188, 189). Overlap between the two pathways is increasingly recognized, as reports of shared components accumulate (190). In fact, endosomes and autophagosomes often converge to form amphisomes before fusing with a lysosome (190).

The same overlap between endosomal and autophagic pathways provides a potential explanation—admittedly speculative—for the puzzling *parkin-Atg7* correlation in PM and synaptic proteins. While existing reports focus on impairment of autophagy caused by endosomal pathway deficits, the degree of overlap in the pathways suggests that impaired endosomal function may also be caused by autophagy deficits. If so, *Atg7* mutants might well have impaired endosomal pathway flux. Such a secondary deficit in the *Atg7* mutants, combined with the primary deficit in *parkin* mutants, might explain the correlation of effect for proteins turned over by the endosomal pathway.

Implications for future work

The findings in this chapter raise the question of what is the "right control" for homozygous null mutants. If possible, I will confirm my existing findings by comparing *parkin* mutants, heterozygote controls, and WT controls within a single experiment. Regardless, the heterozygous effects appear sufficiently important that I would be inclined to use WT controls in future. This would lose the advantage of shared genetic background, but I might be able to minimize the impact of genetic background differences with a different approach. For my WT group in this dissertation, I used different WT genotypes combined from multiple studies. In future, I may use three different control genotypes within a single study, so that each biological replicate for the control group is a different genotype. This would minimize the effects of genetic background differences between strains at the expense of increasing inter-replicate variability.

MATERIALS AND METHODS

Heterozygote control genotypes were *If/CyO* ; $park^{25}/park^{1vA}$ for *parkin* and $Atg7^{d4}/CyO$ or $Atg7^{d77}/CyO$ for *Atg7*. As in Chapter 5, protein categories with < 8 proteins in a given dataset were not analyzed.

When calculating homozygote/WT or heterozygote/WT ratios, only proteins present in both the *parkin* (or *Atg7*) dataset and the WT control dataset were used. As a result, there were sometimes fewer proteins in the analyses using WT controls than in the original heterozygote control analyses (e.g., 137 rather than 156 total mitochondrial proteins for *parkin*). In some direct comparisons of fold change values obtained with heterozygote vs. WT controls (e.g., Fig. 6.1c-d), the values with heterozygote controls may therefore differ slightly from those reported in Chapter 3.

Chapter 7: Conclusions and future directions

In this final chapter, I will review some of the major conclusions and speculations that have emerged from my work, both those specific to the PINK1-Parkin pathway and those that have a more general bearing on mitochondrial protein turnover. I will discuss limitations of my work and mention some plans for further experiments. I will then discuss the field of PINK1-Parkin pathway research as a whole and describe the lines of investigation that I consider most important for the future.

MAJOR CONCLUSIONS: PINK1-PARKIN PATHWAY

Parkin promotes mitophagy *in vivo*

parkin mutations cause significant slowing of overall mitochondrial protein turnover, similar to but less severe than the effect of general autophagy blockade, as would be predicted for a mitochondria-selective turnover mechanism. The effects of *parkin* on individual proteins correlate with the effects of *Atg7*, consistent with the idea that Parkin causes mitochondrial autophagy through Atg7. Although a *parkin*-*Atg7* correlation also exists for some nonmitochondrial protein groups when fold change in half-life is calculated using WT controls, the most likely explanation for the mitochondrial correlation remains that Parkin promotes Atg7-dependent mitophagy. The greater effect of *parkin* mutation on mitochondrial proteins in tissues with high relative mitophagy rates also supports that idea that Parkin promotes mitophagy.

PINK1 appears to promote mitophagy *in vivo*

While *PINK1* mutants surprisingly did not have a deficit in non-RC mitochondrial protein turnover, the effects of *PINK1* on individual non-RC proteins correlated strongly with the effects of *parkin*. Given the literature suggesting increased autophagy in *PINK1*-deficient cells and organisms, the pattern of *PINK1* results seemed best explained by a compensatory increase in an alternative turnover mechanism that affected all proteins equally. The nonmitochondrial protein results from Chapter 5 offer some support for an increase in general autophagy, as large percentages of ribosomal and cytoplasmic proteins showed accelerated turnover in *PINK1* mutants compared to controls.

The PINK1 overexpression experiments, which could have provided additional evidence for the idea that PINK1 promotes mitophagy, failed to do so. However, I do not consider this failure to be evidence against an *in vivo* role for PINK1 in mitophagy. As noted in Chapter 1, the *in vitro* experiments showing mitophagy triggered by PINK1 overexpression also involved overexpressing Parkin. Because coexpressing PINK1 and Parkin in flies has fatal results, I cannot perform a test comparable to those done *in vitro*.

Parkin and PINK1 promote selective turnover of RC proteins

Perhaps my single most surprising finding was the discovery that *parkin* and *PINK1* had marked selective effects on mitochondrial protein turnover, and specifically on many proteins of the respiratory chain. This was especially striking because the RC turnover deficit was the only significant mitochondrial protein turnover deficit in *PINK1* mutants. The finding raises a great many questions. Why do membrane-bound RC subunits show greater effects from *PINK1* and *parkin*? To what extent, if at all, does Atg7 contribute to selective RC turnover? What is the

primary mechanism of the selective turnover? The strong correlation of my own WT mitochondrial half-life data with the Price et al. mouse data (136), shown in Chapter 2, supports the idea that mitochondrial turnover mechanisms may be conserved from fly to mammal. If so, failure of selective RC turnover may be relevant to human neurodegeneration.

Parkin affects turnover of nonmitochondrial proteins

The original concept of Parkin's role in PD was that of an E3 ligase controlling cytoplasmic protein turnover (49). Consistent with this, the PINK1-Parkin pathway appears to influence cytoplasmic protein turnover, as shown by the significant effect of *parkin* on fold change in half-life and the strong correlation between *PINK1* and *parkin* effects. These findings might indicate that the pathway normally regulates cytoplasmic protein turnover through direct ubiquitination, but might also indicate that PINK1-Parkin pathway dysfunction impairs the proteasome.

Parkin also appears to influence turnover via the endocytic/endosomal degradation pathway, and this function does not seem to involve PINK1. Parkin may influence more than one component of the pathway, as *parkin* nulls have large but inconsistent effects on extracellular protein turnover and moderate but consistent effects on other targets of endosomal degradation.

MAJOR CONCLUSIONS: MITOCHONDRIAL PROTEIN TURNOVER

Both total mitochondrial turnover and mitophagy appear to be low in brain

My data indicate that the rate of mitophagy, as well as the percentage of mitochondrial protein turnover accomplished through mitophagy, varies across the tissues of the fly head. In particular, the findings suggest that overall mitochondrial turnover is slow in brain, and that a

comparatively small fraction of this turnover occurs through mitophagy. With the exception of RC proteins, mitochondrial proteins expressed at moderate to high levels in brain also appear to depend less on Parkin-mediated turnover than do proteins with low brain expression. These findings are significant because they do not clearly support the current model of PINK1-Parkin pathway action, which depicts mitophagy as an active and essential quality control pathway in brain. In future, logistics permitting, I may analyze turnover in dissected brains rather than heads to gain more information on this important point.

Mitochondrial protein turnover in fly heads appears highly nonunitary

In Chapter 1, I discussed the early controversy over unitary vs. nonunitary mitochondrial turnover. Based on my own data, I believe that unitary turnover occurs, and in some tissues mitophagy may account for a significant proportion of mitochondrial protein turnover. However, it also appears that a large amount of turnover occurs asynchronously through selective mechanisms, especially in brain. My findings are consistent with the diverse mitochondrial protein half-lives reported by stable isotope labeling studies of protein turnover in mice (136, 137), and also with the findings of Hare and Hodges on asynchronous turnover of RC peptides (132).

FUTURE WORK

Limitations of the current work and potential solutions

One basic limitation of my work is that it does not provide information on whether the PINK1-Parkin pathway preferentially promotes turnover of damaged or depolarized mitochondria. This limitation is difficult to overcome with the technique used here. A more

remediable limitation is the small number of time points, and especially the lack of a zero time point (completely unlabeled flies). More time points will allow me to measure a larger range of half-lives with accuracy, and a zero time point will allow me to test for potential abundance change across the full period of the study.

Another limitation of the current work is the general ill health and weakness of *parkin* mutants, which have a high mortality rate in my studies. It is currently impossible to rule out the possibility that some of the effects noted could be nonspecific consequences of poor health. A potential solution to this dilemma is overexpressing Drp1 or Parkin with a GAL4 driver that drives in thorax but not head (68). The driver would need to be tested carefully to rule out inappropriate expression in head. However, if feasible, this manipulation would produce *parkin* mutants with good general health, without directly affecting protein turnover in the head.

Finally, one of the most significant caveats to my study is the issue of compensatory turnover. Some effects that I currently attribute to differences between *parkin* and *Atg7*, for instance, could be the result of differential compensation. There is no direct way of resolving this issue; however, testing a variety of related genetic manipulations of protein turnover and comparing the results may shed light on the role of compensation.

Proposed experiments

One of my original objectives was to find a reliable method of accelerating mitochondrial turnover, so that I could then test whether absence of Parkin or Atg7 blocks the increase in turnover. I still hope to accomplish this. Exposing flies to a hyperoxic environment, which has been shown to cause mitochondrial abnormalities, is a possible future strategy for increasing turnover (191). Another potential approach is to induce mitochondrial unfolded protein stress by

driving expression of a misfolded mitochondrial enzyme. In a previous study, flies expressing this misfolded protein had mitochondrial defects, which were remedied by Parkin overexpression (162).

I also intend to test the effects of altered mitochondrial dynamics on mitochondrial turnover. Mitochondrial dynamics profoundly influence the *PINK1* and *parkin* phenotypes, and Drp1 overexpression in particular causes remarkable rescue of these mutants. I plan to study the effects of Drp1 overexpression on mitochondrial protein turnover, both in a WT background and in *parkin* mutants. As Drp1 has been seen on mitochondrial "buds" in stressed cells (165), it might rescue selective RC turnover occurring through mitochondrial vesicles. On the other hand, if Drp1 simply facilitates autophagy by increasing the rate of fission, overexpression might rescue the general mitochondrial protein turnover defect but not the RC turnover defect. Another useful way of testing this distinction is mild overexpression of Atg1, an upstream component in both conventional and alternative autophagy.

Testing protein turnover in *Rab9*-deficient flies, which would have a defect in alternative autophagy, would be an excellent complement to the *Atg7* studies. Likewise, proteomic studies of flies with impaired proteasomal functioning would contribute to our understanding of mitochondrial protein turnover. Not only are many individual mitochondrial proteins turned over by the UPS, but if the Chan group is correct, proteasomal protein turnover is necessary for mitophagy (101). Finally, studying manipulations of multiple protein turnover mechanisms may help distinguish secondary from primary effects. By comparing datasets and distinguishing shared defects from unique ones, we may clarify the contributions of each turnover mechanism.

FUTURE DIRECTIONS FOR THE PINK1/PARKIN RESEARCH FIELD

Ten years after Greene and Whitworth developed the *parkin* mutant, the PINK1-Parkin pathway is the focus of very active research. Most of that research is devoted to elucidating the function of the pathway in mitophagy: finding substrates and modifiers of the pathway, discovering new pathway components, and investigating the molecular mechanisms underlying known portions of the pathway. I would like to see research on PINK1 and Parkin broaden to explore more aspects of these proteins' functions and relationship to human health.

One excellent way to widen the focus of the field would be to take a fresh view of the *in vitro* CCCP model of mitophagy. This assay has always been presented as a model of Parkinson disease, which is hypothesized to result from "failure to clear normally occurring damaged mitochondria by mitophagy" (35). For reasons I have described at length, the CCCP model does not seem a good representation of mitochondrial QC under normal physiological conditions, especially in brain; I therefore question its relevance to the pathogenesis of an age-related neurodegenerative disorder. However, the model is directly applicable to another class of major human health problems: cardiac and cerebral ischemia. Ischemia/reperfusion injury is a situation in which cell-wide mitochondrial depolarization actually occurs in nature, and it is also a situation in which eliminating much of a cell's mitochondrial mass is clearly beneficial. Mitochondria damaged by ischemia are frankly dangerous during the immediate post-injury period. These mitochondria can induce apoptosis or necrosis, and can also trigger cardiac arrhythmias through waves of ROS-induced ROS release (192). As noted in Chapter 1, neurons without mitochondria actually survived longer under hypoxia (44). A mechanism for rapid elimination of mitochondria after ischemia would thus be a valuable way to mitigate the severity

of tissue damage—and, in fact, recent work suggests that the PINK1-Parkin pathway is a vital modulator of survival after myocardial infarction (111, 112).

The recent studies of Parkin function in cardiac ischemia, mentioned briefly in Chapter 1, strike me as the most exciting current research in the field. These studies have demonstrated not only that Parkin is recruited to mitochondria *in vivo* after physiologically relevant stress, but that Parkin materially influences the outcome of ischemia. Normal mice and *parkin* null mice were subjected to three brief episodes of cardiac ischemia (preconditioning) before undergoing 20 minutes of ischemia. Preconditioning is normally protective against ischemia-induced cell death. The area at risk for infarction was the same in control and *parkin* null mice, but the final size of infarction was larger in *parkin* nulls (111). Similarly, *parkin* null mice were three times as likely as controls to die in the first week after induced myocardial infarction (112). An earlier study had established that autophagy was necessary for preconditioning-induced cardioprotection, and found a rapid increase of autophagosomes in the area at risk in preconditioned hearts (193). These studies promise to yield valuable information on the mechanisms of cellular response to ischemia. No preconditioning studies on *PINK1* null mice have yet appeared, but these mice develop early and severe congestive heart failure (194). I would encourage all researchers using the CCCP mitophagy model to consider the relevance of their findings to ischemic injury and cardiac function.

I would also encourage researchers to consider the relationship of PINK1 and Parkin to forms of mitochondrial turnover other than mitophagy. I cannot rule out, of course, that failure of mitophagy is actually the correct model for PD. Mitophagy could be particularly active and important in dopaminergic neurons, for instance. It is also possible that impairment of a pathway with low baseline activity could be highly deleterious. But my findings suggest that, in brain,

protein-selective turnover may be a more crucial form of mitochondrial QC than mitophagy. I would therefore like to see vigorous research into mechanisms of selective mitochondrial protein turnover in brain, including mitochondrial proteases, the ubiquitin-proteasome system, and (potentially) mitochondrial vesicles.

Finally, I would like to see a resurgence of Parkin and PINK1 research not directly related to mitochondria. Given my own findings, I am interested in the potential role of Parkin in endocytic/endosomal protein turnover. Also, recent work has suggested that Parkin regulates lipid and glucose metabolism (195, 196). Both the evidence of previous studies and my own data suggest that Parkin is a multifunctional enzyme, involved in a wide variety of processes; it would be a pity to ignore potentially valuable findings because they do not fit the concept of Parkin as a mitochondrial QC factor.

In summary, PINK1 and Parkin appear to play multiple roles in both mitochondrial QC and other essential cellular processes. Research on any of these functions could yield clues to both human health problems and basic cell biology.

References

1. McBride HM, Neuspiel M, & Wasiak S (2006) Mitochondria: more than just a powerhouse. *Curr Biol* 16(14):R551-560.
2. Wallace DC (2012) Mitochondria and cancer. *Nat Rev Cancer* 12(10):685-698.
3. Lill R*, et al.* (2012) The role of mitochondria in cellular iron-sulfur protein biogenesis and iron metabolism. *Biochim Biophys Acta* 1823(9):1491-1508.
4. Wang C & Youle RJ (2009) The role of mitochondria in apoptosis. *Annu Rev Genet* 43:95-118.
5. Mari M*, et al.* (2012) Mitochondrial glutathione: Features, regulation and role in disease. *Biochim Biophys Acta*.
6. Valente EM*, et al.* (2004) Hereditary early-onset Parkinson's disease caused by mutations in PINK1. *Science* 304(5674):1158-1160.
7. Kitada T*, et al.* (1998) Mutations in the parkin gene cause autosomal recessive juvenile parkinsonism. *Nature* 392(6676):605-608.
8. Narendra DP*, et al.* (2010) PINK1 is selectively stabilized on impaired mitochondria to activate Parkin. *PLoS Biol* 8(1):e1000298.
9. Pagliarini DJ*, et al.* (2008) A mitochondrial protein compendium elucidates complex I disease biology. *Cell* 134(1):112-123.
10. Bulteau AL & Bayot A (2011) Mitochondrial proteases and cancer. *Biochim Biophys Acta* 1807(6):595-601.
11. Gregersen N & Bross P (2010) Protein misfolding and cellular stress: an overview. *Methods Mol Biol* 648:3-23.
12. Neutzner A, Youle RJ, & Karbowski M (2007) Outer mitochondrial membrane protein degradation by the proteasome. *Novartis Found Symp* 287:4-14; discussion 14-20.
13. Clarke KJ*, et al.* (2012) A role for ubiquitinylation and the cytosolic proteasome in turnover of mitochondrial uncoupling protein 1 (UCP1). *Biochim Biophys Acta* 1817(10):1759-1767.
14. Margineantu DH, Emerson CB, Diaz D, & Hockenbery DM (2007) Hsp90 inhibition decreases mitochondrial protein turnover. *PLoS One* 2(10):e1066.
15. Nakada K, Sato A, & Hayashi J (2009) Mitochondrial functional complementation in mitochondrial DNA-based diseases. *Int J Biochem Cell Biol* 41(10):1907-1913.
16. Tolkovsky AM (2009) Mitophagy. *Biochim Biophys Acta* 1793(9):1508-1515.
17. Xie Z & Klionsky DJ (2007) Autophagosome formation: core machinery and adaptations. *Nat Cell Biol* 9(10):1102-1109.
18. Murrow L & Debnath J (2012) Autophagy as a Stress-Response and Quality-Control Mechanism: Implications for Cell Injury and Human Disease. *Annu Rev Pathol*.
19. Mizushima N (2007) Autophagy: process and function. *Genes Dev* 21(22):2861-2873.
20. Klionsky DJ*, et al.* (2003) A unified nomenclature for yeast autophagy-related genes. *Dev Cell* 5(4):539-545.
21. Chen Y & Klionsky DJ (2011) The regulation of autophagy - unanswered questions. *J Cell Sci* 124(Pt 2):161-170.
22. Nishida Y*, et al.* (2009) Discovery of Atg5/Atg7-independent alternative macroautophagy. *Nature* 461(7264):654-658.
23. Suzuki K (2013) Selective autophagy in budding yeast. *Cell Death Differ* 20(1):43-48.

24. Di Bartolomeo S, Nazio F, & Cecconi F (2010) The role of autophagy during development in higher eukaryotes. *Traffic* 11(10):1280-1289.
25. Reggiori F, Komatsu M, Finley K, & Simonsen A (2012) Selective types of autophagy. *Int J Cell Biol* 2012:156272.
26. Tuttle DL, Lewin AS, & Dunn WA, Jr. (1993) Selective autophagy of peroxisomes in methylotrophic yeasts. *Eur J Cell Biol* 60(2):283-290.
27. Bernales S, McDonald KL, & Walter P (2006) Autophagy counterbalances endoplasmic reticulum expansion during the unfolded protein response. *PLoS Biol* 4(12):e423.
28. Lamark T & Johansen T (2012) Aggrephagy: selective disposal of protein aggregates by macroautophagy. *Int J Cell Biol* 2012:736905.
29. Fujita N & Yoshimori T (2011) Ubiquitination-mediated autophagy against invading bacteria. *Curr Opin Cell Biol* 23(4):492-497.
30. Ashford TP & Porter KR (1962) Cytoplasmic components in hepatic cell lysosomes. *J Cell Biol* 12:198-202.
31. Kristensen AR*, et al.* (2008) Ordered organelle degradation during starvation-induced autophagy. *Mol Cell Proteomics* 7(12):2419-2428.
32. May AI, Devenish RJ, & Prescott M (2012) The many faces of mitochondrial autophagy: making sense of contrasting observations in recent research. *Int J Cell Biol* 2012:431684.
33. Mendl N*, et al.* (2011) Mitophagy in yeast is independent of mitochondrial fission and requires the stress response gene WHI2. *J Cell Sci* 124(Pt 8):1339-1350.
34. Zhang J & Ney PA (2009) Role of BNIP3 and NIX in cell death, autophagy, and mitophagy. *Cell Death Differ* 16(7):939-946.
35. Youle RJ & Narendra DP (2011) Mechanisms of mitophagy. *Nat Rev Mol Cell Biol* 12(1):9-14.
36. Sandoval H*, et al.* (2008) Essential role for Nix in autophagic maturation of erythroid cells. *Nature* 454(7201):232-235.
37. Ding WX*, et al.* (2010) Nix is critical to two distinct phases of mitophagy, reactive oxygen species-mediated autophagy induction and Parkin-ubiquitin-p62-mediated mitochondrial priming. *J Biol Chem* 285(36):27879-27890.
38. Ding WX & Yin XM (2012) Mitophagy: mechanisms, pathophysiological roles, and analysis. *Biol Chem* 393(7):547-564.
39. De Duve C & Wattiaux R (1966) Functions of lysosomes. *Annu Rev Physiol* 28:435-492.
40. Elmore SP*, et al.* (1997) Detection of mitochondrial depolarization during autophagy by confocal fluorescence resonance energy transfer (CFRET). *Cell Vis J Anal Morphol* 4:170-171.
41. Lemasters JJ*, et al.* (1998) The mitochondrial permeability transition in cell death: a common mechanism in necrosis, apoptosis and autophagy. *Biochim Biophys Acta* 1366(1-2):177-196.
42. Elmore SP, Qian T, Grissom SF, & Lemasters JJ (2001) The mitochondrial permeability transition initiates autophagy in rat hepatocytes. *FASEB J* 15(12):2286-2287.
43. Priault M*, et al.* (2005) Impairing the bioenergetic status and the biogenesis of mitochondria triggers mitophagy in yeast. *Cell Death Differ* 12(12):1613-1621.
44. Xue L, Fletcher GC, & Tolkovsky AM (2001) Mitochondria are selectively eliminated from eukaryotic cells after blockade of caspases during apoptosis. *Curr Biol* 11(5):361-365.

45. Kim I, Rodriguez-Enriquez S, & Lemasters JJ (2007) Selective degradation of mitochondria by mitophagy. *Arch Biochem Biophys* 462(2):245-253.
46. Twig G*, et al.* (2008) Fission and selective fusion govern mitochondrial segregation and elimination by autophagy. *EMBO J* 27(2):433-446.
47. Narendra D, Tanaka A, Suen DF, & Youle RJ (2008) Parkin is recruited selectively to impaired mitochondria and promotes their autophagy. *J Cell Biol* 183(5):795-803.
48. Vives-Bauza C*, et al.* (2010) PINK1-dependent recruitment of Parkin to mitochondria in mitophagy. *Proc Natl Acad Sci U S A* 107(1):378-383.
49. Shimura H*, et al.* (2000) Familial Parkinson disease gene product, parkin, is a ubiquitin-protein ligase. *Nat Genet* 25(3):302-305.
50. Zhang Y*, et al.* (2000) Parkin functions as an E2-dependent ubiquitin- protein ligase and promotes the degradation of the synaptic vesicle-associated protein, CDCrel-1. *Proc Natl Acad Sci U S A* 97(24):13354-13359.
51. Stichel CC*, et al.* (2000) Parkin expression in the adult mouse brain. *Eur J Neurosci* 12(12):4181-4194.
52. Shimura H*, et al.* (2001) Ubiquitination of a new form of alpha-synuclein by parkin from human brain: implications for Parkinson's disease. *Science* 293(5528):263-269.
53. Imai Y*, et al.* (2001) An unfolded putative transmembrane polypeptide, which can lead to endoplasmic reticulum stress, is a substrate of Parkin. *Cell* 105(7):891-902.
54. Yang Y, Nishimura I, Imai Y, Takahashi R, & Lu B (2003) Parkin suppresses dopaminergic neuron-selective neurotoxicity induced by Pael-R in Drosophila. *Neuron* 37(6):911-924.
55. Corti O*, et al.* (2003) The p38 subunit of the aminoacyl-tRNA synthetase complex is a Parkin substrate: linking protein biosynthesis and neurodegeneration. *Hum Mol Genet* 12(12):1427-1437.
56. Ko HS*, et al.* (2005) Accumulation of the authentic parkin substrate aminoacyl-tRNA synthetase cofactor, p38/JTV-1, leads to catecholaminergic cell death. *J Neurosci* 25(35):7968-7978.
57. Staropoli JF*, et al.* (2003) Parkin Is a Component of an SCF-like Ubiquitin Ligase Complex and Protects Postmitotic Neurons from Kainate Excitotoxicity. *Neuron* 37(5):735-749.
58. Um JW*, et al.* (2006) Parkin ubiquitinates and promotes the degradation of RanBP2. *J Biol Chem* 281(6):3595-3603.
59. Ren Y, Zhao J, & Feng J (2003) Parkin binds to alpha/beta tubulin and increases their ubiquitination and degradation. *J Neurosci* 23(8):3316-3324.
60. Munoz-Soriano V, Nieto-Arellano R, & Paricio N (2012) Septin 4, the drosophila ortholog of human CDCrel-1, accumulates in parkin mutant brains and is functionally related to the Nedd4 E3 ubiquitin ligase. *J Mol Neurosci* 48(1):136-143.
61. Choi P*, et al.* (2003) SEPT5_v2 is a parkin-binding protein. *Brain Res Mol Brain Res* 117(2):179-189.
62. Huynh DP, Scoles DR, Nguyen D, & Pulst SM (2003) The autosomal recessive juvenile Parkinson disease gene product, parkin, interacts with and ubiquitinates synaptotagmin XI. *Hum Mol Genet* 12(20):2587-2597.
63. Pridgeon JW, Olzmann JA, Chin LS, & Li L (2007) PINK1 Protects against Oxidative Stress by Phosphorylating Mitochondrial Chaperone TRAP1. *PLoS Biol* 5(7):e172.

64. Plun-Favreau H, *et al.* (2007) The mitochondrial protease HtrA2 is regulated by Parkinson's disease-associated kinase PINK1. *Nat Cell Biol* 9(11):1243-1252.
65. Whitworth AJ, *et al.* (2008) Rhomboid-7 and HtrA2/Omi act in a common pathway with the Parkinson's disease factors Pink1 and Parkin. *Dis Model Mech* 1(2-3):168-174; discussion 173.
66. Petit A, *et al.* (2005) Wild-type PINK1 prevents basal and induced neuronal apoptosis, a protective effect abrogated by Parkinson disease-related mutations. *J Biol Chem* 280(40):34025-34032.
67. Darios F, *et al.* (2003) Parkin prevents mitochondrial swelling and cytochrome c release in mitochondria-dependent cell death. *Hum Mol Genet* 12(5):517-526.
68. Greene JC, *et al.* (2003) Mitochondrial pathology and apoptotic muscle degeneration in Drosophila parkin mutants. *Proc Natl Acad Sci U S A* 100(7):4078-4083.
69. Perez FA & Palmiter RD (2005) Parkin-deficient mice are not a robust model of parkinsonism. *Proc Natl Acad Sci U S A* 102(6):2174-2179.
70. Palacino JJ, *et al.* (2004) Mitochondrial dysfunction and oxidative damage in parkin-deficient mice. *J Biol Chem* 279(18):18614-18622.
71. Stichel CC, *et al.* (2007) Mono- and double-mutant mouse models of Parkinson's disease display severe mitochondrial damage. *Hum Mol Genet* 16(20):3377-3393.
72. Clark IE, *et al.* (2006) Drosophila pink1 is required for mitochondrial function and interacts genetically with parkin. *Nature* 441(7097):1162-1166.
73. Park J, *et al.* (2006) Mitochondrial dysfunction in Drosophila PINK1 mutants is complemented by parkin. *Nature* 441(7097):1157-1161.
74. Poole AC, *et al.* (2008) The PINK1/Parkin pathway regulates mitochondrial morphology. *Proc Natl Acad Sci U S A* 105(5):1638-1643.
75. Yang Y, *et al.* (2006) Mitochondrial pathology and muscle and dopaminergic neuron degeneration caused by inactivation of Drosophila Pink1 is rescued by Parkin. *Proc Natl Acad Sci U S A* 103(28):10793-10798.
76. Deng H, Dodson MW, Huang H, & Guo M (2008) The Parkinson's disease genes pink1 and parkin promote mitochondrial fission and/or inhibit fusion in Drosophila. *Proc Natl Acad Sci U S A* 105(38):14503-14508.
77. Park J, Lee G, & Chung J (2009) The PINK1-Parkin pathway is involved in the regulation of mitochondrial remodeling process. *Biochem Biophys Res Commun* 378(3):518-523.
78. Yu W, Sun Y, Guo S, & Lu B (2011) The PINK1/Parkin pathway regulates mitochondrial dynamics and function in mammalian hippocampal and dopaminergic neurons. *Hum Mol Genet* 20(16):3227-3240.
79. Poole AC, Thomas RE, Yu S, Vincow ES, & Pallanck L (2010) The mitochondrial fusion-promoting factor mitofusin is a substrate of the PINK1/parkin pathway. *PLoS One* 5(4):e10054.
80. Whitworth AJ, *et al.* (2005) Increased glutathione S-transferase activity rescues dopaminergic neuron loss in a Drosophila model of Parkinson's disease. *Proc Natl Acad Sci U S A* 102(22):8024-8029.
81. Matsuda N, *et al.* (2010) PINK1 stabilized by mitochondrial depolarization recruits Parkin to damaged mitochondria and activates latent Parkin for mitophagy. *J Cell Biol* 189(2):211-221.

82. Jin SM, *et al.* (2010) Mitochondrial membrane potential regulates PINK1 import and proteolytic destabilization by PARL. *J Cell Biol* 191(5):933-942.
83. Kulawiak B, *et al.* (2012) The mitochondrial protein import machinery has multiple connections to the respiratory chain. *Biochim Biophys Acta*.
84. Zhou C, *et al.* (2008) The kinase domain of mitochondrial PINK1 faces the cytoplasm. *Proc Natl Acad Sci U S A* 105(33):12022-12027.
85. Lazarou M, Jin SM, Kane LA, & Youle RJ (2012) Role of PINK1 Binding to the TOM Complex and Alternate Intracellular Membranes in Recruitment and Activation of the E3 Ligase Parkin. *Dev Cell* 22(2):320-333.
86. Geisler S, *et al.* (2010) PINK1/Parkin-mediated mitophagy is dependent on VDAC1 and p62/SQSTM1. *Nat Cell Biol* 12(2):119-131.
87. Kim Y, *et al.* (2008) PINK1 controls mitochondrial localization of Parkin through direct phosphorylation. *Biochem Biophys Res Commun* 377(3):975-980.
88. Sha D, Chin LS, & Li L (2010) Phosphorylation of parkin by Parkinson disease-linked kinase PINK1 activates parkin E3 ligase function and NF-kappa B signaling. *Hum Mol Genet* 19(2):352-363.
89. Kondapalli C, *et al.* (2012) PINK1 is activated by mitochondrial membrane potential depolarization and stimulates Parkin E3 ligase activity by phosphorylating Serine 65. *Open Biol* 2.
90. Shiba-Fukushima K, *et al.* (2012) PINK1-mediated phosphorylation of the Parkin ubiquitin-like domain primes mitochondrial translocation of Parkin and regulates mitophagy. *Sci Rep* 2:1002.
91. Shiba K, *et al.* (2009) Parkin stabilizes PINK1 through direct interaction. *Biochem Biophys Res Commun* 383(3):331-335.
92. Um JW, Stichel-Gunkel C, Lubbert H, Lee G, & Chung KC (2009) Molecular interaction between parkin and PINK1 in mammalian neuronal cells. *Mol Cell Neurosci* 40(4):421-432.
93. Wang X, *et al.* (2011) PINK1 and Parkin target Miro for phosphorylation and degradation to arrest mitochondrial motility. *Cell* 147(4):893-906.
94. Narendra D, Kane LA, Hauser DN, Fearnley IM, & Youle RJ (2010) p62/SQSTM1 is required for Parkin-induced mitochondrial clustering but not mitophagy; VDAC1 is dispensable for both. *Autophagy* 6(8):1090-1106.
95. Liu S, *et al.* (2012) Parkinson's disease-associated kinase PINK1 regulates Miro protein level and axonal transport of mitochondria. *PLoS Genet* 8(3):e1002537.
96. Gegg ME, *et al.* (2010) Mitofusin 1 and mitofusin 2 are ubiquitinated in a PINK1/parkin-dependent manner upon induction of mitophagy. *Hum Mol Genet* 19(24):4861-4870.
97. Tanaka A, *et al.* (2010) Proteasome and p97 mediate mitophagy and degradation of mitofusins induced by Parkin. *J Cell Biol* 191(7):1367-1380.
98. Ziviani E, Tao RN, & Whitworth AJ (2010) Drosophila Parkin requires PINK1 for mitochondrial translocation and ubiquitinates Mitofusin. *Proc Natl Acad Sci U S A*.
99. Okatsu K, *et al.* (2012) Mitochondrial hexokinase HKI is a novel substrate of the Parkin ubiquitin ligase. *Biochem Biophys Res Commun* 428(1):197-202.
100. Walczak H, Iwai K, & Dikic I (2012) Generation and physiological roles of linear ubiquitin chains. *BMC Biol* 10:23.
101. Chan NC, *et al.* (2011) Broad activation of the ubiquitin-proteasome system by Parkin is critical for mitophagy. *Hum Mol Genet* 20(9):1726-1737.

102. Yoshii SR, Kishi C, Ishihara N, & Mizushima N (2011) Parkin mediates proteasome-dependent protein degradation and rupture of the outer mitochondrial membrane. *J Biol Chem* 286(22):19630-19640.
103. Olzmann JA*, et al.* (2007) Parkin-mediated K63-linked polyubiquitination targets misfolded DJ-1 to aggresomes via binding to HDAC6. *J Cell Biol* 178(6):1025-1038.
104. Seibenhener ML*, et al.* (2004) Sequestosome 1/p62 is a polyubiquitin chain binding protein involved in ubiquitin proteasome degradation. *Mol Cell Biol* 24(18):8055-8068.
105. Lee JY, Nagano Y, Taylor JP, Lim KL, & Yao TP (2010) Disease-causing mutations in parkin impair mitochondrial ubiquitination, aggregation, and HDAC6-dependent mitophagy. *J Cell Biol* 189(4):671-679.
106. Pankiv S*, et al.* (2007) p62/SQSTM1 binds directly to Atg8/LC3 to facilitate degradation of ubiquitinated protein aggregates by autophagy. *J Biol Chem* 282(33):24131-24145.
107. Okatsu K*, et al.* (2010) p62/SQSTM1 cooperates with Parkin for perinuclear clustering of depolarized mitochondria. *Genes Cells* 15(8):887-900.
108. Gogvadze V, Zhivotovsky B, & Orrenius S (2010) The Warburg effect and mitochondrial stability in cancer cells. *Mol Aspects Med* 31(1):60-74.
109. Sterky FH, Lee S, Wibom R, Olson L, & Larsson NG (2011) Impaired mitochondrial transport and Parkin-independent degeneration of respiratory chain-deficient dopamine neurons in vivo. *Proc Natl Acad Sci U S A* 108(31):12937-12942.
110. Lee S*, et al.* (2012) Mitofusin 2 is necessary for striatal axonal projections of midbrain dopamine neurons. *Hum Mol Genet* 21(22):4827-4835.
111. Huang C*, et al.* (2011) Preconditioning involves selective mitophagy mediated by Parkin and p62/SQSTM1. *PLoS One* 6(6):e20975.
112. Kubli DA*, et al.* (2012) Parkin Deficiency Exacerbates Cardiac Injury and Reduces Survival Following Myocardial Infarction. *J Biol Chem* 288(2):915-926.
113. Mitsuhashi S*, et al.* (2011) Muscle choline kinase beta defect causes mitochondrial dysfunction and increased mitophagy. *Hum Mol Genet* 20(19):3841-3851.
114. Jin SM & Youle RJ (2012) PINK1- and Parkin-mediated mitophagy at a glance. *J Cell Sci* 125(Pt 4):795-799.
115. Ham BK, Li G, Kang BH, Zeng F, & Lucas WJ (2012) Overexpression of Arabidopsis plasmodesmata germin-like proteins disrupts root growth and development. *Plant Cell* 24(9):3630-3648.
116. Greene AW*, et al.* (2012) Mitochondrial processing peptidase regulates PINK1 processing, import and Parkin recruitment. *EMBO Rep* 13(4):378-385.
117. Rakovic A*, et al.* (2012) PTEN-induced putative kinase 1 (PINK1)-dependent ubiquitination of endogenous Parkin attenuates mitophagy: study in human primary fibroblasts and induced pluripotent stem (iPS) cell-derived neurons. *J Biol Chem* 288(4):2223-2237.
118. Cai Q, Zakaria HM, Simone A, & Sheng ZH (2012) Spatial parkin translocation and degradation of damaged mitochondria via mitophagy in live cortical neurons. *Curr Biol* 22(6):545-552.
119. Van Laar VS*, et al.* (2011) Bioenergetics of neurons inhibit the translocation response of Parkin following rapid mitochondrial depolarization. *Hum Mol Genet* 20(5):927-940.
120. Menzies RA & Gold PH (1971) The turnover of mitochondria in a variety of tissues of young adult and aged rats. *J Biol Chem* 246(8):2425-2429.

121. Beattie DS, Basford RE, & Koritz SB (1967) The turnover of the protein components of mitochondria from rat liver, kidney, and brain. *J Biol Chem* 242(20):4584-4586.
122. Swick RW, Rexroth AK, & Stange JL (1968) The metabolism of mitochondrial proteins. 3. The dynamic state of rat liver mitochondria. *J Biol Chem* 243(13):3581-3587.
123. Gross NJ, Getz GS, & Rabinowitz M (1969) Apparent turnover of mitochondrial deoxyribonucleic acid and mitochondrial phospholipids in the tissues of the rat. *J Biol Chem* 244(6):1552-1562.
124. Aschenbrenner B, Druyan R, Albin R, & Rabinowitz M (1970) Haem a, cytochrome c and total protein turnover in mitochondria from rat heart and liver. *Biochem J* 119(2):157-160.
125. Rajwade MS, Katyare SS, Fatterpaker P, & Sreenivasan A (1975) Regulation of mitochondrial protein turnover by thyroid hormone(s). *Biochem J* 152(2):379-387.
126. Fletcher MJ & Sanadi DR (1961) Turnover of rat-liver mitochondria. *Biochim Biophys Acta* 51:356-360.
127. Lusena CV & Depocas F (1966) Heterogeneity and differential fragility of rat liver mitochondria. *Can J Biochem* 44(5):497-508.
128. Von Hungen K, Mahler HR, & Moore WJ (1968) Turnover of protein and ribonucleic acid in synaptic subcellular fractions from rat brain. *J Biol Chem* 243(7):1415-1423.
129. Bailey E, Taylor CB, & Bartley W (1967) Turnover of mitochondrial components of normal and essential fatty acid-deficient rats. *Biochem J* 104(3):1026-1032.
130. Lipsky NG & Pedersen PL (1982) Perturbation by clofibrate of mitochondrial levels in animal cells. Implications for a model of mitochondrial genesis. *J Biol Chem* 257(3):1473-1481.
131. Hare JF & Hodges R (1982) Turnover of mitochondrial matrix polypeptides in hepatoma monolayer cultures. *J Biol Chem* 257(21):12950-12953.
132. Hare JF & Hodges R (1982) Turnover of mitochondrial inner membrane proteins in hepatoma monolayer cultures. *J Biol Chem* 257(7):3575-3580.
133. Alberti KG & Bartley W (1969) The localization of proteolytic activity in rat liver mitochondria and its relation to mitochondrial swelling and aging. *Biochem J* 111(5):763-776.
134. Yen WL & Klionsky DJ (2008) How to live long and prosper: autophagy, mitochondria, and aging. *Physiology (Bethesda)* 23:248-262.
135. Miwa S, Lawless C, & von Zglinicki T (2008) Mitochondrial turnover in liver is fast in vivo and is accelerated by dietary restriction: application of a simple dynamic model. *Aging Cell* 7(6):920-923.
136. Price JC, Guan S, Burlingame A, Prusiner SB, & Ghaemmaghami S (2010) Analysis of proteome dynamics in the mouse brain. *Proc Natl Acad Sci U S A* 107(32):14508-14513.
137. Kim TY*, et al.* (2012) Metabolic labeling reveals proteome dynamics of mouse mitochondria. *Mol Cell Proteomics* 11(12):1586-1594.
138. Findlay GD, Yi X, Maccoss MJ, & Swanson WJ (2008) Proteomics reveals novel Drosophila seminal fluid proteins transferred at mating. *PLoS Biol* 6(7):e178.
139. Matthews DE (1993) Stable isotope methodologies in studying human amino acid and protein metabolism. *Ital J Gastroenterol* 25(2):72-78.
140. MacCoss MJ, Fukagawa NK, & Matthews DE (2001) Measurement of intracellular sulfur amino acid metabolism in humans. *Am J Physiol Endocrinol Metab* 280(6):E947-955.

141. Reinders J, Zahedi RP, Pfanner N, Meisinger C, & Sickmann A (2006) Toward the complete yeast mitochondrial proteome: multidimensional separation techniques for mitochondrial proteomics. *J Proteome Res* 5(7):1543-1554.
142. Lopez MF*, et al.* (2000) High-throughput profiling of the mitochondrial proteome using affinity fractionation and automation. *Electrophoresis* 21(16):3427-3440.
143. Gan JC & Jeffay H (1967) Origins and metabolism of the intracellular amino acid pools in rat liver and muscle. *Biochim Biophys Acta* 148(2):448-459.
144. Smith CB, Deibler GE, Eng N, Schmidt K, & Sokoloff L (1988) Measurement of local cerebral protein synthesis in vivo: influence of recycling of amino acids derived from protein degradation. *Proc Natl Acad Sci U S A* 85(23):9341-9345.
145. Hsieh EJ*, et al.* (2012) Topograph, a software platform for precursor enrichment corrected global protein turnover measurements. *Mol Cell Proteomics*.
146. Helfand SL & Rogina B (2003) Molecular genetics of aging in the fly: is this the end of the beginning? *Bioessays* 25(2):134-141.
147. Sardiello M, Licciulli F, Catalano D, Attimonelli M, & Caggese C (2003) MitoDrome: a database of Drosophila melanogaster nuclear genes encoding proteins targeted to the mitochondrion. *Nucleic Acids Res* 31(1):322-324.
148. Kraft C, Deplazes A, Sohrmann M, & Peter M (2008) Mature ribosomes are selectively degraded upon starvation by an autophagy pathway requiring the Ubp3p/Bre5p ubiquitin protease. *Nat Cell Biol* 10(5):602-610.
149. McCune HJ*, et al.* (2008) The temporal program of chromosome replication: genomewide replication in clb5{Delta} Saccharomyces cerevisiae. *Genetics* 180(4):1833-1847.
150. Hsieh EJ, Hoopmann MR, MacLean B, & MacCoss MJ (2010) Comparison of database search strategies for high precursor mass accuracy MS/MS data. *J Proteome Res* 9(2):1138-1143.
151. Ducret A, Van Oostveen I, Eng JK, Yates JR, 3rd, & Aebersold R (1998) High throughput protein characterization by automated reverse-phase chromatography/electrospray tandem mass spectrometry. *Protein Sci* 7(3):706-719.
152. Kall L, Canterbury JD, Weston J, Noble WS, & MacCoss MJ (2007) Semi-supervised learning for peptide identification from shotgun proteomics datasets. *Nat Methods* 4(11):923-925.
153. Zhang B, Chambers MC, & Tabb DL (2007) Proteomic parsimony through bipartite graph analysis improves accuracy and transparency. *J Proteome Res* 6(9):3549-3557.
154. Juhasz G, Erdi B, Sass M, & Neufeld TP (2007) Atg7-dependent autophagy promotes neuronal health, stress tolerance, and longevity but is dispensable for metamorphosis in Drosophila. *Genes Dev* 21(23):3061-3066.
155. Dagda RK*, et al.* (2009) Loss of PINK1 function promotes mitophagy through effects on oxidative stress and mitochondrial fission. *J Biol Chem* 284(20):13843-13855.
156. Liu S & Lu B (2010) Reduction of protein translation and activation of autophagy protect against PINK1 pathogenesis in Drosophila melanogaster. *PLoS Genet* 6(12):e1001237.
157. Qi Z*, et al.* (2011) Loss of PINK1 function decreases PP2A activity and promotes autophagy in dopaminergic cells and a murine model. *Neurochem Int* 59(5):572-581.
158. Ahmed AU & Fisher PR (2009) Import of nuclear-encoded mitochondrial proteins: a cotranslational perspective. *Int Rev Cell Mol Biol* 273:49-68.

159. Morais VA*, et al.* (2009) Parkinson's disease mutations in PINK1 result in decreased Complex I activity and deficient synaptic function. *EMBO Mol Med* 1(2):99-111.
160. Mortiboys H*, et al.* (2008) Mitochondrial function and morphology are impaired in parkin-mutant fibroblasts. *Ann Neurol* 64(5):555-565.
161. Zhu J & Chu CT (2010) Mitochondrial dysfunction in Parkinson's disease. *J Alzheimers Dis* 20 Suppl 2:S325-334.
162. Pimenta de Castro I*, et al.* (2012) Genetic analysis of mitochondrial protein misfolding in Drosophila melanogaster. *Cell Death Differ* 19(8):1308-1316.
163. Soubannier V*, et al.* (2012) A vesicular transport pathway shuttles cargo from mitochondria to lysosomes. *Curr Biol* 22(2):135-141.
164. Neuspiel M*, et al.* (2008) Cargo-selected transport from the mitochondria to peroxisomes is mediated by vesicular carriers. *Curr Biol* 18(2):102-108.
165. Matarrese P*, et al.* (2005) Galectin-1 sensitizes resting human T lymphocytes to Fas (CD95)-mediated cell death via mitochondrial hyperpolarization, budding, and fission. *J Biol Chem* 280(8):6969-6985.
166. Duttaroy A, Paul A, Kundu M, & Belton A (2003) A Sod2 null mutation confers severely reduced adult life span in Drosophila. *Genetics* 165(4):2295-2299.
167. Paul A*, et al.* (2007) Reduced mitochondrial SOD displays mortality characteristics reminiscent of natural aging. *Mech Ageing Dev* 128(11-12):706-716.
168. Brand M, Jarman AP, Jan LY, & Jan YN (1993) asense is a Drosophila neural precursor gene and is capable of initiating sense organ formation. *Development* 119(1):1-17.
169. Lin DM & Goodman CS (1994) Ectopic and increased expression of Fasciclin II alters motoneuron growth cone guidance. *Neuron* 13(3):507-523.
170. Benjamini Y & Hochberg Y (1995) Controlling the False Discovery Rate: A Practical and Powerful Approach to Multiple Testing. *J R Stat Soc Series B Stat Methodol* 57(1):289-300.
171. Chintapalli VR, Wang J, & Dow JA (2007) Using FlyAtlas to identify better Drosophila melanogaster models of human disease. *Nat Genet* 39(6):715-720.
172. Vargas JL, Roche E, Knecht E, & Grisolia S (1987) Differences in the half-lives of some mitochondrial rat liver enzymes may derive partially from hepatocyte heterogeneity. *FEBS Lett* 224(1):182-186.
173. Boland B*, et al.* (2008) Autophagy induction and autophagosome clearance in neurons: relationship to autophagic pathology in Alzheimer's disease. *J Neurosci* 28(27):6926-6937.
174. Berman SB & Hollenbeck PJ (2012) Exploring the life cycle of mitochondria in neuropsychiatric diseases: Mitochondrial dynamics and quality control. *Neurobiol Dis*.
175. de Vries RL & Przedborski S (2012) Mitophagy and Parkinson's disease: Be eaten to stay healthy. *Mol Cell Neurosci*.
176. Fallon L*, et al.* (2006) A regulated interaction with the UIM protein Eps15 implicates parkin in EGF receptor trafficking and PI(3)K-Akt signalling. *Nat Cell Biol* 8(8):834-842.
177. Doherty GJ & McMahon HT (2009) Mechanisms of endocytosis. *Annu Rev Biochem* 78:857-902.
178. Schwarz LA & Patrick GN (2012) Ubiquitin-dependent endocytosis, trafficking and turnover of neuronal membrane proteins. *Mol Cell Neurosci* 49(3):387-393.

179. Scherz-Shouval R & Elazar Z (2011) Regulation of autophagy by ROS: physiology and pathology. *Trends Biochem Sci* 36(1):30-38.
180. Vincent A*, et al.* (2012) parkin-induced defects in neurophysiology and locomotion are generated by metabolic dysfunction and not oxidative stress. *Hum Mol Genet* 21(8):1760-1769.
181. Grunewald A*, et al.* (2010) Mutant Parkin impairs mitochondrial function and morphology in human fibroblasts. *PLoS One* 5(9):e12962.
182. Heeman B*, et al.* (2011) Depletion of PINK1 affects mitochondrial metabolism, calcium homeostasis and energy maintenance. *J Cell Sci* 124(Pt 7):1115-1125.
183. Amo T*, et al.* (2011) Mitochondrial membrane potential decrease caused by loss of PINK1 is not due to proton leak, but to respiratory chain defects. *Neurobiol Dis* 41(1):111-118.
184. Um JW*, et al.* (2010) Parkin directly modulates 26S proteasome activity. *J Neurosci* 30(35):11805-11814.
185. Dachsel JC*, et al.* (2005) Parkin interacts with the proteasome subunit alpha4. *FEBS Lett* 579(18):3913-3919.
186. Sakata E*, et al.* (2003) Parkin binds the Rpn10 subunit of 26S proteasomes through its ubiquitin-like domain. *EMBO Rep* 4(3):301-306.
187. Livnat-Levanon N & Glickman MH (2011) Ubiquitin-proteasome system and mitochondria - reciprocity. *Biochim Biophys Acta* 1809(2):80-87.
188. Rusten TE & Stenmark H (2009) How do ESCRT proteins control autophagy? *J Cell Sci* 122(Pt 13):2179-2183.
189. Hyttinen JM, Niittykoski M, Salminen A, & Kaarniranta K (2012) Maturation of autophagosomes and endosomes: A key role for Rab7. *Biochim Biophys Acta* 1833(3):503-510.
190. Metcalf D & Isaacs AM (2010) The role of ESCRT proteins in fusion events involving lysosomes, endosomes and autophagosomes. *Biochem Soc Trans* 38(6):1469-1473.
191. Walker DW*, et al.* (2006) Hypersensitivity to oxygen and shortened lifespan in a Drosophila mitochondrial complex II mutant. *Proc Natl Acad Sci U S A* 103(44):16382-16387.
192. Gottlieb RA (2011) Cell death pathways in acute ischemia/reperfusion injury. *J Cardiovasc Pharmacol Ther* 16(3-4):233-238.
193. Huang C*, et al.* (2010) Autophagy induced by ischemic preconditioning is essential for cardioprotection. *J Cardiovasc Transl Res* 3(4):365-373.
194. Billia F*, et al.* (2011) PTEN-inducible kinase 1 (PINK1)/Park6 is indispensable for normal heart function. *Proc Natl Acad Sci U S A* 108(23):9572-9577.
195. Kim KY*, et al.* (2011) Parkin is a lipid-responsive regulator of fat uptake in mice and mutant human cells. *J Clin Invest* 121(9):3701-3712.
196. Zhang C*, et al.* (2011) Parkin, a p53 target gene, mediates the role of p53 in glucose metabolism and the Warburg effect. *Proc Natl Acad Sci U S A* 108(39):16259-16264.

VITA

Evelyn Sandra Vincow was born in Seattle, Washington, and grew up in Syracuse, New York. She attended Harvard University, where she earned a Bachelor of Arts degree in Psychology in 2001. After working in the lab of John Neumaier at the University of Washington, she entered the Neurobiology and Behavior Program, and earned a Doctor of Philosophy degree in 2013.